9-1-2021

MECHANISM OF DNA DAMAGE ASSOSCIATED WITH ESTROGEN RECEPTOR ALPHA – INTERPLAY OF NON-CANONICAL DNA SECONDARY STRUCTURES

AMAN SHARMA
University of Massachusetts Amherst

MECHANISM OF DNA DAMAGE ASSOSCIATED WITH ESTROGEN RECEPTOR ALPHA – INTERPLAY OF NON-CANONICAL DNA SECONDARY STRUCTURES.

A Dissertation Presented

by

AMAN SHARMA

Submitted to the Graduate School of the
University of Massachusetts Amherst in partial fulfillment
of the requirements for the degree of

DOCTOR OF PHILOSOPHY

September 2021

Animal Biotechnology and Biomedical Sciences (ABBS) Graduate Program

MECHANISM OF DNA DAMAGE ASSOSCIATED WITH ESTROGEN RECEPTOR ALPHA – INTERPLAY OF NON-CANONICAL DNA SECONDARY STRUCTURES.

A Dissertation Presented

by

AMAN SHARMA

Approved as to style and content by:

_____
D. Joseph Jerry, Chair

_____
Karen Dunphy, Member

_____
Barbara Osborne, Member

_____
Leonid Pobezinsky, Member

_____
Peter Chien, Member

_____
Rafael Fissore, Department Head
Veterinary and Animal Sciences

MECHANISM OF DNA DAMAGE ASSOSCIATED WITH ESTROGEN RECEPTOR ALPHA – INTERPLAY OF NON-CANONICAL DNA SECONDARY STRUCTURES.

A Dissertation Presented

by

AMAN SHARMA

Approved as to style and content by:

DocuSigned by:
D. Joseph Jerry
D. Joseph Jerry, Chair

DocuSigned by:
Dr. Karen Dunphy
Karen Dunphy, Member

DocuSigned by:
Dr. Barbara Osborne
Barbara Osborne, Member

DocuSigned by:
Dr. Leonid Pobezinsky
Leonid Pobezinsky, Member

DocuSigned by:
Dr. Peter Chien
Peter Chien, Member

DocuSigned by:
Dr. Rafael Fissore
Rafael Fissore, Department Head
Veterinary and Animal Sciences

DEDICATION

This work is completely dedicated to my parents and grandparents for their constant support and love. Also, thanks to my younger brother for being supportive and helpful. This thesis is also dedicated to my advisors under whose constant guidance I have completed this dissertation. They not only enlightened with academic knowledge but also gave me valuable advice and showed me the right path whenever I needed help.

ACKNOWLEDGMENTS

I would like to thank my awesome advisors, D. Joseph Jerry, and Karen Dunphy for giving me the great opportunity to work in their lab and gain expertise in different models such as human breast tissue explants, cellular and *in vivo* model. They have always encouraged me and has been supportive of my ideas to develop me as an efficient researcher.

In addition, I need to thank all the Jerry lab members, past and present, who have helped me along the way including Prabin Dhangada Majhi, Amy Roberts, Amye Black, Mary Hagen, Janhavi Phadkar, Libby Daniele, Aliza Majewski, Anna Gorfinkel, Shakirah Ssebyala, Sandra Barzola and Ceren Goral. Through lab meeting discussions and informal conversations, you helped me develop project ideas and push forward with this work. I am especially thankful for the support of Amy Roberts and Prabin Majhi, who helped me out in my projects intellectually as well as experimentally.

I am also thankful for the guidance of my committee members Barbara Osborne, Peter Chen, and Leonid Pobezinsky throughout my PhD journey. Their support and helpful suggestions at our meetings were crucial to finishing this work. I especially thank Sallie Schneider, Laura Vandenberg, and James Shull for their collaboration over the years. I also want to thank Helen Cousin and Dominique Alfandari for their support during my first lab rotation.

Lastly, I would like to thank my family and friends. I would not have been able to finish this work without their constant motivation and support.

MECHANISM OF DNA DAMAGE ASSOSCIATED WITH ESTROGEN RECEPTOR ALPHA – INTERPLAY OF NON-CANONICAL DNA SECONDARY STRUCTURES.

SEPTEMBER 2021

AMAN SHARMA, B.TECH., SHRI MATA VAISHNO DEVI UNIVERSITY (SMVDU), INDIA

Ph.D., UNIVERSITY OF MASSACHUSETTS AMHERST

Directed by: Professor D. JOSEPH JERRY

ABSTRACT

Breast cancer is the second leading cause of cancer mortality among women. Many risk factors for breast cancer are related to estrogen exposure and high serum estrogen levels. Studies have demonstrated the critical role of estrogen in breast carcinogenesis, but less clear how estrogen acts as an initiator of carcinogenesis. Several mechanisms have been implicated the pathogenic actions of estrogens. 1) Estrogens cause increased proliferation to indirectly introduce mutations that promote breast tumorigenesis. 2) Estrogens can form DNA adducts which may directly promote mutagenesis. 3) Estrogens induce DNA double strand breaks in the breast epithelial cells to promote transcription of estrogen target genes but also replication stress and genomic instability. 4) Estrogen also induces co-transcriptional products, called R-loops, that can lead to DNA damage.

Recent studies have suggested associations between exposures to environmental chemicals may also increase risk of breast cancer. Environmental chemicals such as endocrine disrupting chemicals or xenoestrogens can mimic the effects of estrogen by binding with the receptors and alter the endocrine system. However, there is a lack of

detailed mechanistic understanding. The focus of our first study is to investigate the effects of two xenoestrogens – Benophenone-3 (BP-3) and Propyl Paraben (PP) in the breast epithelial cells at concentrations relevant to human exposures and are commonly found in cosmetics, personal care products and sunscreens. With luciferase reporter assays, our lab confirmed that these two xenoestrogens are able to bind with the estrogen receptor complexes. We showed that 17β-estradiol (E2), BP-3 and PP are able to induce DNA damage via estrogen receptor manner *in vitro* but BP-3 and PP were weakly estrogenic in terms of transcriptional and proliferation responses. The DNA damage response from E2, BP-3 and PP is strongly associated with levels of ERα-mediated DNA: RNA hybrids triplex structures called R-loops. We also showed the induction of DNA damage and R loops from these compounds in mice without inducing transcription of estrogen target genes or proliferation in the mammary epithelial cells. These studies demonstrated that xenoestrogens possess the potential for genotoxic activity mediated by ERα through the formation of R-loops and DNA double-strand breaks.

While all women are exposed to endogenous and exogenous estrogens, only 1 in 8 women are expected to develop breast cancer suggesting that the cancer-promoting effects of estrogen exposure vary among individuals. Our second study demonstrated that E2-induced DNA damage is most pronounced in rodents that are genetically susceptible to mammary tumors and among women who are at high risk of breast cancer. Rodents which are susceptible to hormone-induced mammary tumors, such as BALB/c mice and ACI rats, showed significantly increased levels of DNA damage in the mammary epithelial cells with E2 treatment. E2 induced DNA damage in BALB/c mice was mainly found in ERα positive cells. Strains that are resistant to mammary tumors such as C57BL/6 mice and BN rats

showed little damage with E2. We also found increased E2-induced DNA damage in human breast tissues from women with inherited breast cancer risk alleles affecting DNA double-strand break repair. In contrast, only 1 in 5 of average risk donors exhibited a significant increase in E2 induced DNA damage. Together, these data demonstrate genetic differences in sensitivity to E2-stimulated DNA damage in rodents and that similar variation is observed in normal breast tissues from women.

Lastly, we investigated the mechanism by which E2 and BP-3 induce DNA damage in breast cancer cell lines. We showed that treatment with E2 and BP-3 promotes another non-canonical DNA secondary structure called G quadruplexes (G4s) in ER+ breast cancer cells. Most of the G4s induced by E2 and BP-3 colocalized with R-loops indicating G-loop formation. The induction of G4 formation and DNA damage with E2 and BP-3 in breast cancer cells is mediated by reactive oxygen species (ROS). Therefore, our data suggest a mechanism in which E2 and BP3 induce R loop stabilization is dependent on ROS which contributes to the formation of DNA G4s and colocalize with sites of DNA damage.

TABLE OF CONTENTS

Page

LIST OF TABLES

Table Page

LIST OF FIGURES

CHAPTER -1

INTRODUCTION

Breast cancer and Estrogen Exposure

Breast cancer is the most prevalent cancer type among women worldwide and the second leading cause of cancer related death in women (Siegel et al., 2021). It is a spectrum of many subtypes related to biological characteristics, such as tumor size, lymph node involvement, histological grade, patient's age, estrogen receptors (ERs), progesterone receptor (PRs) and human epidermal growth factor receptor 2 (HER2 or c-erbB2) or triple negative status (lack ER, PR and HER2) (Yersal and Barutca, 2014). The risk factors for breast cancer include age, genetics, obesity, increased breast density, early onset of menarche, late menopause, nulliparity, and late full-term pregnancy (Brooks et al., 2018; Samavat and Kurzer, 2015; Travis and Key, 2003).

Many of these risk factors are related to endogenous estrogen levels. Chronic lifetime exposure to estrogen, through early menarche (RR = 1.3), late menopause (RR = 1.2-2.0), hormone replacement therapy with estrogen and progesterone (RR = 1.2) or having the highest quartile of serum estrogen levels (RR = 1.8-5.0) all increase breast cancer risk in women (Brinton et al., 2009, 1983; Clemons and Goss, 2001; Dall and Britt, 2017; Eliassen et al., 2006; Rossouw et al., 2002; Trichopoulos et al., 1972). These suggest that lifetime exposure to estrogen increases breast cancer risk. Treatment with selective estrogen receptor modulators (SERMs) to inhibit estrogen activity in the breast has been shown to lower breast cancer incidence (Cuzick et al., 2013). Estrogen is also known to

contribute to breast tumor initiation and proliferation (Russo and Russo, 2006; J.-M. Tian et al., 2018).

Estrogen Sensitivity in Rodents

Previous work has identified rodent strains with increased sensitivity or resistance to mammary tumor development in response to carcinogen or estrogen treatment. In DMBA induced models of mammary tumors, the Wistar-Kyoto rat strain is resistant to tumor development while the Wistar-Furth strain is uniquely susceptible (Gould, 1986; Lan et al., 2001). For estrogen-induced mammary tumor models, the ACI strain is uniquely susceptible to estrogen-induced mammary tumors while the Copenhagen and Brown Norway strains are resistant (Dennison et al., 2015; Shull et al., 2018, 1997; Spady et al., 1998). Treatment of susceptible ACI rats with tamoxifen reduces the development of estrogen-induced mammary tumors (Li et al., 2002; Singh et al., 2011), demonstrating the involvement of estrogen receptor signaling in mammary tumor development in the ACI strain. These studies have also identified quantitative trait loci (QTL), regions of the chromosomes linked to mammary tumor susceptibility and resistance (Gould et al., 2004; Haag et al., 2003; Lan et al., 2001; Schaffer et al., 2006).

BALB/c and C57BL/6 strains of mice differ in their responses to E2 and progesterone (P4) (Aupperlee et al., 2008). Hormone-induced mammary tumors have been shown to develop in BALB/c mice whereas C57BL/6 mice are resistant (Girard et al., 2007; Kordon et al., 1993; Lanari et al., 1986; Molinolo et al., 1987). BALB/c mice are also sensitive to radiation-induced mammary tumors when compared with C57BL/6 mice (Ponnaiya et al., 1997; Ullrich et al., 1996). BALB/c mice with heterozygous mutations in

the p53 tumor suppressor gene (*Trp53*) develop spontaneous mammary tumors similar to the susceptibility to breast cancer among women with inherited mutations in *TP53*. In contrast, mammary tumors in C57BL/6-*Trp53*+/- mice are rare (Kuperwasser et al., 2000). This difference in susceptibility to mammary tumors was genetically linked to a locus on mouse chromosome 7 (Blackburn et al., 2007) and involves a greater reliance on repair DSBs in BALB/c-*Trp53*$^{+/-}$ mice through error-prone repair pathways (Böhringer et al., 2013). Taken together, these results illustrate the potential for estrogen to contribute to breast cancer development in certain genetic backgrounds, suggesting unique sensitivity to estrogen exposure. Similarly, genetic polymorphisms and epigenetic alterations may render a subset of women susceptible to carcinogenic effects of estrogens resulting in breast cancer.

Mechanism of Estrogen Signaling: Interplay of Estrogen receptors.

Biological responses to estrogen exposure are mediated through the two nuclear hormone estrogen receptors: estrogen receptor alpha (ERα) and estrogen receptor beta (ERβ). ERα and ERβ are ligand activated transcription factors in the steroid nuclear receptor family encoded by *ESR1* and *ESR2* gene respectively (Heldring et al., 2007). Studies from estrogen receptor knockout mice demonstrate that ERα function is crucial to mammary gland development. ERα knockout mice (αERKO) have rudimentary ductal mammary gland development similar to newborn mice (Bocchinfuso and Korach, 1997). Conversely, ERβ knockout mice (βERKO) mammary glands are indistinguishable from wild type mice (Krege et al., 1998). While ERβ appears dispensible with respect to mammary gland development, deletion of ERβ was shown to speed the onset of mammary

tumors when the p53 tumor suppressor gene is disrupted (Bardo et al., 2017). Therefore, it is possible that ERα and ERβ may play antagonistic roles with respect to the carcinogenic actions of estrogens.

In the classical mechanism, ligand-bound estrogen receptors form homodimers or heterodimers that bind estrogen response elements (ERE) in the DNA **(Figure 1.1**). The estrogen receptor dimers form complexes with other transcriptional coregulatory factors to drive expression of estrogen target genes (Marino et al., 2006; Saville et al., 2000; Yaşar et al., 2017; Yi et al., 2017). Other pathways for estrogen signaling have been identified, including tethered, non-genomic, and ligand-independent pathways (Heldring et al., 2007). The tethered pathway involves ligand-bound estrogen receptor dimer binding to other transcription factors bound to DNA, instead of EREs (Gaub et al., 1990; Saville et al., 2000). Non-genomic estrogen receptor signaling involves either membrane bound estrogen receptors or other membrane bound receptors which in turn activate the estrogen receptors (Heldring et al., 2007; Levin, 2009). However, membrane-bound estrogen receptors are not sufficient to rescue mammary gland development in ERα knockout mice (Pedram et al., 2009). Therefore, it is unclear whether the non-genomic pathway plays a significant role in normal mammary tissue. Ligand-independent pathways involve estrogen receptor phosphorylation by kinases activated by growth factor signaling and are hypothesized to be involved in hormone-independent growth of breast tumors (Coutts and Murphy, 1998; Kato et al., 1995; Shim et al., 2000). Recent work has highlighted the increased complexity of classical estrogen receptor signaling, where estrogen receptors can control the expression of genes without EREs or other transcription factor binding sites through long

range chromatin looping, which brings distant genes into close proximity to where estrogen receptors are bound (Fullwood et al., 2009).

Endocrine Disrupting Chemicals.

Endocrine disrupting chemicals (EDCs) can interfere with normal hormone signaling by mimicking or antagonizing the effects of endogenous hormones but can also alter the synthesis and metabolism of endogenous hormones and their receptors (Fernandez and Russo, 2010; Sonnenschein and Soto, 1998). Xenoestrogens are structurally diverse EDCs that affect estrogen receptor (ER) signaling pathways (Singleton and Khan, 2003). Estrogenic responses to putative xenoestrogens are most often determined by transactivation of ERE-reporters, endogenous gene expression and cell proliferation in ER-expressing MCF-7 and T47D cell lines, where ERα is the dominant subtype (Buteau-Lozano et al., 2002; Vladusic et al., 2000).

Benzophenone-3 (BP-3) is a UV-filter used in personal care products, such as sunscreens, cosmetics and lotions. BP-3 was detected in the urine samples of 96.8% of U.S. population in the National Health and Nutrition Examination Survey (Calafat et al., 2008). BP3 was shown to be a weak agonist of ER at 1 μM levels (Kerdivel et al., 2013; Schlotz et al., 2017; Schlumpf et al., 2010). Exposure to BP3 during pregnancy and lactation in mice resulted in altered mammary gland ductal architecture (LaPlante et al., 2018). Propyl Paraben (PP) is widely used as an anti-microbial agent in food and personal care products. PP was detected in the urine samples of >96% of U.S. population surveyed during 2003-2005 (Ye et al., 2006). PP was shown to be an effective ER-agonist with 1.3-fold induction of gene expression using reporter assays (ERE-CAT reporter) at 10 μM, increased

expression of estrogen-responsive gene Trefoil Factor 1 (*TFF1,* also known as pS2) and increased proliferation of MCF-7 cells at 1 μM (Byford et al., 2002). Proliferation induced by PP was inhibited by ER antagonist (fulvestrant) indicating dependence on ERα. Xenoestrogens, therefore, have the potential to disrupt estrogen receptor signaling by acting as ligands and could either amplify or mitigate the risk of breast cancer posed by estrogen exposure.

Genotoxicity by Estrogen.

Estrogen induces genotoxicity and DNA damage which is considered a major risk factor in breast cancer etiology (Roy and Liehr, 1999; Yager and Davidson, 2006). However, the mechanisms by which estrogen induces carcinogenesis continue to be debated (**Figure 1.2)**. First, estrogen has the potential to act as a direct carcinogen. Estrogen is metabolized by phase I P450 enzymes to form catechol estrogens (16α-OHE2 or 2-OHE2 and 4-OHE2), which can be oxidized to form reactive semiquinone (SQ) intermediates and quinone derivatives. Two such compounds, E2-3-4-Q and E2-2-3-Q form stable DNA adduct or depurinating adducts such as 4-OHE2-1N7Gua and 4-OHE2-1N3Ade, which were associated with increased breast cancer risk (Cavalieri and Rogan, 2016) . The formation of DNA adducts can also generate ROS through redox cycling and are potent inducers of oxidized bases. The oxidized bases can promote DNA single strand breaks (Fussell et al., 2011; Wang et al., 2010). DNA adducts have been correlated with increased cancer risk and act as carcinogenic metabolites. Therefore, apurinic/apyrimidinic sites (AP) are mutagenic if not faithfully processed (Cavalieri et al., 1997; Cavalieri and Rogan, 2016; Zahid et al., 2006). However, estrogen can also initiate DNA damage that is mediated by

ERα. ERα promotes proliferation of the breast epithelium which causes replication-associated DNA damage (Henderson and Feigelson, 2000; Preston-Martin et al., 1990). However, ERα has been shown to recruit Topoisomerase-2β, stimulating DNA double-strand breaks to facilitate transcription of ER target genes (Ju et al., 2006; Williamson and Lees-Miller, 2011). Another mechanism observed in breast cancer cell lines showed that ERα induces expression of APOBEC3B which causes cytidine deamination leading to DNA damage (Periyasamy et al., 2015; Udquim et al., 2020). Recently, 17β-estradiol (E2) was shown to induce DNA damage by promoting ERα-mediated co-transcriptional structures called R loops (Stork et al., 2016). Therefore, estrogen can stimulate carcinogenesis by initiating direct DNA damage as well as through mechanisms mediated by ERα.

R loops: A double edged sword.

R loops are non-B DNA structures that are formed when the nascent RNA hybridizes with the template DNA strand and causes transient displacement of the non-template DNA strand. The term R loop refers to the three-stranded structure formed by the DNA-RNA hybrid and the displaced single-stranded DNA (ssDNA). R loops are a normal consequence of transcription, but the persistence of R loops can induce DNA damage responses that result in DNA double-strand breaks (Aguilera and García-Muse, 2012a; Skourti-Stathaki and Proudfoot, 2014; Sollier and Cimprich, 2015). There are two different types of R loops: Physiological and Pathological.

Physiological R loops: Programmed R loops is a process which requires specific factors and enhanced specifically at certain regions to play a physiological role. Physiological R loops are intermediates that regulate several processes such as Immunoglobulin (Ig) class switch recombination (CSR) of B cells in vertebrates, CRISPR-Cas9 genome editing where guide-RNA forms a DNA:RNA hybrid to mediate Cas9 cleavage, transcription initiation and termination or mitochondrial and bacterial DNA replication (Aguilera and García-Muse, 2012b; Baldacci et al., 1984; García-Muse and Aguilera, 2019; Itoh and Tomizawa, 1980; Jinek et al., 2012; Kreuzer and Brister, 2010; Pohjoismäki et al., 2010; Xu and Clayton, 1996; Yu et al., 2003).

Pathological R loops: R loops play an important role in many cellular processes; however, persistent/unscheduled R loop formation due to defects in R loop resolving or preventing factors is linked towards DNA damage and genomic instability. The relevant mechanism by which unscheduled R loops causes genomic instability is its potential to act as an obstacle to replication fork progression, and therefore, cause fork collapse (Azvolinsky et al., 2009). Several studies have reported DNA damage generated by collisions between replication fork and the transcriptional machinery (Boubakri et al., 2010; Gottipati et al., 2008; Prado and Aguilera, 2005). The displaced ssDNA that is exposed during R loop formation is an excellent substrate and an open target to DNA editing enzymes such as activation induced cytidine deaminase (AID) or Apolipoprotein B mRNA editing enzyme (APOBEC). The DNA modifications activate base excision repair (BER) which creates an abasic site and ultimately a DNA lesion (Burns et al., 2013; Chiarle et al., 2011; Gómez-González and Aguilera, 2007). R loops can also be processed into

DNA double strand breaks (DSBs) by XPF and XPG endonucleases (xeroderma pigmentosum types F and G) involved in nucleotide excision repair (NER) (Sollier et al., 2014) to promote genomic instability. R loops as a source of DSBs can promote chromosomal translocations to promote carcinogenesis (Gostissa et al., 2011; Yang et al., 2014).

Multiple RNA processing factors and helicases have been shown to be involved in the resolution of R loops. Several proteins involved in Fanconi Anemia (FA) pathway such as BRCA1, BRCA2, FANCD2, FANCM and FANCA are recruited to R loop forming regions and their inactivation causes R loop accumulation and DNA damage (Bhatia et al., 2014; Hatchi et al., 2015; Madireddy et al., 2016; Okamoto et al., 2019; Schwab et al., 2015; Silva et al., 2019). In addition, BRCA1 and BRCA2 interact with DNA: RNA hybrid unwinding helicases such as SETX, DDX5 and RNase H2 to promote the efficient resolution of R loops (D'Alessandro et al., 2018; Hatchi et al., 2015; Sessa et al., 2021). Blocking DNA damage response and DNA repair genes (ATR, ATM, CHK1, CHK2, UBE2B, and RAD18) causes R loop accumulation (Barroso et al., 2019). Thus, several mechanisms are used to ensure the stability of the genome and protect from DNA damage mediated by R loops.

DNA G quadruplexes (G4s).

Another non-canonical DNA secondary structure known as G quadruplexes (G4s) is formed at single-stranded guanine-rich DNA sequences. DNA G4s arise from Hoogsteen hydrogen bonding of four guanine residues arranged within a planar G-quartet. Self-stacking of two or more G-quartets generates a G4 structure that is stabilized by

monovalent cations such as K^+ and Na^+ (Kwok and Merrick, 2017). G4 structures are topologically very polymorphic and can arise from the intra- or inter- molecular folding of G-rich strands. Intra-molecular folding requires the presence of four or more G-tracts in one strand, whereas inter-molecular folding can arise from two or more strands giving rise to parallel or anti-parallel structures depending on the orientation of the strands in a G4 (Kwok and Merrick, 2017; Lejault et al., 2021).

Biological functions of DNA G4s.

Protection of Telomeres: In vertebrates, the telomeric repeats $(TTAGGG)_n$ with a double stranded portion that is several kilobases in length and a 3` single stranded overhang which is few hundred bases in length. Telomeres consists of telomeric DNA and telomere binding proteins including TRF1, TRF2, POT1, RAP1, TIN2 and TPP1 which constitute the shelterin protein complex. This complex prevents the ends of the telomere from being recognized as DNA break points by DNA repair machinery. Telomeric DNA repeats are guanine rich and can form alternative secondary structure – the G4 structures (Maizels and Gray, 2013; Rhodes and Lipps, 2015; T. Tian et al., 2018; Varshney et al., 2020). In *S. cerevisiae*, cdc13 knockdown (a component of telomere capping complex) results in telomere instability and rescued by drugs that stabilize G4 structures (Smith et al., 2011). G4s are very resistant to digestion by exonucleases and may provide stability to telomere deprived of capping complex.

Replication: G4 structures could have important roles in replication origins, both in origin initiation positioning and origin timing control. Origin identification by high

throughput sequencing of short nascent DNA strands in four human cells (fibroblasts, embryonic stem cells, induced pluripotent stem cells and HeLa cells) showed that the majority of 250,000 replication origins correspond to G4 structures (Besnard et al., 2012). In addition, human origin recognition complex (ORC) was shown to bind to G4 forming DNA and RNA sequences *in vitro* (Hoshina et al., 2013). Recently, by initiation site-sequencing (*ini-seq*), using replicated DNA in a cell-free system, approximately 25,000 origins were identified in the human genome and 12,000 overlapped with G4 structures (Langley et al., 2016). The mechanism through which G4s influence origin initiation processing is still poorly understood. G4s have also been shown to play a role in the suppression of late origin firing by acting as the binding target of Rap1-interacting factor 1 (Rif1) in fission yeast, suggested to be a key factor in the regulation of DNA replication timing (Kanoh et al., 2015).

Transcription: G4s are considered to be significantly prevalent in human gene promoters. Computational analysis indicated the presence of 300,000 enriched putative quadruplex sequences ($G_{3+}N_{1-7}G_{3+}N_{1-7}G_{3+}N_{1-7}G_{3+}$) in promoters, proximal to transcription start site (TSS) and revealed that 42.7% of human gene promoters contain one or more quadruplex motifs (Huppert and Balasubramanian, 2005). Primers targeting G4s followed by re-sequencing the templates treated with the G4 stabilizer Pyridostatin (PDS) to identify sites of polymerase pausing. This G4-seq method was used to directly identify 716,310 distinct G4 structures in human B lymphocytes (Chambers et al., 2015). More recently, G4-specific antibodies were used to enrich and sequence endogenous G4 motifs (G4-ChIPseq). This showed that G4s are present in transcription-enhancing nucleosome-

depleted promoter regions suggesting that G4 formation leads to increased transcription (Hänsel-Hertsch et al., 2016). In addition, G4s can contribute to CpG islands hypomethylation in promoter regions contributing to elevated gene expression (Mao et al., 2018). Endogenous G4 DNA also acts as a site docking site for transcription factors (Lago et al., 2021; Spiegel et al., 2021). In patient-derived xenograft (PDX) models of breast cancer, increased G4 formation were found at the promoters of highly amplified genes that show increased expression (Hänsel-Hertsch et al., 2020).

Genomic Instability by DNA G4s.

Stable G4 structures can impede the progression of DNA polymerases and stall the replication fork progression leading to DNA damage and genomic instability (Puget et al., 2019; Técher et al., 2017). G4s can acts as trapping sites of oxidative DNA damage caused by reactive oxygen species (ROS). 8-oxoG formation by ROS can affect stability of promoter G4 structures resulting in altered expression levels in reporter gene assays (Cogoi et al., 2010; Fleming et al., 2017; Fleming and Burrows, 2019; Roychoudhury et al., 2020). In the human genome, G4 DNA is enriched at the chromosomal translocational breakpoints associated with various type of cancers, confirming that G4 DNA is a contributing factor to oncogenic transformation (Bacolla et al., 2019, 2016).

Factors resolving DNA G4s.

Several helicases and proteins are involved in G4 resolution and suppressing G4 mediated genomic instability (Lejault et al., 2021; Sauer and Paeschke, 2017). The yeast Pif1 helicase was shown to prevent G4-mediated genomic instability and prevent DNA

strand breaks (Paeschke et al., 2013; Ribeyre et al., 2009). FANCJ helicase together with the ssDNA binding protein RPA facilitates G4 unwinding (Wu et al., 2008). Another G4 helicase known as Bloom Syndrome (BLM) suppresses sister chromatid exchange events in the transcribed genes specifically at the sites of G4 motifs (Wietmarschen et al., 2018). In glioma cells, α-thalassemia mental retardation X-linked (ATRX) loss promotes G4 formation, somatic copy-number alterations, and increased occupancy of BLM at DNA damage sites (Wang et al., 2019). BLM and Werner Syndrome (WRN) helicases interact with RPA mediated by the BRCA1-interacting E3 ubiquitin- protein ligase HERC2 to suppress G4 DNA formation (Wu et al., 2018; Zhu et al., 2021). Recently, regulator of telomere elongation helicase 1 (RTEL1) was shown to suppress both R loops and G4s to avoid transcription-replication conflicts (Kotsantis et al., 2020; Wu et al., 2020). Thus, the formation and resolution of G-quadruplexes need to be regulated in the genome for the appropriate biological function.

When R loops and G4s come together – G loops.

Multiple studies have shown that R loops are more prevalent in genomic regions that are G-rich. During transcription, the non-template DNA strand is displaced allowing G4 structures to form in the single-stranded DNA strand (Ginno et al., 2013, 2012; Reaban et al., 1994; Skourti-Stathaki and Proudfoot, 2014). Recent studies have shown the co-existence of the R-loop and G4 to form a unique stable structure called as “G-loop”, where those G-rich sequences on the non-template strand fold into a G4 structure and R-loops on the template DNA strand (**Figure 1.3**) (Lee et al., 2020). Using electron microscopy, (Duquette et al., 2004), provided the first evidence of the existence of G-loop structure *in*

vitro and in *Escherichia coli*. Another study used G4 ligands, such as Pyridostatin (PDS), to stabilize G4 structures in human cancer cells and observed that G4 ligands induce DNA damage by stabilization of R loops (Magis et al., 2018). In these studies, 50 - 60% of stabilized G4s colocalized with R-loops. Importantly, R loops allow G4 formation and those G4s reversibly stabilize the R loop structure indicating the interrelationship of G4 and R-loop (Tan et al., 2020). The kinetics of R-loop and G4 formation was found to be similar in the cells at different timepoints and failure to resolve these structures promotes DNA damage and delays the repair process. G-loops can promote genomic instability by causing transcription-replication conflicts. Therefore, both G4 and R loops can be potential targets for cancer therapy. One classical example is G4 stabilizer CX-5461 causes synthetic lethality in BRCA deficient tumors and has advanced to clinical trials (Xu et al., 2017).

Objectives in this study.

We understand that estrogenic actions mediated by ERα plays a crucial role to breast carcinogenesis. Recently, co-transcriptional R loops came out to be a major player in terms of estrogen mediated genomic instability. All women are exposed to estrogens but only 1 in 8 women is expected to develop breast cancer which suggest that the genotoxic effects of estrogen could vary among individuals. In our studies, we tried to examine how estrogen and environmental disrupting chemicals can induce DNA damage. In the first part of our study, we investigated the mechanism of ER dependent DNA damage, R loop formation, transcriptional and proliferative responses by the endocrine disrupting chemicals BP3 and PP using *in vitro* and *in vivo* approach with E2 as a positive control. Next, we used different rodent strains that differ in susceptibility to mammary tumors to

determine whether there is a genetic basis for differences in E2 induced DNA damage. We also utilized patient derived breast explant model to determine the differences in E2 mediated DNA damage among average and high-risk women. Lastly, we studied the underlying DNA damage mechanism of E2 and BP3. We hypothesized that E2 and BP3 could favor G4 structures and especially G loop formation which could be the cause of DNA damage.

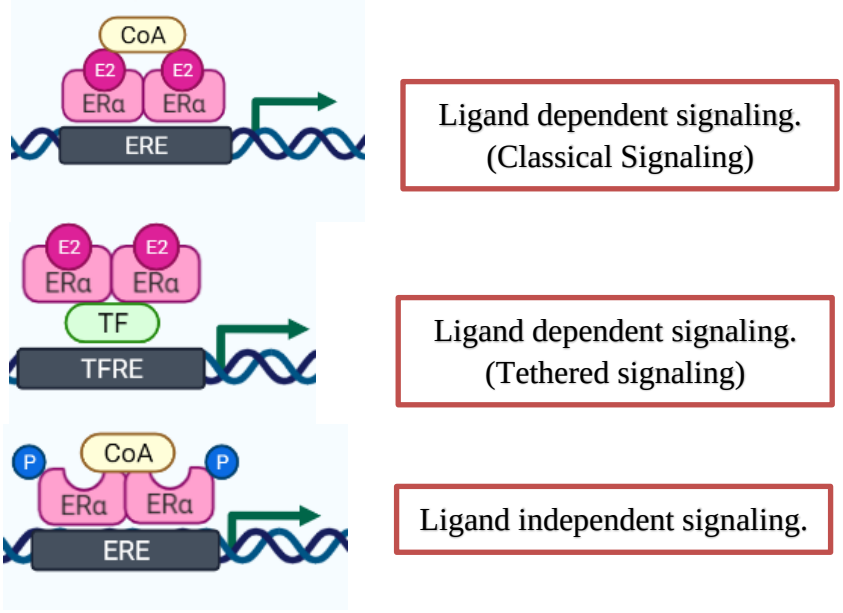

Figure 1.1: Estrogen receptor signaling.

Overview of ligand-dependent and independent mechanisms of estrogen receptor signaling. Direct, ligand-dependent signaling involves ligand-bound estrogen receptor (ER) dimers and coactivators (CoA) binding to estrogen response elements (ERE) in the DNA. Tethered estrogen receptor signaling involves ligand-bound receptor dimers binding to other transcription factors (TF) on the DNA. Ligand-independent signaling involves other growth factor activation, which activates kinases and leads to phosphorylation (P site) of the estrogen receptors. Model generated from bio render.

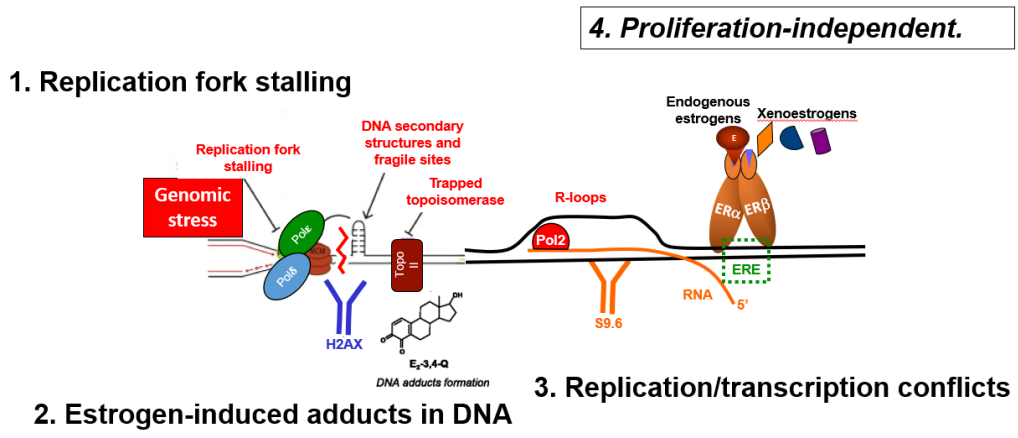

Figure 1.2: Mechanisms of E2 induced genomic instability.

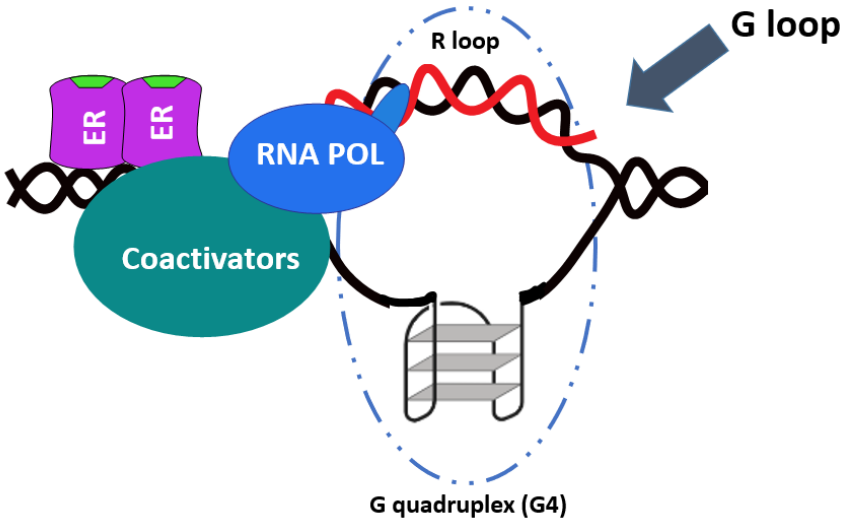

Figure 1.3: Structure of a G loop.

R loop formed on a template strand of DNA and on the non-template strand, a G quadruplex structure is formed. The simultaneous formation of R loop and G quadruplex structure is known as G loop.

CHAPTER -2

EFFECTS OF BENZOPHENONE-3 AND PROPYL PARABEN ON ESTROGEN RECEPTOR – DEPENDENT R-LOOPS AND DNA DAMAGE IN BREAST EPITHELIAL CELLS AND MICE

Published in Environmental Health Perspectives, 2020

https://doi.org/10.1289/EHP5221

Introduction

Endocrine-disrupting chemicals (EDCs) alter the endocrine system by binding directly to the receptors and modulating downstream signaling pathways. Xenoestrogens are structurally diverse EDCs that affect estrogen receptor (ER) signaling pathways. BP3 (Oxybenzone, or 2-Hydroxy-4-methoxybenzophenone, CAS No. 131-57-7) is a UV-filter used in personal care products, such as sunscreens, cosmetics and lotions, with concentrations up to 0.148% (Liao and Kannan 2014) and a maximum allowed concentration of 6% by Food and Drug Administration (FDA) and European commission (EU 2017). BP3 was detected in the urine samples of 96.8% of U.S. population in the National Health and Nutrition Examination Survey (NHANES) 2003-2004 conducted by Centers for Disease Control (CDC) (Calafat et al. 2008). Similarly, PP (propyl parahydroxybenzoate, CAS No. 94-13-3) is widely used as an anti-microbial agent in food and personal care products. While the FDA limits PP to 0.1% in food, currently there is no specific limit for preservatives in personal care products. PP is banned as food preservative and maximum permissible levels in personal care products is 0.4% in the EU (Snodin 2017)

(European Commission 2015). PP was detected in the urine samples of >96% of U.S. population surveyed during 2003-2005 by the CDC (Ye et al. 2006).

Estrogenic responses are determined by the action of two distinct estrogen receptor (ER) subtypes, estrogen receptor α (ERα) and estrogen receptor β (ERβ). Ligand-activated ER recruits co-activators to estrogen response elements (ERE) in promoters of target genes leading to transcription initiation (Shang et al. 2000; Yi et al. 2017). In ERα expressing breast cancer cells, proliferation is among the cellular responses (Henderson et al. 1988; Musgrove and Sutherland 1994). Hence, estrogenic responses to putative xenoestrogens are most often determined by transactivation of ERE-reporters, endogenous gene expression and cell proliferation in ER-expressing MCF-7 and T47D cell lines, where ERα is the dominant subtype (Buteau-Lozano et al. 2002; Vladusic et al. 2000). These studies showed BP3 was a weak agonist of ER at 1 μM (Kerdivel et al. 2013; Schlotz et al. 2017; Schlumpf et al. 2001). BP3 was found in the urine samples of 25 volunteers who used sunscreen containing 4% BP3 twice a day for 5 days suggesting it was readily absorbed through skin (Gonzalez et al. 2006). Metabolites of BP3, such as 2,4-diOH-BP and 2,3,4-triOH BP, were shown to form by oxidation in rat and human liver microsomes (Okereke et al. 1994; Watanabe et al. 2015). 2,4-diOH-BP was detected in the urine samples of women scheduled undergo a diagnostic and/or therapeutic laparoscopy or laparotomy as part of the ENDO study (Kunisue et al. 2012) and was shown to have higher ER transactivation potential compared to BP3 (Watanabe et al. 2015). BP3 and BP3 metabolite 4,4'-dihydroxybenzophenone were also detected in 27 of the 79 breast milk samples from mothers who had normal pregnancy and delivery and participated in the Breast Milk Bank of the Blood and Tissue Bank of Catalonia (Spain) (Molins-Delgado et al. 2018). Exposure

of BP3 during pregnancy and lactation in mice resulted in altered mammary gland ductal architecture that persisted for weeks after exposures ended (LaPlante et al. 2018). Long-term exposure of MCF-7 breast cancer cells to 100 µM BP3 for >20 weeks increased the motility of these cells (Alamer and Darbre 2018). This was also observed in estrogen non-responsive cell line MDA-MB-231 suggesting alternate pathways of BP3 actions at this dose. Similarly, PP was shown to be an effective ER-agonist with 1.3-fold induction of gene expression using reporter assays (ERE-CAT reporter) at 10 µM, increased expression of estrogen-responsive gene Trefoil Factor 1 (*TFF1*, also known as pS2) and increased proliferation of MCF-7 cells at 1 µM (Byford et al. 2002). Proliferation induced by PP was inhibited by ER antagonist (fulvestrant) indicating dependence on ERα. PP also increased cell motility (increased scratch closure) in both short-term (7 days) and long term (20 weeks) treatments in the MCF-7 cell line (Khanna et al. 2014).

In addition to stimulating cell proliferation and motility, estrogen also induces genotoxicity and DNA damage and is considered a major risk factor in breast cancer etiology (Roy and Liehr 1999; Yager and Davidson 2006). Estrogen has been shown to induce DNA damage by 1) metabolic activation of estrogen and 2) hormonal carcinogenesis (Santen et al. 2009). E2 is metabolized to form catechol estrogens (16α-OHE2 or 2-OHE2 and 4-OHE2), which can be oxidized to form reactive semiquinone (SQ) intermediates and quinone derivatives. Two such compounds, E2-3-4-Q and E2-2-3-Q form stable DNA adduct or depurinating adducts such as 4-OHE2-1N7Gua and 4-OHE2-1N3Ade, which were associated with increased breast cancer risk, but micromolar levels of E2-3-4-Q and E2-2-3-Q were required to show DNA adduct formation *in vitro* (Cavalieri and Rogan 2016). The SQ and quinone derivatives can also generate ROS through redox

cycling, which can be genotoxic (Fussell et al. 2011; Wang et al. 2010). Similarly, ER-independent DNA damage was shown in ERα-negative cell lines using the COMET assay (Rajapakse et al. 2005), *cII* mutagenesis assay (Zhao et al. 2006) or LOH (Huang et al. 2007; Russo et al. 2003). The concentrations of E2 or 4-OHE2 used in these studies were ≥ 70nM, with the exception of Russo et al. 2003 who reported increased clonal efficiency of MCF10F cells at 0.007nM. However, the median 17β-estradiol level during pregnancy is 74 nM and < 2 nM in normal cycling women **(Table 1.1)** and the level of circulating estradiol metabolites are 100-fold lower (Xu et al. 2007; Ziegler et al. 2010). Clinical data show that in postmenopausal women with ER+ early breast cancer, endocrine therapy with an aromatase inhibitor was associated with significantly lower recurrence than tamoxifen therapy (EBCTCG 2015), which could be either because of lower levels of estrogen metabolites or reduced ER activation. Epidemiological data show that for a given level of total estrogen, increased levels of 4-OHE2, 2-OHE2 and 16-OHE2 are associated with reduced risk in breast cancer (Dallal et al. 2014; Moore et al. 2016; Sampson et al. 2017) or no independent association with risk (Sampson et al. 2017). Although an earlier study reported 4-OHE2 levels to be associated with higher breast cancer risk (Fuhrman et al. 2012). Hence, the impact of metabolic activation of estrogen at physiologically relevant concentrations on DNA damage remains to be demonstrated.

Hormonal carcinogenesis is postulated to act through ER to initiate lesions as well as stimulate progression of tumors. E2 treatment stimulated renal tumors in male Syrian hamsters (Liehr et al. 1988). Tamoxifen (TAM) reduced tumors but did not alter levels of DNA-adducts suggesting the primary effect of E2 being mediated by ER. Similarly, blockage of ER activation through selective estrogen receptor modulators (SERMs) such

as TAM and raloxifene reduced the incidence of breast cancer by 50-75 % in women (Cummings et al. 1999; Cuzick and International Breast Cancer Intervention 2001; Martino et al. 2004). Bilateral oophorectomy and hysterectomy in women under 40 years of age reduced breast cancer later in life by 75% (Feinleib 1968). Administration of aromatase inhibitor (exemestane) for 35 months to a cohort of post-menopausal women with Gail score of 1.66, prior atypical ductal/lobular hyperplasia or ductal carcinoma *in situ* treated with mastectomy but non-carriers for BRCA1/2 and no prior invasive ductal carcinoma resulted in 65% relative reduction of breast cancer (Goss et al. 2011). Mobley and Brueggemeier (2004) showed that 8-oxo-dG production with BSO (buthionine sulfoximine)+ E2 (10nM) + H2O2 treatment could be reduced with TAM treatment in ER-positive MCF7 cells but not in ER-negative MDA-MB-231 cells suggesting DNA damage was at least partially ER-mediated (Mobley and Brueggemeier 2004). Stork et. al (2016) a showed lack of DNA damage marker γH2AX in MCF10A cells following treatment of 10 nM and 100 nM E2 for 24 h (Stork et al. 2016). In T47D cells, E2 mediated γH2AX was diminished with treatment of ER inhibitors like TAM or fulvestrant (Periyasamy et al. 2015). ER signaling stimulates proliferation which was causally linked to tumorigenesis by increasing the probability of replication errors which are propagated in daughter cells (Henderson and Feigelson 2000; Preston-Martin et al. 1990). Therefore, E2 can be considered as a carcinogen through its actions on progression of cancer that was initiated by other factors.

The studies involving DNA damage by E2 have used different cell lines, tissues and endpoints. Therefore, there is no consistent way to discriminate the contribution of ER-

dependent and ER-independent mechanisms across published studies. It is possible that both mechanisms contribute to E2 mediated carcinogenesis.

Recent studies have shown that ER stimulation leads to transcription-coupled DNA damage suggesting a distinct mechanism. Interaction of ERα with chromatin forms transcriptional co-activator/co-repressor complexes to initiate transcription (Chao et al. 2002; Fullwood et al. 2009; Shang et al. 2000). The open chromatin in these ERα complexes were susceptible to DNA damage by formation of RNA:DNA triplex structures called R-loops (Stork et al. 2016). Therefore, estrogen can stimulate carcinogenesis by initiating direct DNA damage mediated by ERα and proliferation that expands the population of breast cells.

Bioassays of transcriptional activities have been valuable in rapidly assessing the risk posed by xenoestrogens. However, it is unclear if the transcriptional activities of xenoestrogens reflect their potential mutagenic activity mediated by ERα. DNA damage by selective ERα agonists such as Diethylstilbestrol (DES) and 4,4',4''-(4-Propyl-[1*H*]-pyrazole-1,3,5-triyl) *tris*phenol (PPT) (Periyasamy et al. 2015) suggest that transcriptional DNA damage needs to be assessed to determine potential breast cancer risk posed by xenoestrogens. In this study, we evaluated effects of two xenoestrogens, BP3 and PP, which differ in structure and transcriptional potency and compared these with E2.

Materials and Methods

Cell culture:

T47D (ATCC #HTB-1330), T47DKBluc (ATCC #CRL-2865) and MCF-7(ATCC #HTB 22) cells were passaged in growth media containing phenol-red free (PRF) DMEM-F12 (Sigma #D6434) or MEM 1x (Gibco #51200-038) with 10% heat inactivated FBS (Omega Scientific # FB-02) and 10 µg/ml insulin (Sigma #9278), 2 mM L-glutamine (Hyclone # SH30034.01), gentamycin 15 µg/ml (Gibco #15750-060) and 1X antibiotics/antimycotics (AB/AM, Gibco #15240-062) and incubated at 37ºC with 5% CO_2. For experiments, cells were grown in clearing media with charcoal-stripped serum (CSS) (MEM 1x with 10% charcoal-dextran treated FBS (Omega Scientific #FB-04), 10 µg/ml insulin and 2 mM L-glutamine) for 24-72 h before being plated for experiments.

The 76N-Tert cell line, a human mammary epithelial cell line immortalized with expression of human telomerase reverse transcriptase (TERT), was a gift from Dr. Vimla Band (Zhao et al. 2010). These cells were grown in F-media (250 mL DMEM (- pyruvate) (Gibco #11965-092), 250 mL Ham's F12 (Gibco #11765-054), 5% FBS, 250 ng/mL hydrocortisone (Sigma #H4001), 10 ng/mL human epidermal growth factor (Tonbo Biosciences # 21-8356-U100), 8.6 ng/mL cholera toxin vibrio (Millipore Sigma # 227035), 1 µg/mL human insulin solution, and 1X antibiotic-antimycotic) and passaged every 2-3 days.

Generation of 76N-Tert-*ESR1* cells.

An inducible ERα (*ESR1*) construct was generated using the pINDUCER14 vector (Meerbrey et al. 2011). Specifically, FLAG tag sequence was amplified from pFLAG-

CMV-2 (Andersson et al. 1989) using forward primer 5'-ATACCGGTACCATGGACTACAAAGACGATGACGAC-3' and reverse primer 5'-TCGACCGGTACGCGTGCGATCGCTGAATTCGCGGCAAG-3'. The amplified FLAG sequence was then cleaned using the Monarch PCR & DNA Cleanup Kit (NEB #T1030) and ligated into pINDUCER14 by digesting both plasmids with *AgeI*, performing dephosphorylation with shrimp alkaline phosphatase (NEB #M0371S), gel electrophoresis, and extracting from agarose gel (DNAland Scientific #GP1001). Sequencing of pINDUCER14-FLAG confirmed the FLAG sequence was inserted.

ESR1 was amplified from a plasmid expressing *ESR1* made in our lab (pIRES-hrGFPII-ESR1, unpublished data). pIRES-hrGFPII-ESR1 contained the *ESR1* cDNA sequence (Open Biosystems #MHS6278-211691051) in the multiple cloning site of the pIRES-hrGFPII vector (Stratagene #240157). *ESR1* was amplified from pIRES-hrGFPII-ESR1 using forward primer 5′- GCAGAAATGACCATGACCCTCCACACCAAAGC-3′ and reverse primer 5′- TAAACGCGTTCAGACCGTGGCAGGGAAACCCT-3′. Ligation of *ESR1* into pINDUCER14-FLAG was done by digesting both plasmids with *EcoRI* and *MluI* and then performing dephosphorylation, cleanup, and extraction as described above. Two linker sequences (Linker A: AATTGCGCGATCGCGG, Linker B: AATTCCGCGATCGCGC) between FLAG and *ESR1* were added to keep the *ESR1* sequence in-frame. Sequencing of this final pINDUCER14-FLAG-*ESR1* confirmed that all inserts were in the correct orientation relative to the vector, both FLAG and *ESR1* were in frame, and the *ESR1* sequence was identical to the *Homo sapiens ESR1* gene (Sequencing Primers: F: CGGTGGGAGGCCTATATAAG, M: GCTACCATTATGGAGTCTGG, R:

ACTTATATACGGTTCTCCCC). This final construct was referred to as pIND-*ESR1* and expressed a constitutive GFP reporter and ERα with N-terminal FLAG tag.

In addition, 293T cells were cultured in DMEM: F12 (Sigma #D8900) supplemented with 10% FBS, 15 µg/mL gentamycin (Gibco #15750-060), and 1X antibiotic/antimycotic. Cells were lifted with 0.05% trypsin and plated in 60 mm tissue culture dishes at 2.5 x 10^6 cells per dish for next day use. 293T cells were then transfected with 3.5 µg pIND-*ESR1*, 3 µg psPAX2 (Addgene #12260) (gag, pol, and rev packaging vector) and 2 µg pMD2.G (Addgene #12259) (vsv-g packaging vector) in antibiotic free media using Lipofectamine 2000 (Thermo Fisher Scientific). Media was refreshed after 24 hours and viral media was collected at 48 and 54 hours post initial transfection. Viral media from transfected 293T was filtered using a 0.45 µM filter (Corning #431220) and added to 76N-Tert cells twice, 6 hours apart, in a 1:1 ratio with F-media. After 24 hours, viral media was removed and replaced with F-media. Following cell expansion, the cells were pooled and resuspended in 1% FBS/PBS. Selection of the stably transduced cells was performed by FACS for GFP+ cells using FACSAria II (Becton-Dickinson). 76N-Tert uninfected cells were used as a control to set the background fluorescence. Approximately 5% cells were GFP+ suggesting pINDUCER14-FLAG-*ESR1* expression. The GFP+ cells were collected to 90% purity. These cells were expanded and referred to as 76N-Tert-*ESR1*.

Luciferase reporter assay

T47DKBluc cells were grown in clearing media for 72 h and plated in a 24 well plate at 10 x 10^5 cells/well density. After 24 h cells were treated with 10 nM E2 (17β-estradiol, Sigma #E2758), 10 nM fulvestrant (F, ICI 182, 780, Tocris #1047), 0.5 to 50 µM

BP3 (Sigma #H36206) or 0.5 to 50μM PP (Sigma #P53357). Stock solutions were prepared in DMSO (Sigma #D8418), then diluted to working concentrations in media. Luciferase assays were performed using the Promega Dual-Luciferase Reporter Assay (Promega # E1910). Cells were lysed in 1X Passive Lysis Buffer after treatment for 24 h and then stored at -20°C. Luciferase activity was determined in lysates by using the Polar Star OPTIMA plate reader (BMG Labtech) and expressed in relative light units (RLU). Treatments were compared to 10nM E2 included on the plate and relative transactivation activity (RTA) is defined as percent transactivation compared to 10nM E2.

RT-qPCR

RNA from T47D cells, MCF-7 Cells or flash-frozen 4th mammary gland was isolated with TRIzol (Thermofisher Scientific #15596018) and Direct-zol RNA MiniPrep Plus (Zymo Research #R2072). cDNA was prepared from 1 μL of RNA in 20 μL reaction mix with Protoscript II First Strand cDNA Synthesis Kit (New England Biolabs #E6560S) following the standard protocol provided by manufacturer. qPCR for *TFF1*, progesterone receptor (*PGR/Pgr*) and Amphiregulin (*AREG/Areg*) was performed using primers in **Table 2.3** (Integrated DNA Technology) and iTaq Universal SYBR Green Supermix (Biorad, #1725121) on CFX96 Real-Time System thermocycler (Bio-Rad). Each run (96 well qPCR plate) included an inter-run calibrator to normalize across experiments. No house-keeping gene was included in the experiment to avoid possible variation due to treatments. Results represent average of 3 experiments. Data was analyzed with ΔΔCt method and relative fold change in expression of target gene was compared between control and treatments.

Cell proliferation assay

T47D cells grown in clearing media for 72 h was plated as 100µl of cells suspension having 5000 or 10000 cells per well on five 96 well plates (one for each day). The 96 well plate had 12 cell-free wells for a blank and 7 wells per treatment on each plate. After 24h, media was changed in appropriate wells on each plate to reach the desired final concentration of E2 (0.5 nM), BP3 (5, 50 µM) or PP (1, 10 µM) in the given wells. All plates were maintained in a 37ºC, 5% CO_2 incubator until media was exchanged, on one plate per day, for 10% Alamar Blue in plating media. Plates were read at the same time each day at 4 hr and 8 hr after media exchange on a BioTek Synergy 2 plate reader (Winooski, VT) at 570nm and 600nm. Percent alamar blue reduction was calculated as per equation 5 on the Alamar Blue protocol:

$$Percent\ reduced = \frac{(117216 \times \text{test well } A_{570}) - (80586 \times \text{test well } A_{600})}{(155677 \times \text{mean (negative control wells } A_{600})) - (14652 \times \text{mean (negative control wells } A_{570}))} \times 100$$

Immunostaining

T47D, MCF7, 76N-Tert or 76N-Tert-ESR1 cells were grown in clearing media for 48 h and plated on 20 mm glass uncoated coverslips in 12 well plates with a density of 2 x 10^5 cells/well. After 24h of growth, cells were treated with 10 nM E2, 1 or 5 µM BP3, and 1 or 5 µM PP with or without 1 µM fulvestrant for 24h. **γH2AX/53BP1/ERα:** Cells were fixed in ice-cold methanol (100%) for 10 mins and quenched with 0.1 M Glycine for 15

mins. Cells were washed with 1X PBS, blocked in 2% BSA/PBS with 0.1% Triton-X 100 for 1hr at room temperature (RT), incubated overnight with anti-γH2AX antibody (Cell Signaling # 9718S), anti-ERα antibody (Santa Cruz Biotechnology #sc-8002) or anti-53BP1 antibody (Abcam # ab36823) at 4°C followed by 1 hour with anti-rabbit AlexaFluoro-488-conjugated secondary antibody (Cell Signaling #8889S) or anti-mouse AlexaFluoro-488-conjugated (Cell Signaling #4408S) at RT. **S9.6**: Cells were fixed in ice-cold 100% methanol for 10 min at -20°C, permeabilized in 100% acetone for 1 min at RT, blocked for 30 min in saline sodium citrate pH 7 (SSC, 4X), 3% BSA, 0.1% Triton-X and incubated with S9.6 antibody (Kerafast #ENH001) for 2hr at RT followed by 1h with anti-mouse AlexaFluoro-596-conjugated secondary antibody (Life Technologies #A11062) or anti-mouse AlexaFluoro-488-conjugated (Cell Signaling #4408S). For each treatment, two replicates of slides were stained with one set of replicates treated with RNase H (NEB #M0297L) for 4hr at 37°C prior to incubation with primary antibody. Stained cells were mounted with Vectashield mounting medium containing DAPI (Vector Laboratories # H-1200). Slides were imaged at 60X (immersion oil) with Nikon A1 Spectral Confocal microscope. Analysis of γH2AX and S9.6 intensity per nucleus or foci per nucleus was calculated using Nikon analysis software, where DAPI was used as a mask for the nucleus.

Western blot

Cells from MCF7 grown in growth media, 76N-Tert (parental), 76N-Tert-ESR1, 76N-Tert-ESR1 grown in F-media treated with doxycycline for 24h and 76N-Tert-ESR1 treated with doxycycline and 10nM E2 for 24h were lysed with ice cold RIPA lysis buffer (50 mM Tris–HCl, pH 8.0; 150 mM NaCl; 1 mM EDTA; 1% Triton X-100; 1% Sodium

deoxycholate; 0.1% SDS; 1% protease inhibitors (Sigma-Aldrich # P8340), 1% phosphatase inhibitor #2 (Sigma-Aldrich # P5726), and 1% phosphatase inhibitor #3 (Sigma-Aldrich # P0044). Homogenate was centrifuged at 13,000 rpm for 15 minutes at 4°C to remove cellular debris. Protein quantification was performed using BCA protein assay (Thermo Scientific # 23225). Equal amounts of protein (28 μg) were separated by SDS-PAGE on 10% acrylamide under denaturating conditions and then blotted onto PVDF membrane (Millipore # IPVH00010). Non-specific binding was blocked with 5% non-fat dry milk in TBST (Tris-buffered saline and Tween 20 containing 10 mM Tris-HCl, pH 7.5; 150 mM NaCl; 0.05% Tween-20) for 1 hour. The blot was incubated with 1:100 anti-ERα antibody (Abcam # ab16660) overnight at 4°C. After incubation, the blot was washed with TBST and then incubated with HRP-conjugated secondary antibody (1:5000, GE Healthcare # NA934V) for 1 hour. Bands were detected using enhanced chemiluminescence solution and visualized using G-box imaging system (Syngene). The blot was washed with TBST and incubated with anti-β actin antibody (1:5000, Sigma # A1978) overnight at 4°C. After washing with TBST and HRP secondary antibody incubation for 1hour (1:5000, GE Healthcare # NA931C) bands were detected with enhanced chemiluminescence and G-box system. Expected molecular weights were 67 kDa (ERα) and 42 kDa (β actin).

Animal treatment

Forty mature female mice (8 weeks old) BALB/c mice were purchased from Jackson Laboratory and housed in temperature-controlled facilities with a set temperature of 64-79 °F and humidity of 30-70%, 12-hour alternating day/night light cycle and fed

LabChow 5058 ad libitum. All procedures were in accordance with the national guidelines for the care and use of animals and approved by the University of Massachusetts Amherst's Institutional Animal Care and Use Committee.

The mice were ovariectomized before treatment. Briefly, each mouse was anaesthetized with a mix of isoflurane and oxygen. The flanks were shaved, sterilized with betadine, and cleaned with alcohol. An incision was made to the skin on the right flank. The underlying muscle layer was nicked to reveal a small hole through which ovary was pulled out by grasping the periovarian fat. A Serrifin clamp was used to hold the ovary. After making sure the blood vessels were constricted to prevent breeding, the ovary was cut from the uterine horn. The periovarian fat was restored into the peritoneum. The peritoneum was closed with one or two stiches and the skin was closed with 9 mm wound clips. The procedure was repeated on the contralateral side. The mouse was monitored for a week post-procedure and wound clips were removed after 10 days. After 1 week of recovery, the mice were randomized to four groups and began an acute oral treatment via pipette with vehicle control (tocopherol-stripped corn oil) (n = 7) or one of three different compounds E2 (n = 8), BP3 (n = 12) and PP (n =12) for 4 days. Each mouse was administered 1 μL of oil per gram of body weight to deliver 250 μg/kg/d E2, 3000 μg/kg/d BP3 or 10000 μg/kg/d PP or vehicle control. For BP3 and PP, these doses represent the toxicologically no-adverse-effect-level (NOAEL) doses for each compound based on development and reproductive toxicity assays (Scientific Committee on Consumer Products 2005, 2008; Soni et al. 2001).

Six hours prior to sacrifice all of the mice were treated with 5 Gy dose of γ-irradiation. Then two hours before sacrifice all mice were injected intraperitoneally with

70 µg/g body weight of BrdU (Sigma Aldrich; Cat# B5002) that was previously prepared at 10 mg/ml in PBS and filter sterilized. The mice were sacrificed using carbon dioxide followed by cervical dislocation. Whole blood was collected by cardiac puncture and tissues were harvested. One of the 4th mammary gland was fixed in 10% NBF and transferred to 70% alcohol prior to paraffin-embedding. The other 4th mammary gland was cleared of lymph node and stored in -70°C. The whole blood was allowed to coagulate at RT for 20 min and then spun down at 2000 x g for 10 min at 4°C to retrieve the serum.

Immunostaining of mouse mammary gland

Freshly cut 4 µM paraffin-embedded sections were deparaffinized/rehydrated with 100% xylenes 3 times for 5 min each, 2 times with 100% ethanol for 5 min each, 95% ethanol for 3 min and 70% ethanol for 3 min. Samples were rinsed with PBS. Antigen-unmasking was performed by boiling the samples in 1 mM EDTA for 1 hr. Samples were cooled down to RT and then treated with SSC 0.2X with gentle shaking at RT for 20 min. Samples were blocked in 3% BSA in PBS with 0.5% Tween-20 for 1 hr at RT. Primary antibody incubation was done with monoclonal S9.6 antibody (Kerafast #ENH001) or anti-H2AX antibody (Cell Signaling # 9718S) for overnight at 4°C. After primary incubation, samples were washed 3 times with PBS containing 0.5% Tween-20 and then incubated with anti-mouse AlexaFluoro-488-conjugated (Cell Signaling #4408S) or anti-rabbit AlexaFluoro-488-conjugated secondary antibody (Cell Signaling #8889S) for 1 hr at RT. Samples were washed 2 times with PBS containing 0.5% Tween-20 and 2 times with PBS and then mounted with Vectashield mounting medium containing DAPI. Slides were imaged at 60X with Nikon A1 Spectral Confocal microscope. Analysis of S9.6 intensity

per nucleus or foci per nucleus were calculated using Nikon analysis software, where DAPI was used as a mask for the nucleus. IHC for Ki-67 was performed on a DakoCytomation autostainer using 1:1000 D2H10 primary antibody (cell signaling #9027T) and the Envision HRP detection system (Dako, Carpinteria, CA). Positive cells were counted using ImageJ software. A total of 1200 cells were counted per slide to determine percent Ki67 positive.

ELISA

The serum from whole blood that was harvested from all the mice were quantified using a 17β-estradiol specific enzyme-linked immunosorbent assay (ELISA) (Calbiotech # ES 180S- 100).

Statistical analyses

Unless specified, data were analyzed by one-way analysis of variance (ANOVA) followed by Tukey's honestly significant difference (HSD) multiple-range test using GraphPad Prism 8 statistical analysis software or R program (R Core Team 2013). The difference between control and fulvestrant/RNase H treated groups were evaluated with two-way ANOVA followed by Bonferroni correction. Results are presented as mean ± standard error of the mean (SEM). Data were considered statistically significant at $p < 0.05$. Growth curves were fitted to linear regression model and slopes were compared between control and treatment conditions. Slopes and 95% confidence interval are reported in **Table 2.2**.

Results

DNA damage and *TFF1* gene expression in cells treated with E2, BP3 or PP

We monitored γH2AX foci as a measure of DNA damage in T47D cells treated with the compounds for 24h. A dose-dependent increase in γH2AX intensity was observed following E2 treatment **(Figure 2.1A)**. Treatment with either BP3 or PP also led to an increase in γH2AX intensity. Treatment with BP3 at 1 or 5 μM increased γH2AX intensity compared to the control ($p < 0.0001$) although we did not observe a dose-dependent increase (1μM BP3 vs 5μM BP3, **Figure 2.1B**). PP treatment also resulted in significantly increased γH2AX intensity at 1 and 5μM compared to the control ($p < 0.0001$). The γH2AX intensity due to PP treatment was dose-dependent, similar to E2 treatment (1μM PP vs 5μM PP, $p < 0.0001$) **(Figure 2.1C)**. We confirmed the DNA damage with immunostaining of 53BP1, a DNA damage response factor, which localizes to the sites of DNA damage and forms ionization radiation induced foci. Similar to γH2AX intensity, we observed dose-dependent increases in 53BP1 nuclear intensity following treatment with E2 (10-100 nM) and PP (1-5μM) compared to control in both T47D and MCF-7. BP3 treatment (1-5 μM) showed increased nuclear 53BP1 intensity over control in both T47D and MCF-7, but only MCF-7 showed dose-dependent increase **(Figure 2.1D and E)**. We also observed a dose-dependent increase in nuclear γH2AX intensity in MCF-7 with treatment of E2 (10 – 100 nM), BP3 (1 – 30μM) and PP (1 – 30μM) **(Figure 2.1F)**.

The effect on γH2AX by these compounds was contrasted with the mRNA expression of estrogen-responsive gene *TFF1*. Treatment with 10nM E2 stimulated a 13.1-fold increase in expression of the estrogen-responsive gene *TFF1*, whereas responses to 5

μM BP3 or PP did not differ significantly from the control **(Figure 2.2A)**. The transcriptional responses to E2 were blocked by treatment with fulvestrant (ICI 182,780, 1 μM) demonstrating the dependence on ER. Blocking ER with fulvestrant also significantly reduced the effect of E2 on γH2AX intensity (**Figure 2.2B**, $p < 0.0001$) and inhibited γH2AX intensity in response to 5μM BP3 ($p < 0.0001$) and 5μM PP ($p < 0.0001$) suggesting that the induction of DNA damage was, in part, dependent upon ER. However, the γH2AX foci induced by E2 and BP3 was incompletely blocked by fulvestrant compared to its inhibition of *TFF1* expression.

Estrogenic response in cells treated with BP3 and PP.

Reporter assays provide a sensitive means to evaluate estrogenic activity on a minimal promoter whereas endogenous genes containing estrogen responsive elements provide physiologically relevant targets. 10nM E2 is sufficient to saturate ER responses in these assays, hence it was used as positive control that is relevant to physiologic E2 levels (2-70nM) in women **(Table 2.1)**. T47D-KBluc cells harbor an integrated ERE-luciferase reporter in which BP3 showed a lowest-observed-effect at 5μM with transactivation increasing to a maximum 37% relative transactivation activity (RTA) compared to 10nM E2 **(Figure 2.3A left)**. In contrast, PP showed 4.7% RTA at 0.5 μM and increased to 288% at 50 μM. To estimate the transactivation activity of the compounds at levels that are relevant to human exposure, we used the published urinary levels of BP3 and PP **(Table 2.1)**. At concentrations measured in the 95th percentile of pregnant women, BP3 had 27.16±6.2% and PP had 104.07±20.98% RTA (**Figure 2.3A right**, white, and black arrows respectively). Expression of endogenous ER target genes *AREG* and *PGR* were also

quantified in T47D and MCF-7 cell lines **(Figure 2.3B and C)**. Treatment of BP3 and PP at 1 µM resulted in no significant changes in mRNA expression of *AREG* and *PGR*, a concentration that led to significant increases in DNA damage in both T47D and MCF7 cells **(Figure 2.1)**. Proliferation induced by these compounds was also compared to control treatment to provide an additional measure of their bioactivity **(Figure 2.3D, Table 2.2)**. PP stimulated significant proliferation of T47D cells at 10µM but not at 1µM PP. However, BP3 had marginal effect at 5 or 50µM. Low concentrations of BP3 and PP only marginally increased cell numbers compared to control.

R-loop formation in cells treated with E2, BP3 or PP

R-loop formation was investigated as a possible mechanism of DNA damage using the S9.6 antibody to specifically detect DNA: RNA hybrids. While we observed a basal level of R-loop foci in the vehicle-treated control in T47D cells, nuclear S9.6 foci were significantly increased with 5µM of BP3 or PP treatment and comparable to responses with 10nM E2. Addition of RNase H to the cells treated with 5µM BP3 or PP or 10nM E2 abolished the S9.6 intensities, confirming the specificity of S9.6 nuclear staining **(Figure 2.4A and B)**. Similarly, increased of R-loops formation was obtained with 10nM E2, 5µM BP3 or 5µM PP treatment of MCF-7 cells which was abrogated following RNase H addition post-fixation **(Figure 2.4C)**.

R-loop formation in normal breast epithelial cell line treated with E2, BP3 or PP

Next, we asked if R-loops form in normal breast epithelial cells in response to exposures of BP3 and PP. The 76N-Tert cells do not express endogenous *ESR1* providing a null background to test ERα-stimulated R-loops. The cells were stably infected with an inducible human *ESR1* (pINDUCER-*ESR1*, **Figure 2.5A**). ERα expression in 76N-Tert-*ESR1* was confirmed with western blot **(Figure 2.5B)**. MCF-7 cell lysate was used as a positive control. Immunofluorescence showed 90% of the 76N-Tert-*ESR1* cell population were GFP+ (ERα expressing) **(Figure 2.5B)**.

In the parental 76N-Tert cell line, which does not express ERα, treatment with 10nM E2, 5μM BP3 or 5μM PP showed low nuclear S9.6 staining. After induction of ERα with doxycycline, 5μM BP3 or PP increased number of nuclear S9.6 foci significantly over vehicle-treated control and comparable to 10nM E2 treatment. RNase H treatment reduced nuclear S9.6 foci in 10nM E2 treated as well as 5 μM BP3 or PP treated 76N-Tert-*ESR1* cell line induced with doxycycline ($p<0.0001$, **Figure 2.5C & D**).

Evaluation of R-loop formation and DNA damage in mice treated with E2, BP3 or PP

To evaluate the relevance of exposure to xenoestrogens *in vivo*, we treated ovariectomized BALB/c mice orally with E2 (250μg/kg/day), BP3 (3,000 μg/kg/day) or PP (10,000 μg/kg/day) for 4 days **(Figure 2.6A)**. These doses were used in experiments evaluating effects of chronic exposures on mammary gland development (LaPlante et al., 2018). We observed 3.8-fold higher nuclear S9.6 staining in the mammary epithelium of E2 treated animals over control treated animals. Exposure to BP3 also induced 2.5-fold

higher nuclear S9.6 staining in the mammary epithelial cells whereas PP induced 3.8-fold higher compared to control-treated animals (**Figure 2.6B & C**). Nuclear γH2AX intensity in the mammary gland of E2 and BP3 treated animals was significantly higher than animals treated with vehicle control **(Figure 2.6D)**. While oral treatment of E2 stimulated proliferation as shown by higher Ki-67 straining and transcriptional activation of ER-target genes (*Areg* and *Pgr*) in the mammary gland, neither BP3 nor PP elicited significant responses **(Figure 2.6 E-H)**. Similarly, elevated serum levels of 17β-estradiol and uterine weight was only observed in E2 treated mice **(Figure 2.6I)**.

DISCUSSION

Exposure of xenoestrogens was implicated in breast cancer risk (Pastor-Barriuso et al. 2016) as well as resistance to breast cancer treatment (Goodson et al. 2011; Warth et al. 2018) due to their endocrine actions. The median urinary level of BP3 was 0.137µM and PP was 0.161µM in non-pregnant women in participating in the NHANES by CDC (Calafat et al. 2010; Woodruff et al. 2011). The serum levels of BP3 were reported to be approximately 0.87µM (200 µg/L) following exposure in women (Janjua et al. 2004; Matta et al. 2019; Tarazona et al. 2013). In addition, the urinary concentrations of xenoestrogens observed in pregnant women was higher than the general population with median urinary concentrations of BP3 and PP being 0.47µM and 0.253 µM, respectively and the 95th percentile concentrations in pregnant women being 29.5µM BP3 and 3.26µM PP **(Table 2.1)**. This raises the possibility that women may have higher exposure during pregnancy due to use of creams and lotions or that absorption and metabolism may be altered in pregnancy. These compounds were also found in normal tissues of women undergoing mastectomy for primary breast cancer (Barr et al. 2012; Barr et al. 2018) and in milk collected during the period of sunscreen use from 3 different cohorts of mothers of singleton child (Schlumpf et al. 2010). However, based on measures of transcriptional activity in MCF7 human breast cancer cell lines (Byford et al. 2002; Kerdivel et al. 2013), typical exposures to BP3 and PP would appear to pose a minimal risk for breast cancer through ER mediated transcriptional activation of target genes.

Estrogens and their metabolites have been shown to induce direct DNA damage. However, DNA damage by catechol estrogens from ER-negative cell lines requires concentrations that are 100-fold greater than the average circulating concentrations in

women (Cavalieri and Rogan 2016; Savage et al. 2014; Xu et al. 2007). BP3 and PP were shown to have the potential to cause DNA damage independent of ER transactivation, based on experiments on ER-negative cell lines. For example, treatment of BP3 (10 μM) induced γH2AX foci in normal human keratin cell lines (Kim et al. 2018) and PP (50 μM) showed 8-hydroxy-2-deoxyguanosine (8-OHdG) release in Vero cells (derived from Monkey kidney) (Martín et al. 2010). However, these levels exceeded typical concentrations measured in human populations **(Table 2.1)**.

In the breast, epithelial cells with functional ERα, we observed DNA damage at physiologic concentrations of E2. BP3 and PP also caused DNA damage at low concentrations (1-5μM) **(Figure 2.1)**. Both the nuclear γH2AX and 53BP1 foci were diminished by fulvestrant suggesting ERα dependency of DNA damage. At these low concentrations (1μM of PP and 1-5μM of BP3), we did not observe ER-mediated transcriptional response in target genes. Instead, we observed R-loop formation. We also observed increases in R-loops and γH2AX in the mammary epithelial cells of ovariectomized BALB/c mice orally treated with BP3 or PP at doses designed to model environmental exposures in humans **(Figure 2.6D)**. The doses of BP3 and PP used in mice were not sufficient to affect transcription of *Areg* or *Pgr* **(Figure 2.6E-F)** or proliferation of mammary epithelium **(Figure 2.6G-H)** compared to control treatments. Nor were they sufficient to alter uterine weights compared to the control treatment in ovariectomized mice **(Figure 2.6J)**. This finding for BP3 was supported by a previous study (LaPlante et al. 2018). These results with BP3 and PP are consistent with the idea that in mammary epithelial cells of human and mice the formation of R-loops and DNA damage is ER-dependent but is separable from gene transcription and proliferative responses.

ER-mediated DNA double strand breaks was shown to form by collision of R-loop formed during active transcription (co-transcriptional R-loop) and replication fork in MCF7 cells (Stork et al. 2016). Alternatively, R-loop formation can occur with RNA Polymerase II pausing which results in no increase of gene expression but leads to DNA damage (Hatchi et al. 2015; Shivji et al. 2018; Zhang et al. 2017). Indeed, our results showed that, BP3 and PP induced formation of R-loops and DNA damage (Figure 1.7) but did not lead to detectable increases in full-length transcripts of *TFF1*, *AREG* or *PGR*.

Experiment performed using a normal breast epithelial cell line 76N-Tert expressing inducible ERα treated with E2, BP3 and PP provided: 1) additional evidence that the R-loop formation and DNA damage were ERα-dependent and 2) that normal breast epithelial cells were susceptible to DNA damage by xenoestrogens. This raises the possibility that a subset of women bearing variants of R-loop processing factors may be particularly susceptible to the genotoxic effects of xenoestrogens such as BP3 and PP. More than 300 R-loop binding proteins have been identified (Wang et al. 2018). A number of such factors were recently shown to be involved in the resolution of R-loops to limit DNA damage including TopI (Tuduri et al. 2009), BRCA1(Hatchi et al. 2015), BRCA2 (Shivji et al. 2018), SETX (Cohen et al. 2018; Hatchi et al. 2015), Aquaris (Sollier et al. 2014), THO/THREX complex (Bhatia et al. 2014; Gómez-González et al. 2011), BuGZ, Bub (Wan et al. 2015). For example, recruitment of BRCA1/SETX was important for R-loop mediated transcriptional termination. As a consequence, the mutational rate of termination regions where BRCA/SETX co-localize was higher in BRCA1-deficient tumors compared to BRCA1-WT tumors (Hatchi et al. 2015). Premalignant breast lesions such as atypical hyperplasia expressed higher levels of ERα (Gregory et al. 2019), and

thus, may be especially sensitive to the genotoxic effects of these xenoestrogens. Therefore, limiting exposure to personal care products and foods containing these chemicals may be valuable for this subset of women.

However, the present studies do not show a direct risk of exposure to these compounds on subsequent breast cancer. While chronic exposure to low levels of DNA damage has the potential to induce mutations that either initiate or promote carcinogenesis, the experiments were not designed demonstrate a causal effect of BP3 or PP on mammary tumors or breast carcinogenesis. The DNA damage observed was associated with the formation of ERα-dependent R-loops, but it is unclear whether ERβ also contributes to the formation of R-loops or may mitigate this. While many tissues express ERs, they vary in the levels of ERα and ERβ as well as expression of DNA repair factors and proficiency of resolving R-loops. Therefore, this mechanism of DNA damage may be limited to the breast epithelium of a subset of individuals. It is also unclear how combinations of environmental xenoestrogens may interact to augment or dissipate the genotoxicity through competing actions on ER. Nonetheless, the data presented here reveal a need to consider the unique potential for genotoxicity of environmental xenoestrogens in tissues expressing ERs.

These studies demonstrated that xenoestrogens possessed the potential for genotoxic activity that was mediated by ERα through the formation of R-loops and DNA double strand breaks. These genotoxic effects were observed at concentrations well below those necessary for detectable transcriptional activation. Therefore, R-loop forming capacity provides a valuable endpoint to consider when evaluating the safety and activity of environmental chemicals. The inducible expression of ERα in normal breast cells provides a tool with which to quantify the variation in sensitivity to these compounds

among individuals and to determine if a subset of individuals is preferentially susceptible to the genotoxic activities.

.

Table 2.1: Estimation of estrogen and xenoestrogens concentrations of estradiol(E2), benzophenone-3(BP-3), or propyl paraben (PP) in urine/blood samples of women and female mice.

Ligand	Median (μM)	90th or 95th percentile (μM)	Relative transactivation activity at 90th or 95th percentile (% RTA vs. E_2)	References
BP-3 (urine)				
Non-Pregnant	0.137	6.70[b]	18.91 ± 6.62%	Woodruff et al. 2011
Pregnant	0.47	29.5[b]	27.16 ± 6.2%	Philippat et al. 2013
PP (urine)				
Non-Pregnant	0.161	1.98[b]	64.27 ± 20.5%	Calafat et al. 2010
Pregnant	0.253	3.26[b]	104.07 ± 20.98%	Philippat et al. 2013
E_2 (blood)				
Human				
Ovulatory	0.0003–0.0018			Clarke et al. 1997
Luteal	0.0002–0.0008			O'Leary et al. 1991
Pregnant	0.074	0.118[a]		Schock et al. 2016
Mouse	<0.0003			Majewski et al. 2018

[a]90th percentile of exposure in the given population.
[b]95th percentile of exposure in the given population.

Table 2.2: Slopes of growth curve effect of Estradiol (E2), Benzophenone-3 (BP3), or Propylparaben (PP) on T47D cells.

Growth Curve	Slope	95% CI
Control DMSO	0.0107	-0.006811 to 0.02821
0.5nM E2	0.08495	0.06604 to 0.1039
1μM PP	0.01856	0.003943 to 0.03318
10 μM PP	0.06387	0.05225 to 0.07550
5μM BP3	0.0202	0.008131 to 0.03226
50μM BP3	0.01581	0.0009721 to 0.03064

Table 2.3: Sequences of primers.

Target	Sequence (5′ to 3′)
qPCR Primers	
TFF1 (human)	F: CCCCTGGTGCTTCTATCCTAA
	R: GATCCCTGCAGAAGTGTCTAAAA
AREG (human)	F: CGGAGAATGCAAATATATAGAGCAC
	R: CACCGAAATATTCTTGCTGACA
PGR (human)	F: TTTAAGAGGGCAATGGAAGG
	R: CGGATTTTATCAACGATGCAG
Pgr (mouse)	F: GACCACATCAGGCTCAATGCT
	R: GGTGGGCCTTCCTAACGAG
Areg (mouse)	F: GTCACTATCTTTGTCTCTGCCA
	R: CCTCCTTCTTTCTTCTGTTTCTCC

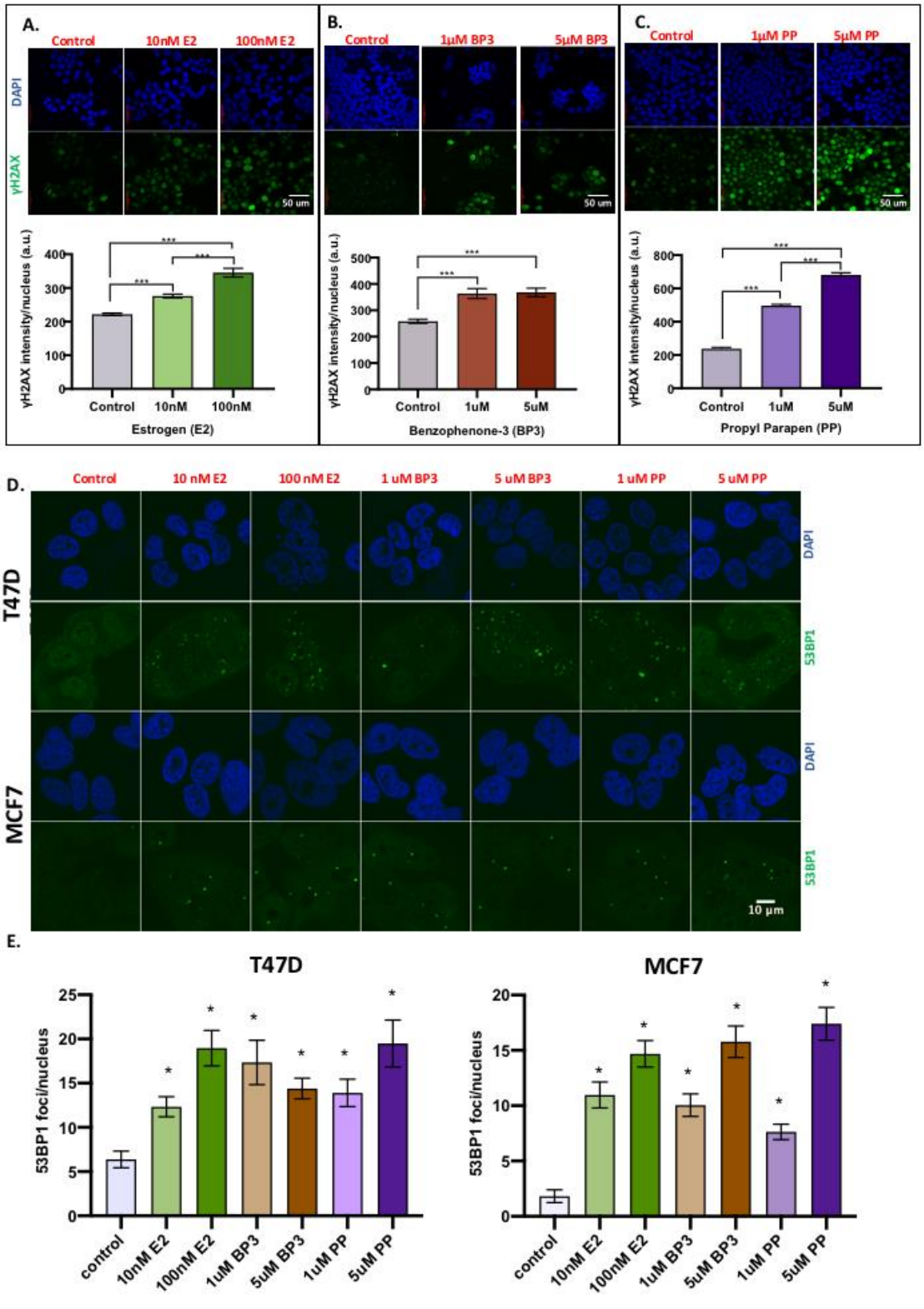
A.
Control
10nM E2
100nM E2
DAPI
γH2AX
50 um
γH2AX intensity/nucleus (a.u.)
Control
10nM
100nM
Estrogen (E2)
B.
Control
1μM BP3
5μM BP3
50 um
γH2AX intensity/nucleus (a.u.)
Control
1uM
5uM
Benzophenone-3 (BP3)
C.
Control
1μM PP
5μM PP
50 um
γH2AX intensity/nucleus (a.u.)
Control
1uM
5uM
Propyl Parapen (PP)
D.
Control
10 nM E2
100 nM E2
1 uM BP3
5 uM BP3
1 uM PP
5 uM PP
T47D
MCF7
DAPI
53BP1
10 μm
E.
T47D
MCF7
53BP1 foci/nucleus
control
10nM E2
100nM E2
1uM BP3
5uM BP3
1uM PP
5uM PP

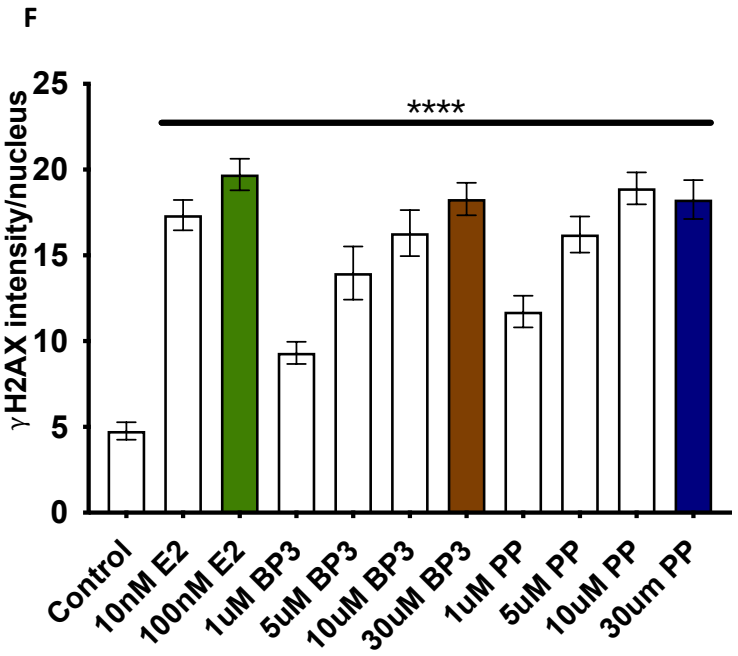

Figure 2.1. Evaluation of DNA damage in cells treated with 17β-Estradiol (E2), Benzophenone-3 (BP3), or Propylparaben (PP) for 24 hours.
Immunofluorescence (upper panel) and quantification (lower panel) of nuclear γH2AX intensity in T47D cells treated with (**A**) 10 or 100nM E2 (**B**) 1 or 5μM BP3 and (**C**) 1 or 5μM PP. (**D**). Immunofluorescence of 53BP1 staining with 10 or 100nM E2, 1 or 5μM BP3 and 1 or 5μM PP in T47D (upper panel) and MCF-7 (lower panel). (**E**) Quantification of nuclear 53BP1 of treatments in **(D)** in T47D (left panel) and MCF-7 (right panel). **(F)** Quantification of nuclear γH2AX intensity in MCF-7 cells following 17β-estradiol (E2) 10-100nM, Benzophenone-3 (BP3) 1-30μM or Propylparaben (PP) 1-30μM treatment. ***$p < 0.0001$, *$p < 0.01$ compared control with treatments using one-way analysis of variance (ANOVA) followed by Tukey's honestly significant difference (HSD) multiple-range test. n = 3 biological replicates. Scale bar = 50 μM (**A-C**), 10 μM (**D**). All graphs show mean ± SEM. *Data collection in collaboration with Prabin. D. Majhi.*

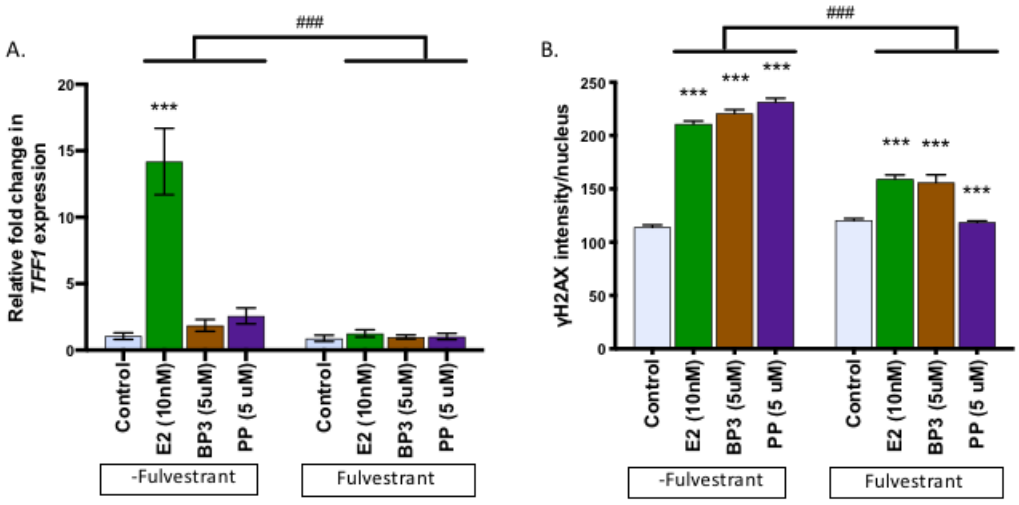

Figure 2.2. *TFF1* expression and γ-H2AX intensity in T47D cells treated with 17β-estradiol (E2), benzophenone-3 (BP-3), or propylparaben (PP) for 24h with or without the ER antagonist fulvestrant.

(A) Inhibition of *TFF1* expression following treatment of 10 nM E2, 5μM BP-3, and 5μM PP when cotreated with fulvestrant (ICI 182 780, 1μM) compared with 10 nM E2, 5μM BP-3, and 5μM PP treatments without fulvestrant. **(B)** Quantification of nuclear γ-H2AX following cotreatment of fulvestrant (1μM) with E2 (10 nM), BP-3 (5μM), or PP (5μM) compared with E2 (10 nM), BP-3 (5μM), or PP (5μM) without fulvestrant treatment, respectively. ***p<0.0001 compared control to xenoestrogens treatment and $^{###}$p<0.001 compared with negative fulvestrant and with positive fulvestrant using multiple comparison for 2-way ANOVA. n=3 biological replicates. All graphs show mean ± SEM. *Data collection in collaboration with Prabin. D. Majhi*.

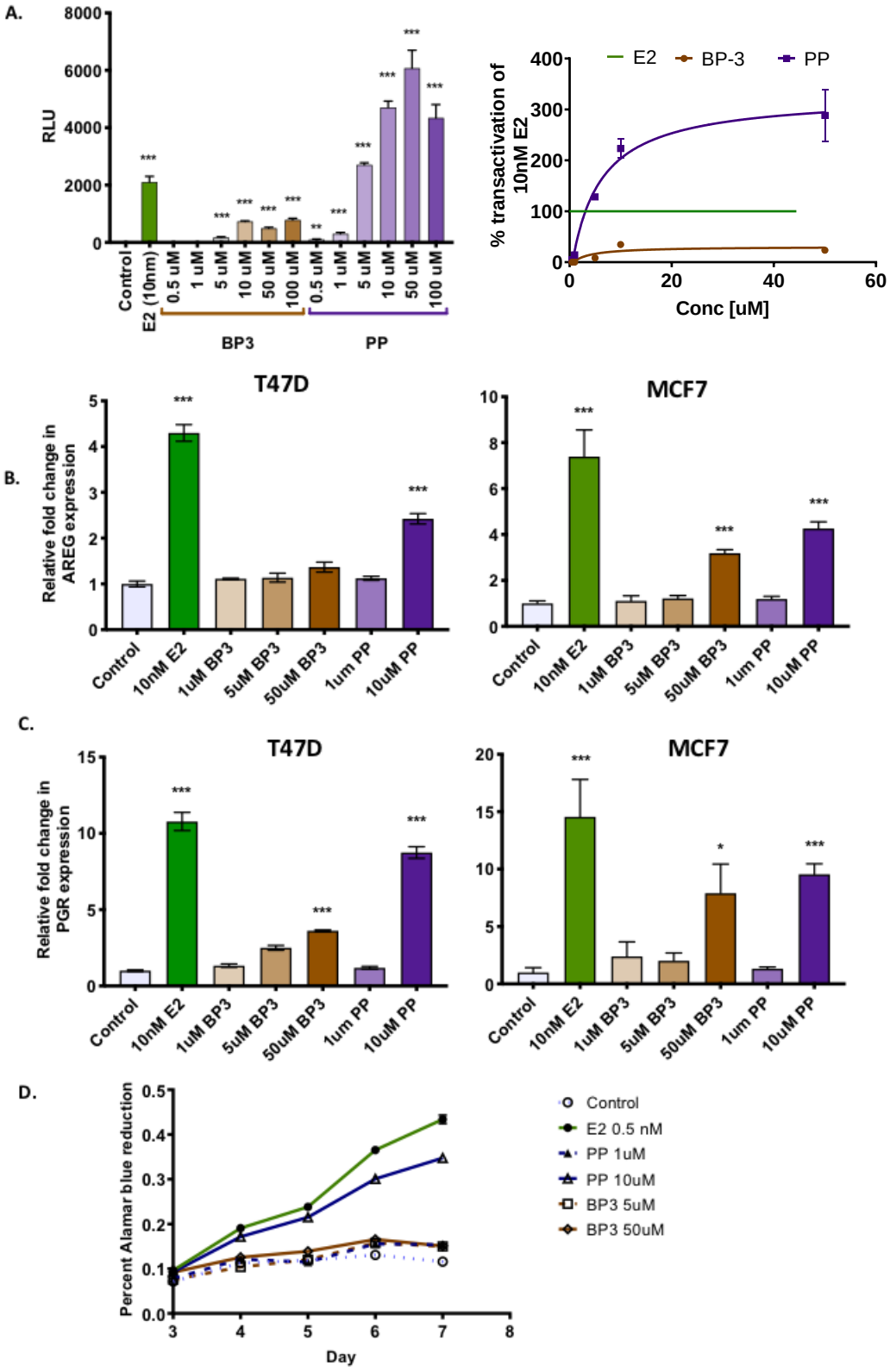

Figure 2.3. Evaluation of estrogen receptor transactivation and proliferation in cells treated with 17β-estradiol (E2), benzophenone-3 (BP-3), or propylparaben (PP) for 24h.

(A) (Left) Transactivation response (in relative light unit, RLU) of T47D-KBluc cells in response to 10nM E2 (green), 0.5–100μM BP-3 (brown), and 0.5–100μM PP (violet) treatment. (Right) Dose-response curve of luciferase reporter assay in T47D-KBluc cells treated with 17β-estradiol (E2) 10-100nM, Benzophenone-3 (BP3) 1-30μM or Propylparaben (PP) 1-30μM treatment. Dose-response curves were plotted using three-parameter dose response curve. Error bars represent standard deviation (SD). n = 3 biological replicates. The arrows represent the levels of 95%ile exposure in pregnant women i.e., BP3 (white arrow; 29.5 μM) PP (Black, 3.26 μM). Expression of endogenous genes AREG **(B)** and PGR **(C)** with E2 (10 nM), BP-3 (1 or 5μM), or PP (1 or 10μM) treatment as relative fold change over control in T47D (left panel) and MCF-7 (right panel). *p<0.05 and ***p<0.0001 compared control with treatments using one-way analysis of variance (ANOVA) followed by Tukey's honestly significant difference (HSD) multiple-range test. n=3 biological replicates. **(D)** Proliferation of 47D cell as percent of Alamar Blue reduction in response to E2 (0.5nM), PP (1 or 10μM), BP-3 (5μM), or control. The confidence intervals of the slope are reported in Table 2. All graphs show mean ± SEM.
Data collection in collaboration with Prabin. D. Majhi, Amy L. Roberts and Karen A. Dunphy.

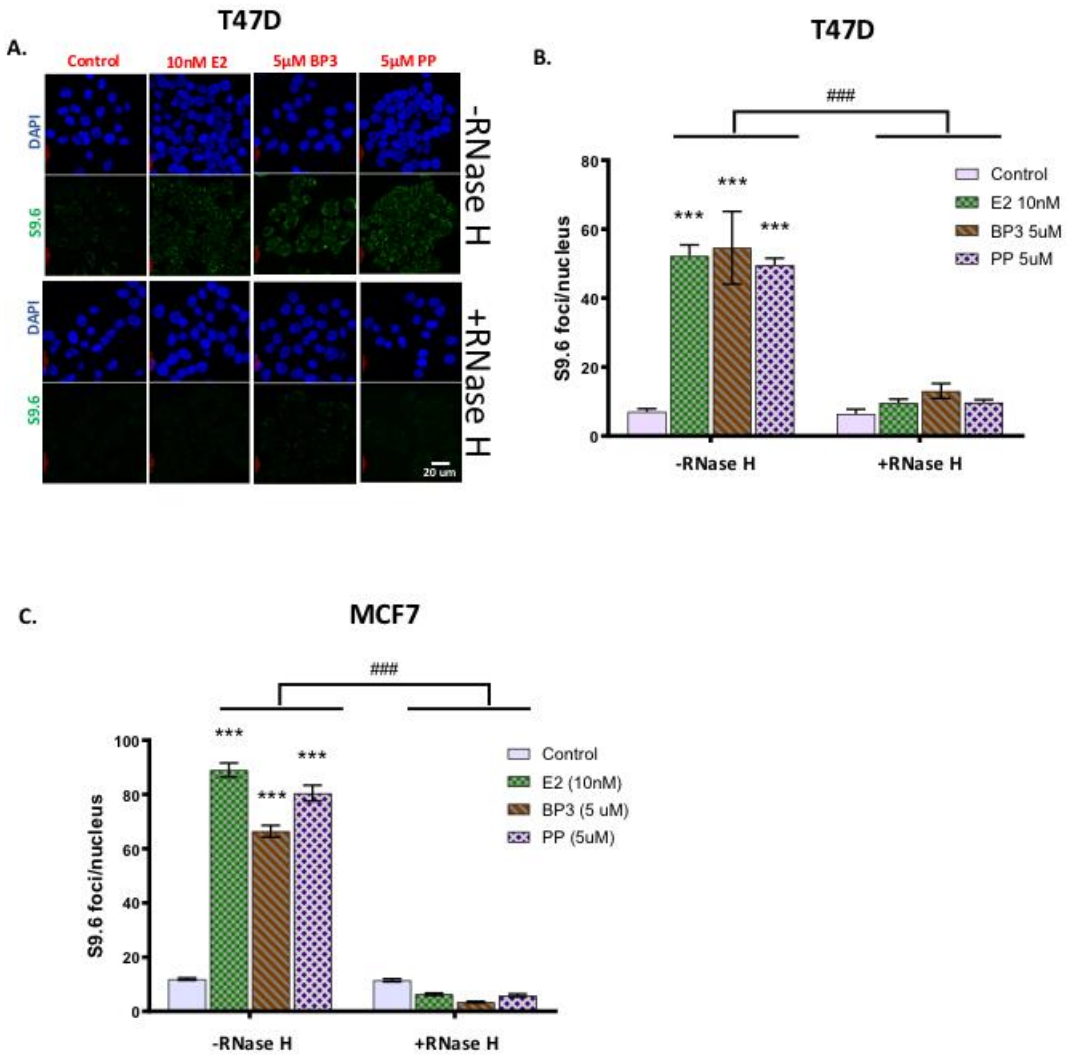

Figure 2.4. R-loop formation in T47D and MCF7 cells treated with 17β-estradiol (E2), benzophenone-3 (BP-3), or propylparaben (PP) or vehicle with or without RNase H. **(A)** Immunostaining of R-loop with S9.6 antibody and DAPI in T47D cells treated with E2 (10nM), BP-3 (5μM) or PP (5μM) without and with RNase H treatment following fixation. Scale bar=20μM. **(B)** Quantification of the nuclear S9.6 intensity in T47D. **(C)** Quantification of nuclear S9.6 intensity in MCF-7. ***p<0.0001 compared control with xenoestrogens treatment and $^{###}$p<0.001 compared negative RNase H and with positive RNase H using multiple comparison for 2-way ANOVA. n=3 biological replicates. All graphs show mean ± SEM. *Data collection in collaboration with Prabin. D. Majhi.*

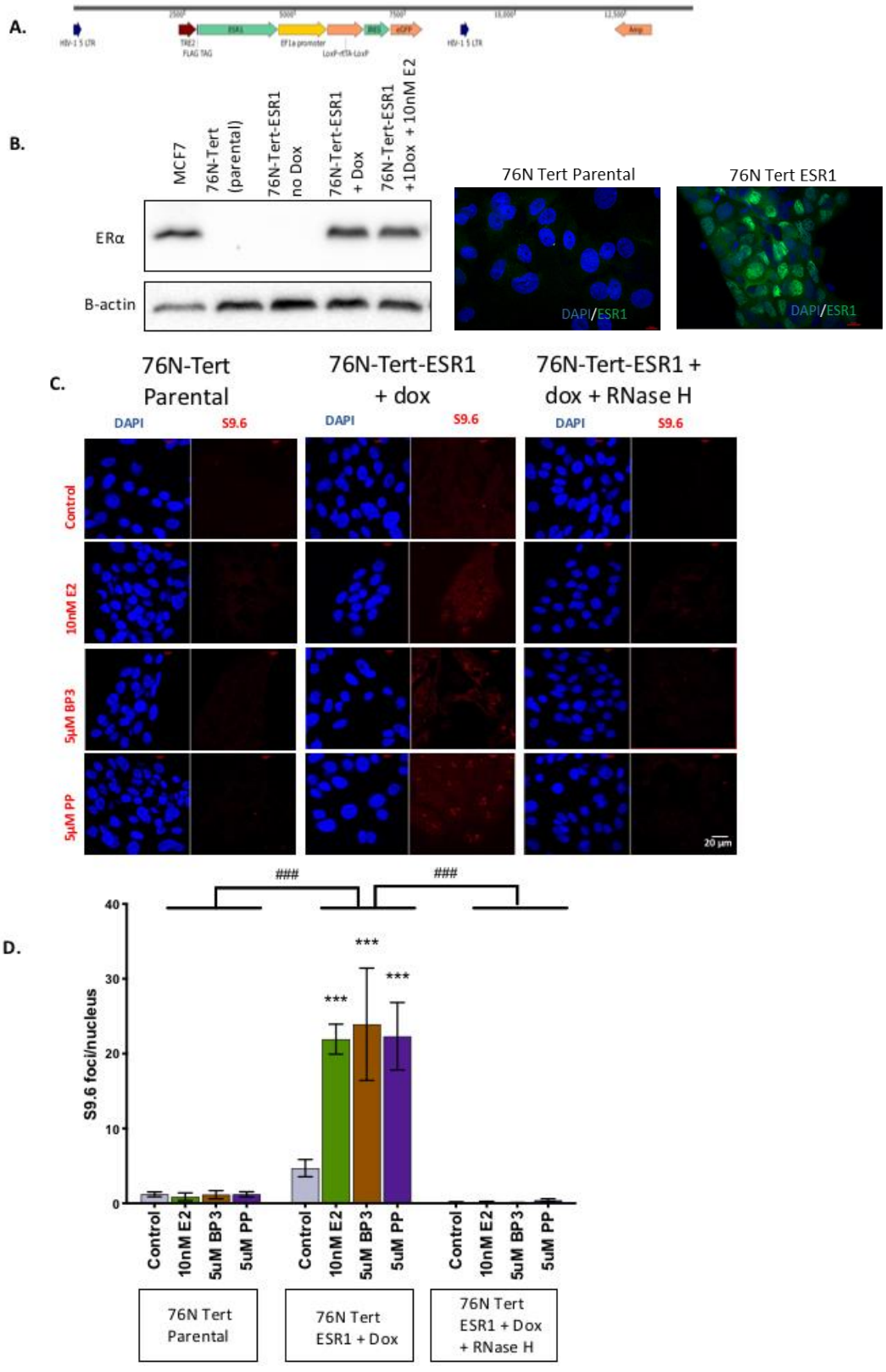
A.
B.
MCF7
76N-Tert (parental)
76N-Tert-ESR1 no Dox
76N-Tert-ESR1 + Dox
76N-Tert-ESR1 +1Dox + 10nM E2
ERα
B-actin
76N Tert Parental
76N Tert ESR1
DAPI/ESR1
C.
76N-Tert Parental
76N-Tert-ESR1 + dox
76N-Tert-ESR1 + dox + RNase H
DAPI
S9.6
Control
10nM E2
5μM BP3
5μM PP
20 μm
D.
S9.6 foci/nucleus
###
***
Control
10nM E2
5uM BP3
5uM PP
76N Tert Parental
76N Tert ESR1 + Dox
76N Tert ESR1 + Dox + RNase H

Figure 2.5. Characterization of 76N-Tert-*ESR1* and R-loop formation in 76N-Tert-*ESR1* following treatment with 17β-estradiol (E2), benzophenone-3 (BP-3) or propylparaben (PP) with and without RNase H.

(A) Map of pIN-ESR1 construct *ESR1* insertion next to doxycycline(dox) inducible TRE2 promoter. **(B) (Left)** Western blot ERα (upper panel) with MCF-7 as positive control (lane 1), 76N-Tert parental (lane 2), 76N-Tert-*ESR1* without dox (lane 3), 76N-Tert-*ESR1* with dox (lane 4), and 76N-Tert-*ESR1* with dox and E2 (10nM) treatment and β-actin as loading control (lower panel). **(Right)** Immunofluorescence with anti- ERα (green) and DAPI (blue) showing ERα expression in > 90% of the 76N- Tert-*ESR1* cell population. Scale bar = 10 μM **(C)** Immunostaining with S9.6 antibody and DAPI with 10nM E2, 5μM BP-3, or 5μM PP treatment to parental 76N-Tert cells (upper panel), to 76N-Tert-ESR1 with dox induction (middle panel) without or with RNase H treatment (lower panel). Scale bar=20μM. **(D)** Quantification of nuclear S9.6 intensity in **(C)**. ***$p<0.0001$ compared control with xenoestrogens treatment and $^{###}p<0.001$ compared among 76N-Tert Parental, 76N-Tert with dox and E2 (10nM) negative RNase H and 76N-Tert with dox and E2 (10 nM) positive RNase H using multiple comparison for 2-way ANOVA. n=3 biological replicates. All graphs show mean ± SEM. *Data collection in collaboration with Amy Black and Prabin D. Majhi.*

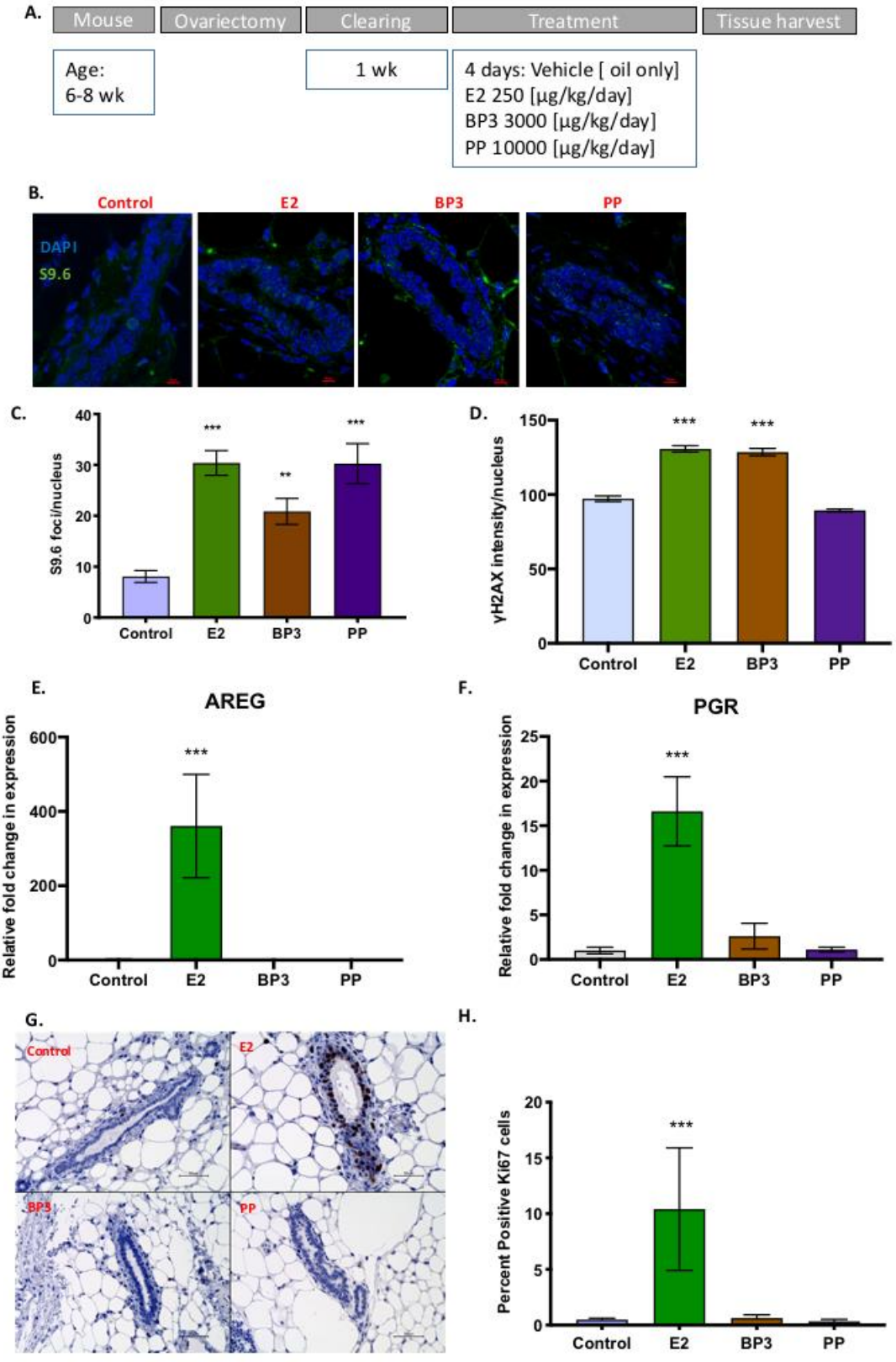
A.
Mouse
Ovariectomy
Clearing
Treatment
Tissue harvest
Age:
6-8 wk
1 wk
4 days: Vehicle [oil only]
E2 250 [µg/kg/day]
BP3 3000 [µg/kg/day]
PP 10000 [µg/kg/day]
B.
Control
E2
BP3
PP
DAPI
S9.6
C.
S9.6 foci/nucleus
Control
E2
BP3
PP
D.
γH2AX intensity/nucleus
E.
AREG
Relative fold change in expression
F.
PGR
G.
H.
Percent Positive Ki67 cells

I

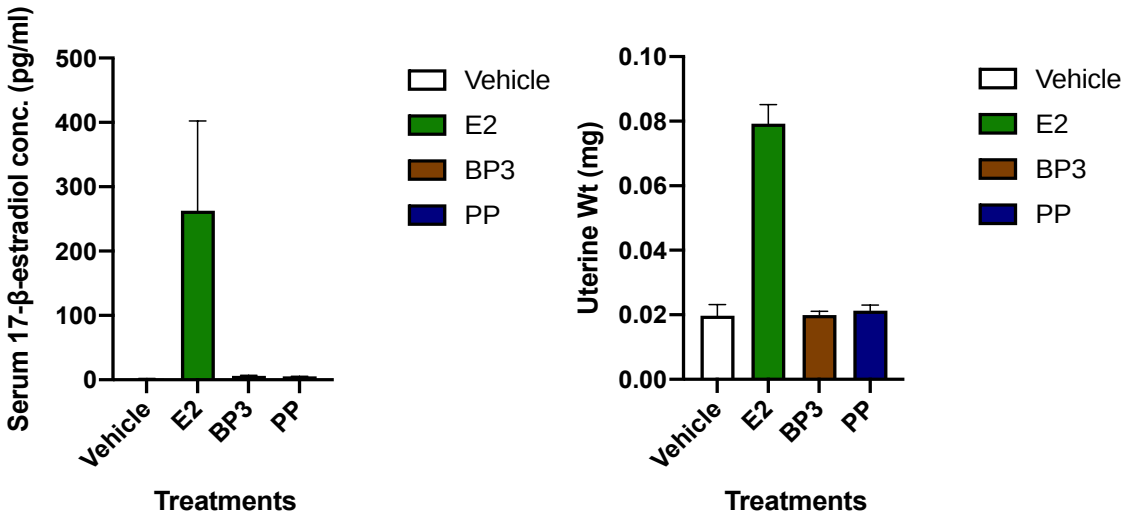

Figure 2.6. Acute exposure of xenoestrogens in mice.
(A) Schematic of experimental design and exposure period. **(B)** Immunostaining of mouse mammary epithelium with S9.6 antibody harvested from mice treated with E2, BP-3, or PP. Each image shows a ductal structure with luminal and myo-epithelial cell nucleus (blue) and R-loop (green) inside the nucleus. Scale bar =10μM. Quantification of the immunostaining data for S9.6 **(C)** and γ-H2AX **(D).** Expression of *Areg* **(E)** and *Pgr* **(F)** from mouse mammary gland. n=3 biological replicates. **(H).** Ki67 straining of luminal epithelial cells **(G)** and percent of Ki67 strained cells per luminal cells counted. **(I)** Serum 17-β-estradiol (E2) levels **(A)** and uterine weight **(B)** from mice treated with E2 (250μg/ml), Benzophenone-3 (BP3, 3000μg/ml) or Propylparaben (PP, 10000 μg/ml) treatment. Scale bar=50μM [Number of biological replicates (*n*): control (5), E2 (8), BP-3 (12), PP (10)] ***p<0.0001, **p<0.01 compared control with treatments using one-way analysis of variance (ANOVA) followed by Tukey's honestly significant difference (HSD) multiple-range test. All graphs show mean ± SEM. *Data collection in collaboration with Aliza R. Majewski and Lynn M. Chuong.*

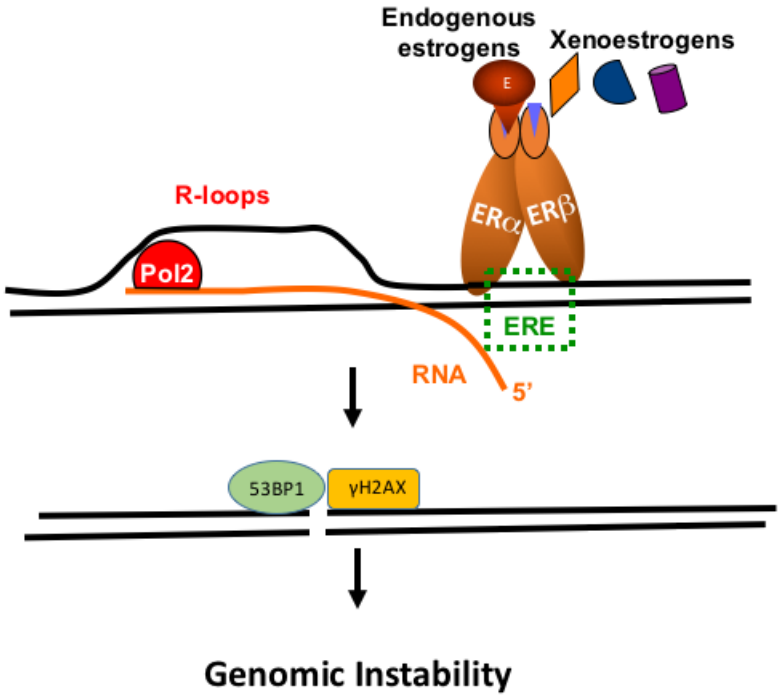

Figure 2.7. A schematic model for ER-dependent DNA damage.
E2 or xenoestrogens binding to the ER recruit ER to the estrogen response element (ERE) in the promoter and forms R-loop. Persistence of R-loop in the promoter introduces DNA damage.

CHAPTER -3

Estrogen mediated DNA damage in the mammary epithelium differs among strains of rodents and among women.

Introduction

Estrogens play a central role in mammary gland development by promoting epithelial cell proliferation and ductal elongation during puberty (Manavathi et al., 2013; Vrtačnik et al., 2014). However, longer lifetime exposure to estrogens due to early menarche and late menopause are associated with increased breast cancer risk (Clemons and Goss, 2001; Dall and Britt, 2017). Women with estradiol levels in the highest quartile had 2.1-fold higher relative risk compared to the lowest quartile (Eliassen et al., 2006). This carcinogenic effect of estrogen may, in part, be due to reactive metabolites that cause depurination or form stable DNA adducts. But the concentrations of estrogens that induce these effects in vitro exceed the levels typically found in women (Cavalieri and Rogan, 2016; Okoh et al., 2011; Santen et al., 2009). This mechanism does not account for the preferential risk of breast cancer as cells in all tissues would be similarly vulnerable to the direct mutagenic consequences of these adducts. The breast epithelial cells expressing estrogen receptor alpha (ERα) appear to be particularly susceptible as approximately 70% of breast cancer cases are positive for ERα (Waks and Winer, 2019). This is a striking enrichment as only 5-10% of normal breast epithelial cells are ERα-positive (Clarke et al., 1997). Blockade of ERα activation through selective estrogen receptor modulators reduced

the breast cancer incidence by 50% – 75% in women (Cummings et al., 1999; Cuzick et al., 2013; Martino et al., 2004). Therefore, the ERα+ breast epithelial cells appear to be vulnerable to pathogenic actions of estrogens.

Estrogen receptors have been shown to be involved in mutagenic actions caused by exposure to estrogens. Two nuclear estrogen receptors, estrogen receptor alpha (ERα) and estrogen receptor beta (ERβ), contribute to the intracellular responses to estrogens. The ligand-bound estrogen receptor complex can form homodimers or heterodimers that bind estrogen response elements (ERE) in the DNA forming complexes with other transcriptional coregulatory factors to drive expression of estrogen target genes (Marino et al., 2006; Saville et al., 2000; Yaşar et al., 2017; Yi et al., 2017). The genes encoding the progesterone receptor (*PGR*) and amphiregulin (*AREG*) growth factor have EREs that have been well-characterized (Ciarloni et al., 2007; Lin et al., 2007; Manavathi et al., 2013; Palaniappan et al., 2019). ERα is a primary effector of estrogen actions in mammary tissue and has been shown to participate in DNA damage by several mechanisms. First, ERα is necessary for the proliferation of the breast epithelium which can also cause replication-associated DNA damage (Henderson and Feigelson, 2000; Preston-Martin et al., 1990). Second, ERα has been shown to recruit Topoisomerase-2β, stimulating DNA double-strand breaks which facilitate transcription of ER target genes (Ju et al., 2006; Williamson and Lees-Miller, 2011). A third mechanism observed in breast cancer cell lines showed that ERα induces expression of APOBEC3B which causes cytidine deamination leading to DNA damage (Periyasamy et al., 2015; Udquim et al., 2020). Recently, 17β-estradiol (E2) and endocrine-disrupting chemicals were shown to induce DNA damage by

promoting ERα-mediated co-transcriptional structures called R loops (Majhi et al., 2020; Stork et al., 2016). R loops are formed when the nascent RNA hybridizes with the template DNA strand causing transient displacement of the non-template strand. R loops are a normal consequence of transcription, but if they persist due to either the genomic context or a lack of resolvases, the single-stranded non-template strand can cause DNA damage responses that result in DNA double-strand breaks (Aguilera and García-Muse, 2012a; Skourti-Stathaki and Proudfoot, 2014; Sollier and Cimprich, 2015). These ERα-mediated DNA damage mechanisms would result in preferential mutagenesis of the ERα+ luminal breast epithelial cells and contribute to carcinogenesis.

While all women are exposed to endogenous and exogenous estrogens, only 1 in 8 women is expected to develop breast cancer suggesting that the cancer-promoting effects of estrogen exposure vary among individuals. Genome-wide association studies have identified >180 alleles that modify the risk of breast cancer (Ahmed et al., 2009; Easton et al., 2007; Hunter et al., 2007; Stacey et al., 2007; Wendt and Margolin, 2019). Polymorphisms in ERα have been identified that contribute to inherited breast cancer risk (Hu et al., 2017; Lipphardt et al., 2013; Yu et al., 2011). However, differences in environmental and lifestyle factors account for nearly 70% of breast cancer risk (Möller et al., 2016; Mucci et al., 2016). Therefore, interactions between inherited risk alleles and environmental exposure to estrogenic chemicals may play a significant role in the development of breast cancer but have remained elusive due to the challenges in measuring environmental exposures across a woman's lifetime and limitations in statistical power to detect effects (Rudolph et al., 2016).

Studies in rodents provide a powerful alternative approach for understanding the combined effects of estrogen exposure and heritable differences in sensitivity to environmental exposures(Jerry et al., 2018). BALB/c and C57BL/6 strains of mice differ in their responses to E2 and progesterone (P4) (Aupperlee et al., 2008). Hormone-induced mammary tumors have been shown to develop in BALB/c mice whereas C57BL/6 mice are resistant (Girard et al., 2007; Kordon et al., 1993; Lanari et al., 1986; Molinolo et al., 1987). BALB/c mice are also sensitive to radiation-induced mammary tumors when compared with C57BL/6 mice (Ponnaiya et al., 1997; Ullrich et al., 1996). BALB/c mice with heterozygous mutations in the p53 tumor suppressor gene (*Trp53*) develop spontaneous mammary tumors similar to the susceptibility to breast cancer among women with inherited mutations in *TP53*. In contrast, mammary tumors in C57BL/6-*Trp53*+/- mice are rare (Kuperwasser et al., 2000). This difference in susceptibility to mammary tumors was genetically linked to a locus on mouse chromosome 7 (Blackburn et al., 2007) and involves a greater reliance on repair DSBs in BALB/c-*Trp53*$^{+/-}$ mice through error-prone repair pathways (Böhringer et al., 2013). Therefore, hormonal exposures and mechanisms affecting proficiency of DNA repair play important roles in determining risk of mammary tumorigenesis.

Rats also exhibit striking differences in susceptibility to mammary tumors. The Brown Norway (BN) strain is resistant to estrogen-induced mammary tumors while the August Copenhagen Irish (ACI) strain is susceptible. Genetic loci that modify susceptibility to E2 have been mapped in crosses between the ACI and BN strains rats (Shull et al., 2018). Using comparative genomic hybridization (CGH), the tumors in ACI were found to have recurrent chromosomal aberrations (Adamovic et al., 2007) suggesting

that differences in the fidelity of DNA repair may contribute to susceptibility to mammary tumors in ACI rats.

The goal of our study was to investigate the effects of genetic background on E2-mediated DNA damage, R loop formation, and transcriptional responses in the mammary epithelium of rodents. DNA damage and R loops were significantly higher in BALB/c mice compared to C57BL/6 mice in response to acute treatment with E2 for 4 days or chronic exposure for 28 days. Accumulation of γH2AX foci were most pronounced in the ERα+ cells of BALB/c mice. Higher doses of E2 (0.25 vs 0.75mg/kg/d) stimulated greater proliferation in both strains, but levels of γH2AX were increased in only the BALB/c mice. The differences in DNA damage and R loops between strains were not associated with differences in levels of ERα. Elevated levels of γH2AX were also observed in the mammary epithelium of ACI rats following E2 treatment, but not in the BN strain. Breast tissue explant cultures from women also exhibited striking variation in levels of E2-induced DNA damage in the epithelial cells. In breast explant cultures from donors with inherited breast cancer risk, E2 stimulated significantly higher levels of DSBs. In contrast, only 1 in 5 of average risk donors exhibited a significant increase in DSBs in the presence of E2. Together, these data demonstrate genetic differences in sensitivity to E2-stimulated DNA damage in rodents and that similar variation is also observed in normal breast tissues from women. Variation in levels of the pathogenic effects of E2 may provide a biomarker associated with sensitivity to breast cancer.

Materials and Methods

Experiments in mice

Female BALB/c and C57BL/6 mice (7 weeks old) were purchased from Jackson Laboratory. The mice were housed in temperature-controlled facilities with a set temperature of 64-79 °F and humidity of 30-70%, 12-hour alternating day/night light cycle and fed Lab Chow 5058 ad libitum for one week prior to use in experiments. The 17β-estradiol (designated E2) used in these experiments was obtained from Sigma-Aldrich (E2758-250MG). All procedures were under the national guidelines for the care and use of animals and approved by the University of Massachusetts Amherst's Institutional Animal Care and Use Committee.

In experiments with ovariectomized, each mouse was anesthetized with a mix of isoflurane and oxygen. The flanks were shaved, sterilized with betadine, and cleaned with alcohol. An incision was made to the skin on the right flank. The underlying muscle layer was nicked to reveal a small opening through which the ovary was exteriorized by grasping the periovarian fat. A serrafin clamp was used to hold the ovary. A suture ligature was applied to prevent breeding, then the ovary was cut from the uterine horn. The periovarian fat was restored into the peritoneum. The peritoneum was closed with one or two stitches and the skin was closed with 9 mm wound clips. The procedure was repeated on the contralateral side. The mouse was monitored for a week post-procedure and wound clips were removed after 10 days. After 1 week of recovery, the mice of strain were randomized to two groups and began an acute oral treatment via pipette with vehicle control

(tocopherol-stripped corn oil) (n = 5) or E2 (n = 5) for 4 days. Each mouse was administered 1μL of oil per gram of body weight to deliver 0.25 mg/kg/day E2 or vehicle control.

For ovary intact animals, ovariectomy was not performed and the E2 dose was increased to 0.75 mg/kg/day. For acute treatment of 4 days, mice of each strain were simply randomized to two groups and began treatment via drinking water with vehicle control (only water) (n=5) or E2 (n=5) for 4 days. For chronic treatment of 28 days, mice were treated with vehicle control (only water) (n=5) or E2 (n=10) for 28 days.

The mice were sacrificed using carbon dioxide followed by cervical dislocation. One 4th mammary gland was fixed in 10% NBF and transferred to 70% alcohol within 12 h followed by paraffin-embedding. The contralateral 4th mammary gland was cleared of lymph node and stored in -80°C for RNA isolation.

Experiments in rats

Details of animal care, treatment, tissue collection, fixation, and processing of samples were explained in (Ding et al., 2013). Slides of ACI and BN mammary gland tissue samples were received from Dr. Shull's lab. Briefly, 9 weeks old female rats of each strain were treated with E2 for 7 days, released from subcutaneous Silastic implants containing 27.5 mg of E2. Methods for preparing and surgically implanting the hormone delivery tubes have been described previously (Shull et al., 1997)**.** Control-treated rats from each strain received empty implants. The rats were euthanized (by decapitation with a rodent guillotine) following 7 days of treatment. Mammary gland tissues were collected, fixed, processed, and embedded in paraffin. Sections were cut and mounted on slides.

Human breast patient-derived explant cultures (PDEs)

Explant culture and treatment were described previously in detail (Dunphy et al., 2020) Briefly, human breast tissue samples were collected from female donors undergoing reduction mammoplasty or mastectomy surgery. Fresh breast tissues were cut using microtome and sections were placed on top of surgical foam (Ethicon) in 60mm plastic dishes and maintained in Basal Media in a humidified incubator with 5% CO2 at 37 °C. Tissues were cultured in Basal Media containing phenol red-free DMEM: F12 (Sigma-Aldrich), 10% charcoal-stripped fetal bovine serum (FB-04, Omega Scientific), 10ng/mL human epidermal growth factor (21–8356-U100, Tonobo Biosciences), and antibiotic-antimycotic (15,240,062, Gibco) for up to 3 days to clear from endogenous hormones. Tissues were maintained in either Basal or supplemented with 10nM E2 for up to additional 4 days. Tissues were processed and paraffin embedded. Fresh sections were cut and mounted on slides.

Immunostaining

Freshly cut 4-5 μM paraffin-embedded sections were deparaffinized/rehydrated with 100% xylenes 3 times for 5 min each, 2 times with 100% ethanol for 5 min each, 95% ethanol for 3 min and 70% ethanol for 3 min. Samples were rinsed with PBS. Antigen retrieval was performed by boiling the samples in 1 mM EDTA (pH 8.0) for 30 mins and cooled for 30 mins at RT. For dual staining of ERα and γH2AX, antigen retrieval was performed using 10mM Sodium Citrate buffer containing 0.05% Tween-20 (pH 6.0). Tissues were incubated in 1% Triton-X 100 in PBS for 30 mins at RT. Samples were then treated with SSC 0.2X with gentle shaking at RT for 20 min. Samples were washed 3 times

with TBS containing 0.5% Tween20. Samples were blocked in 10% goat or rabbit serum in PBS with 0.5% Tween-20 for 1 hr at RT. Primary antibody incubation was done with monoclonal S9.6 antibody (Kerafast #ENH001), anti-H2AX antibody (Cell Signaling # 9718S), or anti-ERα (Millipore, 06-935) for overnight at 4°C. After primary incubation, samples were washed 3 times with TBS containing 0.5% Tween-20 and then incubated with anti-mouse AlexaFluoro-488-conjugated (Cell Signaling #4408S) or anti-rabbit AlexaFluoro-488-conjugated secondary antibody (Cell Signaling #8889S) for 2 hr. Samples were washed 3 times with TBS containing 0.5% Tween-20 and then mounted with Vectashield mounting medium containing DAPI. Slides were imaged at 60X with a Nikon A1 Spectral Confocal microscope. Analysis of S9.6 or γH2AX foci per nucleus and ERα positive cells were calculated using Nikon analysis software, where DAPI was used as a mask for the nucleus. IHC for Ki-67 was performed on a Dako Cytomation autostainer using 1:1000 D2H10 primary antibody (cell signaling #9027T) and the Envision HRP detection system (Dako, Carpinteria, CA). Positive cells were counted using ImageJ software. A total of 1200 cells were counted per slide to determine percent Ki-67 positive.

RT-qPCR

RNA from the mammary gland was isolated with TRIzol (Thermofisher Scientific #15596018) and Direct-zol RNA Miniprep Plus (Zymo Research #R2072). cDNA was prepared from 1 µL of RNA in 20 µL reaction mix with Protoscript II First Strand cDNA Synthesis Kit (New England Biolabs #E6560S) following the standard protocol provided by the manufacturer. qPCR for Estrogen receptor alpha (*ESR1*), progesterone receptor (*Pgr*), Amphiregulin (*Areg*), Apolipoprotein B Editing Complex 3 (*Apobec3*), and

Cytokeratin18 (*Krt18*) was performed using primers in Table 1 (Integrated DNA Technology) and iTaq Universal SYBR Green Supermix (Biorad, #1725121) on CFX96 Real-Time System thermocycler (Bio-Rad). Each run (96 well qPCR plate) included an inter-run calibrator to normalize across experiments. Data were analyzed with ΔΔCt method and relative fold change in expression of the target gene was compared between control and treatments.

Statistical Analysis

Unless specified, data were analyzed by one-way analysis of variance (ANOVA) followed by Tukey's honestly significant difference (HSD) multiple-range test using GraphPad Prism 9 statistical analysis software. Results are presented as mean ± standard error of the mean (S.E.M.). Data were considered statistically significant at $p < 0.05$.

Results

E2 induces DNA damage and R loops in BALB/c mice but not C57BL/6 mice.

Effects of estrogen were compared in BALB/cJ and C57BL/6J mice because they differ in their susceptibility to mammary tumors. Female mice were ovariectomized and endogenous hormones were allowed to clear for 7 days. The mice were then treated with E2 (0.25 mg/kg/d) for 4 days **(Figure 3.1A)**. This dose of E2 mimics levels during early pregnancy (Majewski et al., 2018; Majhi et al., 2020). First, we compared proliferation in the mammary epithelium using Ki-67. The frequency of cells positive for Ki-67 was increased significantly with E2 treatment as compared to the control treatments **(Figure 3.1B)**. The proliferative responses to E2 treatment in the mammary epithelium were similar for both strains **(Figure 3.1B and C)**. Immunostaining with phosphorylated histone H2AX (γH2AX), a marker of DNA-double stranded breaks, was used to assess E2-induced DNA damage in the luminal mammary epithelium. The number of γH2AX foci was increased significantly in BALB/cJ with E2 treatment compared to the control-treated mice. However, the C57BL/6J showed no increase in γH2AX foci with E2 treatment **(Figure 3.1D and E)**. Co-transcriptional R loop (DNA: RNA hybrid) structures were shown to be precursors of E2- induced DNA double-strand breaks (Majhi et al., 2020; Stork et al., 2016). Therefore, immunostaining with an R loop-specific antibody (S9.6) was used to detect the presence of these structures in the mammary epithelium. BALB/cJ mice showed a significant increase in S9.6 foci with E2 treatment as compared to the control mice. In contrast, we did not observe any induction of S9.6 foci by E2 treatment in C57BL/6J mice **(Figure 3.1F and G)**. Estrogen target genes (*Pgr* and *Areg*) were increased significantly

in the mammary tissues of both strains by E2 treatment **(Figure 3.1H and I)**. However, the levels of *Pgr* and *Areg* were increased to a greater extent ($p<0.001$) in BALB/cJ mice when compared with C57BL/6J mice. These data show that E2 stimulates R loops and DNA double strand breaks in BALB/cJ, but not C57BL/6J mice. As both strains had equivalent proliferation at 4 days of E2 treatment, the differences in γH2AX is not attributed to replication-associated DNA damage.

Enrichment of E2-induced DNA damage in ERα positive mammary epithelial cells in BALB/c mice.

To determine which mammary epithelial cells are experiencing E2-induced DNA damage, we performed dual immunofluorescence to detect both γH2AX and estrogen receptor alpha (ERα) in the luminal mammary epithelial cells of ovariectomized mice treated with or without E2 for 4 days as described in Figure 1A. Both strains had similar proportions of ER-α positive cells (37-40%) in the luminal epithelium and were unchanged by E2 treatment **(Figure 3.2A and B)**. The number of γH2AX foci/nucleus was greater in the ER-α positive cells in both strains compared to the ER-α negative cells, but E2-induced γH2AX foci were only observed in BALB/cJ mammary epithelium **(Figure 3.2A and 3.2C)**. While the number of γH2AX foci was greatest in mammary epithelial cells with detectable levels of ERα, there was also a significant increase of γH2AX foci in the ER-α negative population of cells in BALB/cJ mice. However, the levels of γH2AX foci in ERα-negative cells of C57BL/6J mice were not increased **(Figure 3.2C)** despite similar proliferative responses **(Figure 3.1C)**. We also generated frequency distributions for the

proportions of cells with increasing numbers of γH2AX foci to determine if there were different populations within the percentage of ERα positive cells **(Figure 3.2D)**. In the control-treated mice, the majority of ERα-positive cells had fewer than 5 γH2AX foci **(Figure 3.2E)**. There was a small shift in the distribution for C57BL/6J mice toward increased proportions of cells with up to 10 foci/cells but was not significant **(Figure 3.2D and E)**. In contrast, E2 treatment in BALB/cJ mice resulted in 70% of the ERα-positive cells with >10 foci/nucleus. Therefore, ERα-positive cells in BALB/cJ mice are preferentially susceptible to DNA damage with physiologic levels of E2, while C57BL/6J mice were resistant.

Effect of short-term high E2 dose on DNA damage and R loops in ovary intact mice.

As elevated levels of E2 are associated with an increased risk of breast cancer in women, we wanted to determine if higher doses of E2 may be necessary to induce DNA damage in C57BL/6J mice. In this experiment, ovary-intact BALB/cJ and C57BL/6J mice treated with a 3-fold higher dose of E2 (0.75 mg/kg/day, referred to as 3xE2) in drinking water to allow continuous exposure for 4 days **(Figure 3.3A)**. The proliferative response shown by Ki-67 staining indicates that treatment with 3xE2 significantly increased the proliferation rates (37.98% and 36.90% in BALB/cJ and C57BL/6J, respectively) in their mammary gland epithelium **(Figures 3.3B and C)**. These levels of proliferation were greater than the 18% of Ki-67 positive cells observed in ovariectomized mice treated with 0.25mg/kg/d **(Figure 3.1C)** indicating dose-dependent responses at up to 0.75mg/kg/d. Even with the higher dose of E2 and increased proliferation, there was not a significant

difference in γH2AX foci in the mammary epithelium of C57BL/6J compared to control treatment **(Figure 3.3D and 3E)**. There was a modest increase with E2 treatment in BALB/cJ mice, but it did not reach statistical significance. The difference may be blunted by the presence of endogenous estrogens in the ovary-intact mice. However, the number of S9.6 foci/nucleus were increased significantly in the mammary epithelium of both BALB/cJ and C57BL/6J mice by the 3xE2 treatment **(Figures 3.3F and 3G)**. Though R loops appear to be induced by E2 in both strains, the number of foci/nucleus was higher in BALB/cJ compared to C57BL/6J. Overall, the effect of E2 on DNA damage and co-transcriptional R loops was similar to that observed with the 0.25mg/kg/d dose in Figure 2.1, but the fold changes appear to be blunted by the endogenous levels of E2 in the ovary-intact mice.

Effect of chronic exposure to high E2 dose on DNA damage and R loops in ovary intact mice.

Pregnancy is a period during which there are sustained increases in estrogens as well as other growth factors. The mammary gland undergoes dramatic proliferation in response to these hormones followed by differentiation. To evaluate the effect of sustained increases in E2, ovary intact BALB/cJ and C57BL/6J mice were treated for 28 days with E2 (0.75 mg/kg/day, 3x) in drinking water **(Figure 3.4A)**. In contrast to the dramatic proliferation at 4 days (~37% in **Figure 3.3C**), the proliferative fraction of cells returned to near baseline levels (2% to 3%) in the mammary epithelium of both strains of mice treated with E2 for 28 days **(Figure 3.4B and 4C)**. The Ki-67 levels did not differ between the Control- and E2-treated groups. Although proliferative responses had declined, there

was a sustained elevation of γH2AX foci in E2-treated BALB/cJ mammary epithelium whereas there was no difference between Control- and E2 treated C57BL/6J mice **(Figure 3.4D and 4E)**. Chronic treatment with E2 also increased R loop levels in BALB/cJ mice compared to controls but no significant difference due to E2-treatment in C57BL/6 mice **(Figure 3.4F and 4G)**. Therefore, the strain-specific sensitivity to E2-induced DNA damage in BALB/cJ but not C57BL6J mice was observed across the time course of treatments of 4 to 28 days and was not associated with changes in proliferation or physiologic states of the mammary gland.

Expression of estrogen receptors and target genes with acute and chronic treatments.

Transcriptional responses were also examined to compare the effects of the 3xE2 dose in ovary-intact mice. As E2 stimulates proliferation of the luminal epithelium, expression of ERα target genes was normalized to *Krt18* levels (**Figure 3.5 G and H**) to adjust for potential differences in populations of cells. Administration of E2 resulted in decreased *Pgr* mRNA levels at both 4 and 28 days in BALB/cJ mice (**Figures 3.5 A and 5B**). *Areg* mRNA was also decreased by treatment with E2 for 28 days (**Figures 3.5C and D**). In C57BL/6J mice, levels of *Pgr* were increased after 28 days of E2, but not at 4 days (**Figure 3.5A and B**). *Areg* expression was unchanged by E2 in C57BL/6J mammary tissues as well (**Figures 3.5C and D**). Expression of *Esr1* (encoding ERα) was decreased to varying degrees in both strains (**Figures 3.5E and F**) which may reflect feedback inhibition in response to administration of E2. The results in ovary-intact mice differ from responses in ovariectomized mice and indicate that endogenous levels of E2 in mice with normal ovarian cycles are sufficient to maintain the expression of ERα target genes (*Areg*

and *Pgr*). Therefore, the increased numbers of γH2AX foci and R loops in mammary tissues of BALB/cJ mice following E2 treatment does not appear to be due to a global increase in transcription.

The DNA editing enzyme APOBEC3B causes base damage and was induced by E2 in human breast cancer cells (Periyasamy et al., 2015; Udquim et al., 2020). Therefore, we compared the mRNA levels of *Apobec3* in BALB/cJ and C57BL/6J mice. There were no significant changes in *Apobec3* expression in the E2-treated mice compared to controls (**Figure 3.5 I and J**). Levels of *Apobec3* differed between strains, but levels were lower in BALB/cJ mice. Therefore, Apobec*3* does not appear associated with the greater DNA damage observed in BALB/cJ mammary tissues.

E2 induced DNA damage in the mammary epithelium of susceptible ACI rat strain.

Rat strains have also been shown to vary dramatically in their responses to E2. The ACI strain is susceptible to E2-induced mammary tumors and has led to the identification of genetic modifiers through crosses with the resistant BN strain. However, these strains have not been screened for differences in DNA damage and repair pathways. Ovary-intact rats from both ACI and BN strains were treated continuously with E2 for 7days, then tissues were harvested and analyzed for γH2AX foci. E2 treatment in ACI rats resulted in significant increases in γH2AX foci in the mammary epithelium compared to the control treated ACI rats (**Figure 3.6A and B**). In contrast, the BN strain did not show induction of γH2AX foci with E2 treatment. These results demonstrate that the DNA damaging effects of E2 are also observed in rats and are associated with susceptibility to mammary tumors.

DNA damage by E2 in human breast explant tissues

Prior studies had observed E2-induced DNA damage in breast cancer cell lines but had not examined effects in normal breast tissues. We used the *ex-vivo* culture of patient-derived explants (PDEs) to compare the effects of estrogen among women. PDEs were maintained in basal media or supplemented with 10nM E2 for up to 4 days. PDEs from donors undergoing prophylactic mastectomies due inherited genetic risk alleles were designated "High Risk". Responses were compared with donors undergoing reduction mammoplasty and did not have familial risk, and therefore, were considered "Average Risk" of breast cancer. The mean number of γH2AX foci/nucleus was increased by E2 but was not statistically significant within the risk groups (**Figure 3.7A**). The High-Risk patients exhibited a higher baseline level of γH2AX as well as a further increase induced by E2. Comparison between the risk groups, the effect of E2-induced DNA damage was greater in this sample of High Risk compared to the Average Risk tissues ($p=0.01$). The range of γH2AX foci/nucleus was greater in the E2 treated breast epithelium (% of cells) of High-Risk donors when compared with Average Risk donors (**Figure 3.7B**). The results indicate that there is variation in DNA damage caused by E2 among women and may reach pathogenic levels in a subset of individuals.

To assess the variation in the general population, we analyzed PDEs from 3 additional women undergoing reduction mammoplasty and did not have a family history of breast cancer, and therefore, presumed to be "Average Risk". The tissues were maintained in basal media or treated with 10nM E2. The donors had similar baseline levels of γH2AX foci and variable increases in foci with E2 treatment (**Figures 3.7C and D**). Among this group, only donor 184 had significantly higher levels of γH2AX foci/nucleus

in response to E2 compared to the basal media control ($p<0.0001$). The distribution of damage in donor 184 showed that increased γH2AX foci/nucleus was broadly distributed across the breast epithelial cells **(Figure 3.7E)**. In these experiments with tissues from Average Risk donors, we observed a significant increase in E2-induced DNA damage in the breast epithelium in only 1 out of 5 individuals suggesting that this method can provide insights into possible risks posed by exposure to estrogens for a subset of women.

Discussion

A wealth of data has demonstrated the critical role of estrogen in breast carcinogenesis. Both dose and duration of exposure to ovarian hormones are associated with differences in the incidence of breast cancer (Eliassen et al., 2006) (Tamimi et al., 2016). The "pathogenic effect" of estrogens is often attributed to the mitogenic effects in ERα-positive breast cell tumors. While estrogen can have a promotional role in breast cancer cells, it is less clear how estrogen acts as an initiator of carcinogenesis. However, in normal mammary epithelium, ERα rarely colocalizes with markers of proliferation in mice, rats, or human breast (Anderson and Clarke, 2004; Blance et al., 2009; Clarke, 2004; Russo et al., 1999). In the normal epithelium, estrogens act indirectly by stimulating production of growth factors by the ERα-positive cells. The growth factors are secreted and act in a paracrine fashion to induce proliferation in the adjacent ERα-negative cells. Studies in genetically engineered mice have shown that epidermal growth factor receptor (EGFR) ligands such as amphiregulin (AREG) act as paracrine growth factors to mediate the mitogenic effects of estrogens (Ciarloni et al., 2007). Pregnancy is a period of intense proliferation needed to expand the ductal epithelium in preparation for lactation and estrogen concentrations are approximately ten-fold higher in women during pregnancy compared to postmenopausal women. Rather than increasing risk, the hormones during pregnancy ultimately confer a long-term reduction of risk by as much as 50% (Albrektsen et al., 2005; Chie et al., 2000; MacMahon et al., 1970). Indeed, we find no difference in proliferation between BALB/cJ and C57BL/6J mice in response to E2 after 4 days (**Figures 3.1C, 3.3C**). This proliferative burst is quickly resolved, and tissues return to baseline levels of proliferation by 28 days of E2 (**Figures 3.4C**). In rats, the ACI strain had a more

prolonged proliferative response than in the BN strain (Harvell et al., 2000). Proliferative responses in PDEs of normal breast showed varied responses to E2 (Dunphy et al., 2020). Therefore, there is not a consistent relationship between the effect of E2 on proliferation and its activity initiating breast cancer.

Recent studies in breast cancer cells have shown that estrogen can have genotoxic effects mediated by ERα that are not dependent on replication-induced DNA damage. E2 was shown to have an initial induction of DNA double-strand breaks within 2 hours of stimulation (Ju et al., 2006; Sasanuma et al., 2018). The transcription-associated damage was shown to be important for the expression of target genes of ERα but was transient. In addition to the acute DNA damage response, E2 was shown to stimulate even higher levels of γH2AX foci at 24 h after E2 stimulation (Stork et al., 2016). Using ChIP-sequencing, both γH2AX and R loops were shown to be localized to transcribed regions indicating more persistent damage. The E2-induced damage at 24 h was suggested to be due to stalling of replication forks at sites of transcription resulting in DNA double-strand breaks to allow replication to be re-started. However, environmental xenoestrogens were shown to also stimulate nuclear γH2AX foci in ERα-positive cell lines (Majhi et al., 2020), but at concentrations $1/10^{th}$ that required for proliferation. These experiments showed the presence of E2-induced the DNA damage that was ERα-dependent in the absence of proliferative responses.

In our studies, we demonstrate that E2 stimulates DNA damage which provides a mutagenic stimulus for initiating a carcinogenic cascade. However, E2-induced DNA damage is not uniform among strains. Both the BALB/cJ mice and ACI rats are more

susceptible to mammary tumorigenesis (Blackburn et al., 2007; Lanari et al., 1986; Ponnaiya et al., 1997; Shull et al., 2018). These strains also showed greater numbers of γH2AX foci in the luminal mammary epithelium in response to E2 (**Figures 3.1E and 3.6B**). In BALB/cJ mice, the DNA damage was enriched in the ERα-positive cells (**Figure 3.2C**). In contrast, strains that are more resistant to mammary tumors, C57BL/6J mice and BN rats, showed little DNA damage following E2 treatment.

BALB/cJ mice also had higher levels of R loops that are frequently associated with regions of nascent transcription. Therefore, the elevated expression of ERα target genes in BALB/cJ mice compared to C57BL/6J (*Pgr* and *Areg*; **Figure 3.1**) may reflect the underlying mechanisms regulating transcriptional activation of ERα. Suppression of transcription-associated DNA damage was shown to diminish expression of ERα target genes such as *TFF1* in breast cancer cell lines. Alternatively, APOBEC3B was shown to bind to ERα causing deamination near promoters which resulted in DNA double-strand breaks in breast cancer cell lines (Periyasamy et al., 2015). However, only one form of APOBEC3 is found in the mouse genome and it does not retain cytidine deaminase activity (MacMillan et al., 2013). The mouse APOBEC3 transcripts are polymorphic between BALB/c and C57BL/6 mice resulting in decreased translation and lower protein levels in BALB/c mice (MacMillan et al., 2013; Okeoma et al., 2009). There was no increase in expression of *Apobec3* in response to E2 in the mouse tissues from either strain (**Figure 3.5I and J**). Therefore, APOBEC3B is unlikely to account for the E2-induced γH2AX observed in the mouse mammary epithelium. While co-transcriptional R loops have been

implicated as potential genomic threats, it is unclear if they provide a sufficiently sensitive biomarker of risk associated with estrogen exposure.

The E2-induced DNA damage was evident with prolonged treatment with E2. Treatment of BALB/cJ mice with E2 for 28 days resulted in 3-fold more nuclear γH2AX foci in the mammary epithelium while there was no change from baseline in C57BL/6J mice (**Figure 3.4E**). At this time, proliferation had returned to baseline and transcriptional responses in ERα target genes were minimally affected by E2 (**Figures 3.5D and E**). Therefore, neither proliferative responses nor transcriptional activation account for the DNA damage observed in BALB/cJ mice though the presence of R loops induced by E2 continued to be observed (**Figure 3.4G**). These data suggest that E2 stimulates continual DNA damage in BALB/cJ mice which can contribute to their susceptibility to mammary tumors.

The critical role of DNA damage and repair pathways has become increasingly important in determining breast cancer risk and guides the selection of therapies. High penetrance risk alleles affecting the functions of *BRCA1, BRCA2, PALB2* emphasize the importance of canonical homologous recombination in assuring genomic stability. While this mechanism is present in all cells, the fact that breast cancer is the most common tumor type in carriers of pathogenic mutations suggests that breast tissue is keenly sensitive to disruptions in the repair of DNA double-strand breaks through homologous recombination. Deficiencies in canonical homologous recombination can lead to a greater reliance on the repair of DNA double-strand breaks using the lower fidelity single-strand annealing pathway and ALT-end joining pathways. Increased reliance on these lower fidelity pathways for the repair of DNA double-strand breaks is associated with an increased risk

of breast cancer (Keimling et al., 2012). Utilization of single-strand annealing (SSA) and ALT-EJ to repair DNA double-strand breaks is 3-fold greater in BALB/c compared to C57BL/6 mice (Böhringer et al., 2013). The differences in DNA repair between these strains are genetically linked to the *Suprmam1* locus on mouse chromosome 7 (Blackburn et al., 2007). Therefore, susceptibility to mammary tumors in BALB/c mice may be due to combined effects of low levels of DNA double-strand breaks caused by E2 and their repair by error-prone SSA mechanisms. The levels of γH2AX induced by E2 treatment were also greater in breast tissues from women with strong familial risk associated with defects in DNA double strand break repair (**Figure 3.7A**) compared to tissues from average risk women. These data offer a common theme among rodents and humans where the prevalence of γH2AX foci induced by estrogen interacts with the proficiency of DNA double-strand repair mechanisms to determine the risk of developing breast cancer. Levels of γH2AX have been considered as a biomarker of prognosis in breast cancers. Here we have used quantification of nuclear foci to provide a refined quantification of DNA damage in normal breast epithelium that can be applied to analyses of breast tumors as well.

Our results support a mechanism in which estrogen exposure preferentially causes DNA double-strand breaks mediated by ERα. However, the extent of the damage appears to be augmented when DNA double-strand break repair pathways are defective. BALB/c mice are more sensitive to DNA damage which appears to be associated with genetic polymorphisms that affect non-homologous end-joining (Yu et al., 2001) as well as increased homology-directed repair through error-prone pathways (Böhringer et al., 2013). The results are consistent with data showing that E2 stimulated hyperplastic lesions in BALB/c-*Scid* mice (Itou et al., 2020) that have a defective non-homologous end-joining

due to mutations in *Prkdc*. DNA damage in these mice was blocked by treatment with Fulvestrant, and therefore, is dependent on ERα. We also found increased E2-induced DNA damage in human breast tissues from women with inherited breast cancer risk alleles affecting DNA double-strand break repair. In contrast to average-risk women where ERα-positive breast cancers have a good prognosis, ERα-positive breast cancers among women with pathogenic mutations in *BRCA1* or *BRCA2* have a 3-fold higher recurrence rate and risk of death (Metcalfe et al., 2019; Vocka et al., 2019). It appears that DNA double-strand breaks are necessary to facilitate transcription of ERα target genes which, in repair-proficient individuals, is promptly repaired using high fidelity pathways. However, in individuals with impairments of DNA double-strand break repair, the DNA damage in ERα-positive cells can reach pathogenic levels and initiate the carcinogenic cascade.

Table 3.1. Sequence of primers

Target	Sequence (5′ to 3′)
Esr1	F: AGTGTCTGTGATCTTGTCCAG
	R: TGTGTGCCTCAAATCCATCA
Pgr	F: GACCACATCAGGCTCAATGCT
	R: GGTGGGCCTTCCTAACGAG
Areg	F: GTCACTATCTTTGTCTCTGCCA
	R: CCTCCTTCTTTCTTCTGTTTCTCC
Apobec3	F: TTCACCCGTCTCCCTTCA
	R: GCACTTTCAGTACTTTGTCATGG
Krt18	F: GCCACTACTTCAAGATCATCGAA
	R: GCTAGTTCTGTCTCATACTTGACT

Table 3.2. Details of patient derived breast explant donors:

Patient ID	**Age**	**Type of Surgery**	**Risk Category**
184	27	Reduction mammoplasty	Average
237	18	Reduction mammoplasty	Average
243	45	Reduction mammoplasty	Average
814	23	Reduction mammoplasty	Average
772	44	Reduction mammoplasty	Average
833	42	Prophylactic mastectomy	High
812	45	Prophylactic mastectomy	High

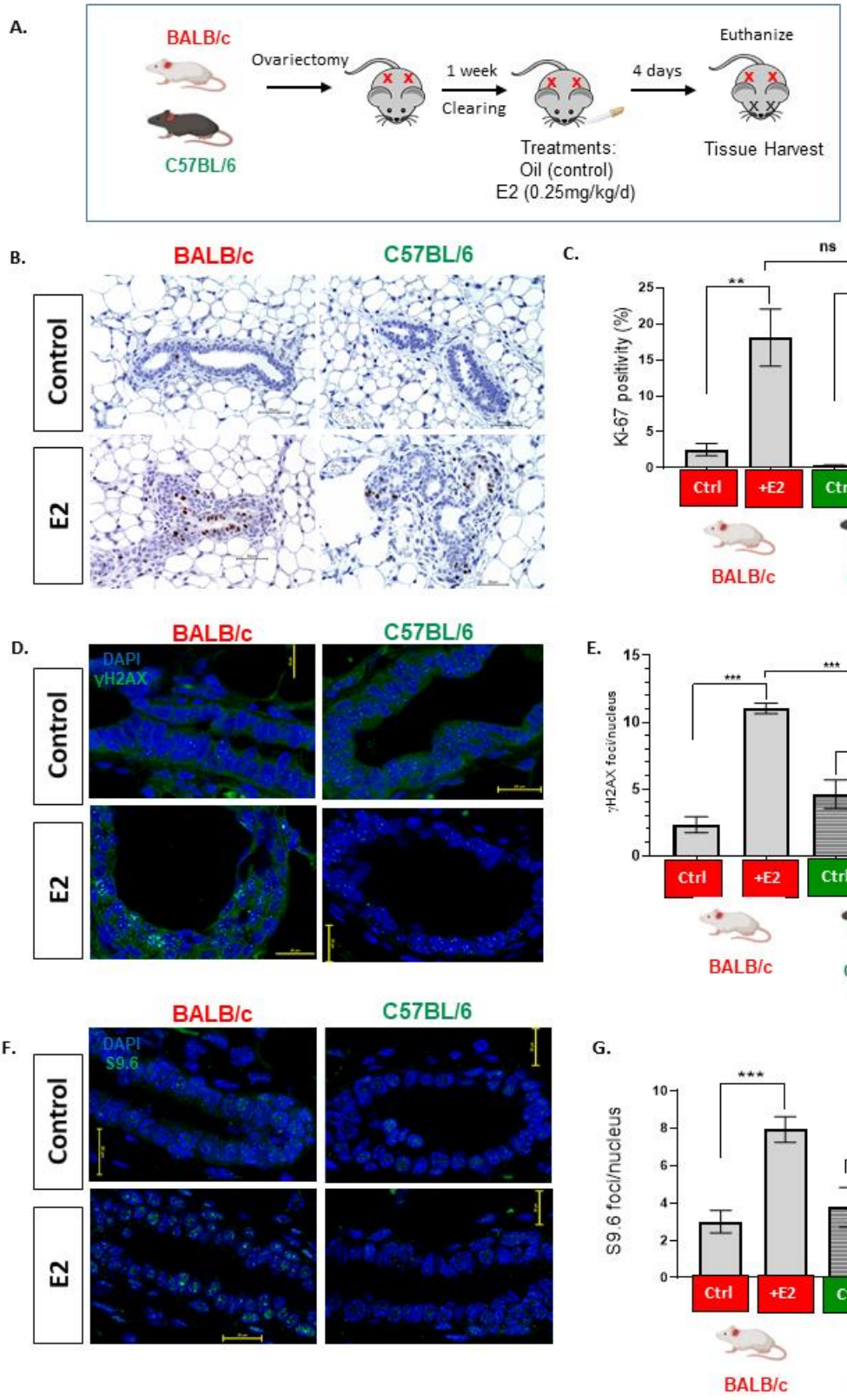
A.
BALB/c
C57BL/6
Ovariectomy
1 week
Clearing
4 days
Euthanize
Treatments:
Oil (control)
E2 (0.25mg/kg/d)
Tissue Harvest
B.
BALB/c
C57BL/6
Control
E2
C.
ns
**
**
Ki-67 positivity (%)
25
20
15
10
5
0
Ctrl
+E2
Ctrl
+E2
BALB/c
C57BL/6
D.
BALB/c
C57BL/6
DAPI
γH2AX
Control
E2
E.
***
***
n.s.
γH2AX foci/nucleus
15
10
5
0
Ctrl
+E2
Ctrl
+E2
BALB/c
C57BL/6
F.
BALB/c
C57BL/6
DAPI
S9.6
Control
E2
G.
***
ns
S9.6 foci/nucleus
10
8
6
4
2
0
Ctrl
+E2
Ctrl
+E2
BALB/c
C57BL/6

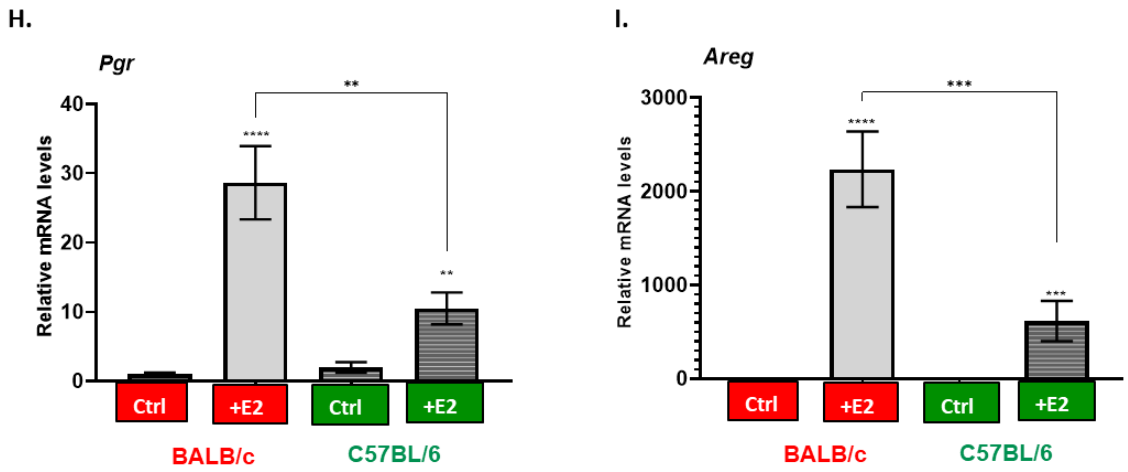

Figure 3.1. Effect of acute (4 days) 1x E2 treatment on mammary gland in ovariectomized BALB/c and C57BL/6 mice.

(A) Workflow of experimental design and animal treatment. **(B)** Proliferation marker: Ki-67 staining of mouse mammary epithelial cells. Scale bar = 50µM **(C)** Percentage of Ki-67-stained cells were counted (n=5 for BALB/c control and C57BL/6 control, n=8 for BALB/c E2, n= 6 for C57BL/6 E2). **(D)** Immunostaining of mouse mammary epithelium with γH2AX antibody harvested from BALB/c and C57BL/6 mice treated with control (n=3) or E2 (n=5). Each image shows a ductal structure with a nucleus stained with DAPI (blue) and γH2AX (green). Scale bar = 20µM. **(E)** Quantification of immunostaining data of γH2AX foci inside the nucleus. **(F)** Immunostaining of mouse mammary epithelium with S9.6 antibody for R loops in BALB/c and C57BL/6 mice treated with control (n=3) or E2 (n=5). Scale bar = 20µM. **(G)** Quantification of immunostaining data of S9.6 foci inside the nucleus. Gene Expression of **(H)** *Pgr* **(I)** *Areg* in mammary gland tissues from ovariectomized mice treated with control or E2 (0.25mg/kg/d) for 4 days (n=5) or E2 (n=5). ***p > 0.0001 compared to control with treatments using one-way analysis of variance (ANOVA) followed by Tukey's honestly significant difference (HSD) multiple-range test. All graphs show mean ± SEM. *Data collection in collaboration with Prabin. D. Majhi and Amy L. Roberts.*

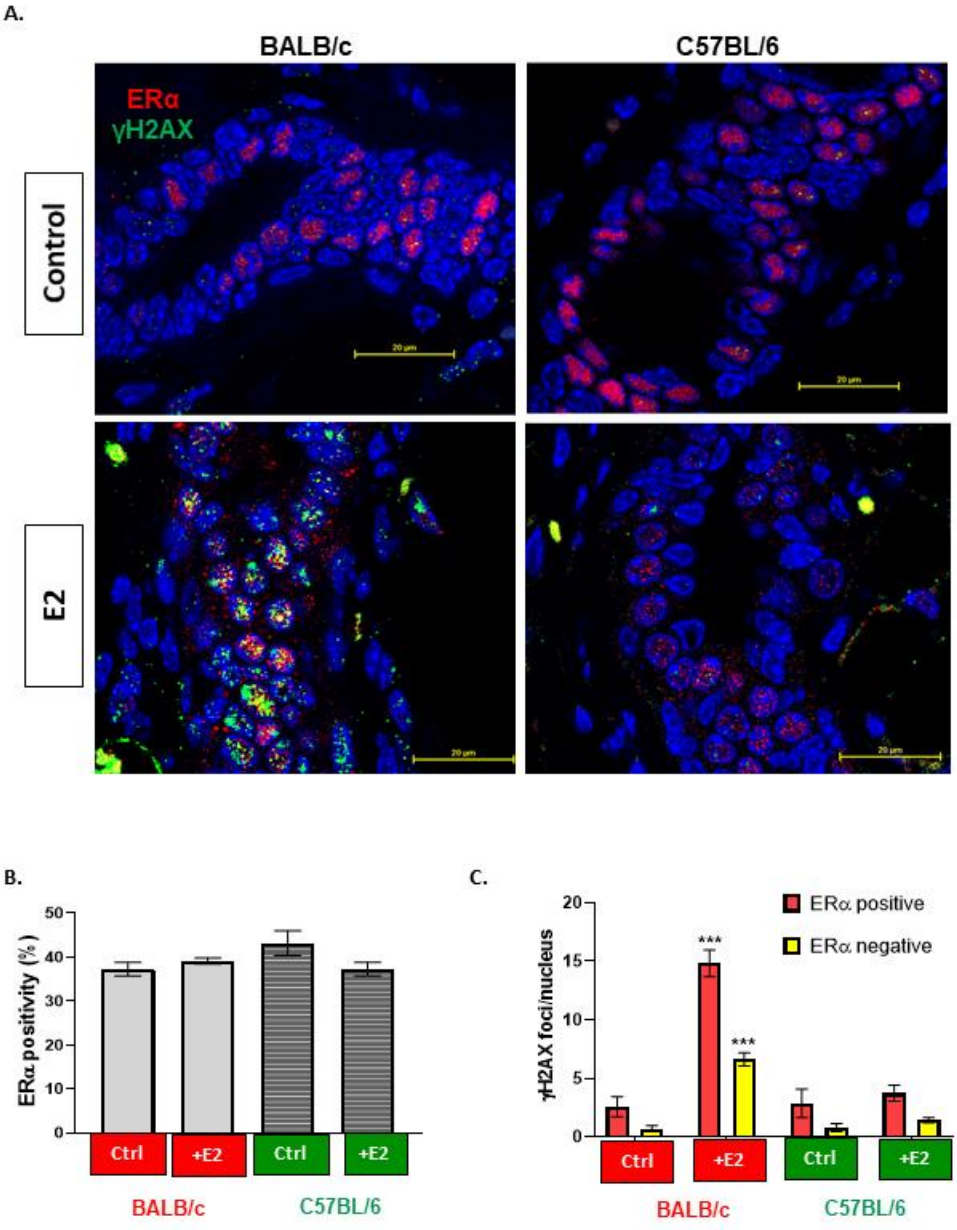
A.
BALB/c
C57BL/6
ERα
γH2AX
Control
E2
B.
ERα positivity (%)
50
40
30
20
10
0
Ctrl
+E2
Ctrl
+E2
BALB/c
C57BL/6
C.
γH2AX foci/nucleus
20
15
10
5
0
ERα positive
ERα negative
***
***
Ctrl
+E2
Ctrl
+E2
BALB/c
C57BL/6

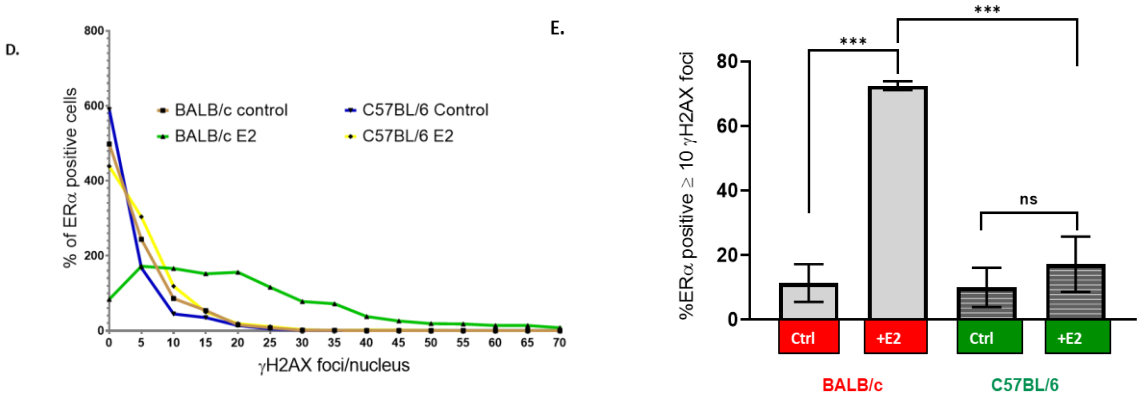

Figure 3.2. Localization of DNA damage in mammary gland epithelium of 4 days treated BALB/c and C57BL/6 ovariectomized mice.

(A) Dual immunostaining on mouse mammary epithelium with γH2AX antibody and ER-alpha harvested from BALB/c and C57BL/6 mice treated with control (n=5) or E2 (n=5). Each image shows a ductal structure with a nucleus stained with DAPI (blue), ER-alpha (Red), and γH2AX (green). Scale bar = 20μM. **(B)** Quantification of total ER-alpha positivity (%) in the dual immunostaining. **(C)** Quantification and comparison of γH2AX foci inside the nucleus of ER-alpha positive versus ER-alpha negative cells. **(D)** Distribution of the number of γH2AX foci per nucleus in each ERα positive cell from BALB/c and C57BL/6 mice treated with control or E2 (0.25mg/kg/d) for 4 days (control n=5, E2 treated n=5). **(E)** Percentage of ERα positive cells with greater than equal to 10 γH2AX foci per nucleus in the mammary epithelium of BALB/c and C57BL/6 mice treated with control or E2 (0.25mg/kg/d) for 4 days (control n=5, E2 treated n=5). ***p > 0.0001 compared to control with treatments using one-way analysis of variance (ANOVA) followed by Tukey's honestly significant difference (HSD) multiple-range test. All graphs show mean ± SEM. *Data collection in collaboration with Karen A. Dunphy.*

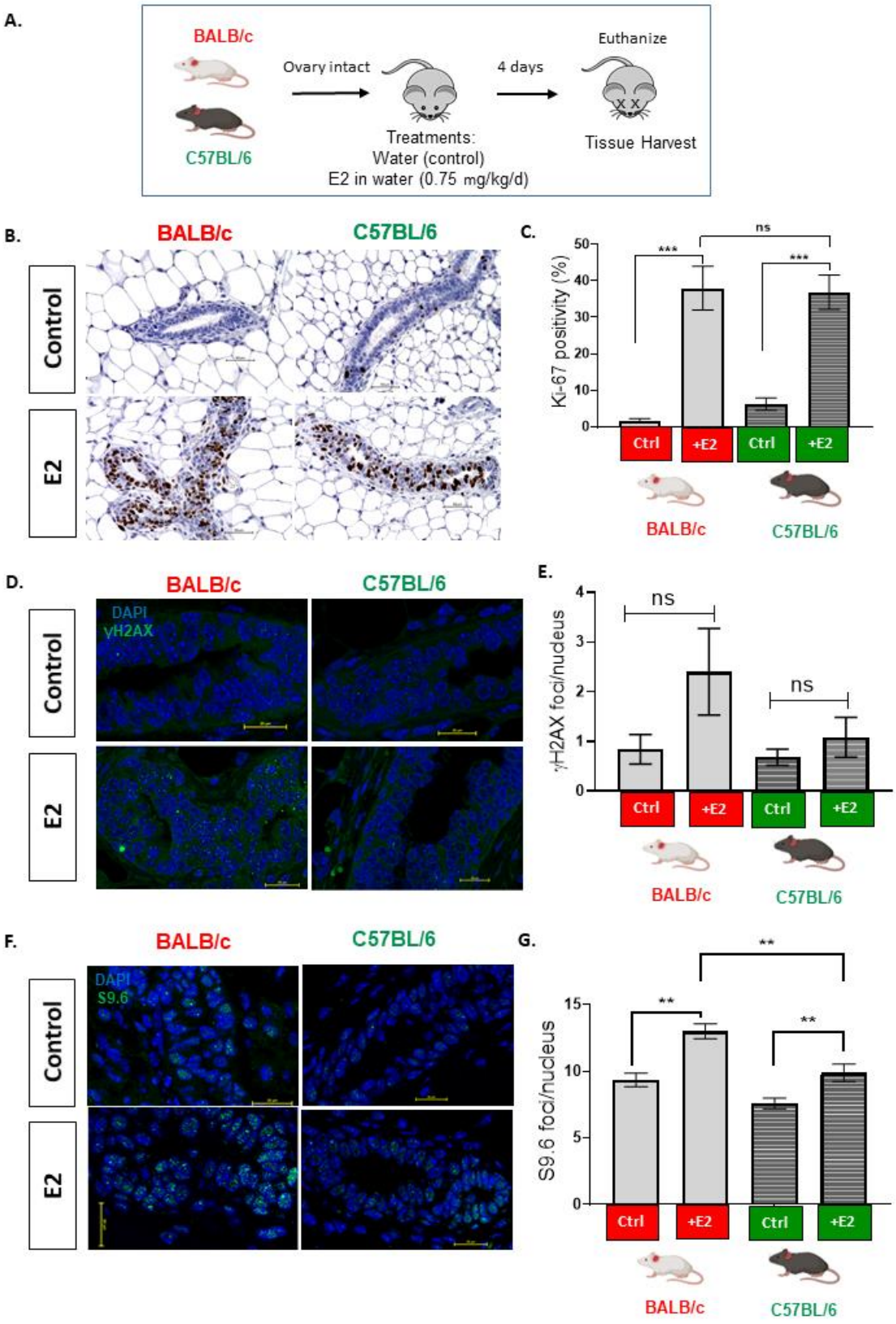
A.
BALB/c
C57BL/6
Ovary intact
4 days
Euthanize
Treatments:
Water (control)
E2 in water (0.75 mg/kg/d)
Tissue Harvest
B.
BALB/c
C57BL/6
Control
E2
C.
Ki-67 positivity (%)
ns
***
***
Ctrl
+E2
Ctrl
+E2
BALB/c
C57BL/6
D.
BALB/c
C57BL/6
Control
E2
DAPI
γH2AX
E.
γH2AX foci/nucleus
ns
ns
Ctrl
+E2
Ctrl
+E2
BALB/c
C57BL/6
F.
BALB/c
C57BL/6
Control
E2
DAPI
S9.6
G.
S9.6 foci/nucleus
**
**
**
Ctrl
+E2
Ctrl
+E2
BALB/c
C57BL/6

Figure 3.3. Effect of acute (4 days) 3xE2 treatment on mammary gland in ovary intact BALB/c and C57BL/6 mice.

(A) Workflow of experimental design and animal treatment. **(B)** Proliferation marker: Ki-67 staining of mouse mammary epithelial cells in BALB/c and C57BL/6 treated with control (n=5) or E2 (n=5). Scale bar = 50μM. **(C)** Percentage of Ki-67-stained cells were counted. **(D)** Immunostaining of mouse mammary epithelium with γH2AX antibody harvested from BALB/c and C57BL/6 mice treated with control (n=5) or E2 (n=5). Each image shows a ductal structure with a nucleus stained with DAPI (blue) and γH2AX (green). Scale bar = 20μM. **(E)** Quantification of immunostaining data of γH2AX foci inside the nucleus. **(F)** Immunostaining of mouse mammary epithelium with S9.6 antibody for R loops in BALB/c and C57BL/6 mice treated with control (n=5) or E2 (n=5). Scale bar = 20μM. **(G)** Quantification of immunostaining data of S9.6 foci inside the nucleus. ***p > 0.0001 compared to control with treatments using one-way analysis of variance (ANOVA) followed by Tukey's honestly significant difference (HSD) multiple-range test. All graphs show mean ± SEM. *Data collection in collaboration with Amy L. Roberts.*

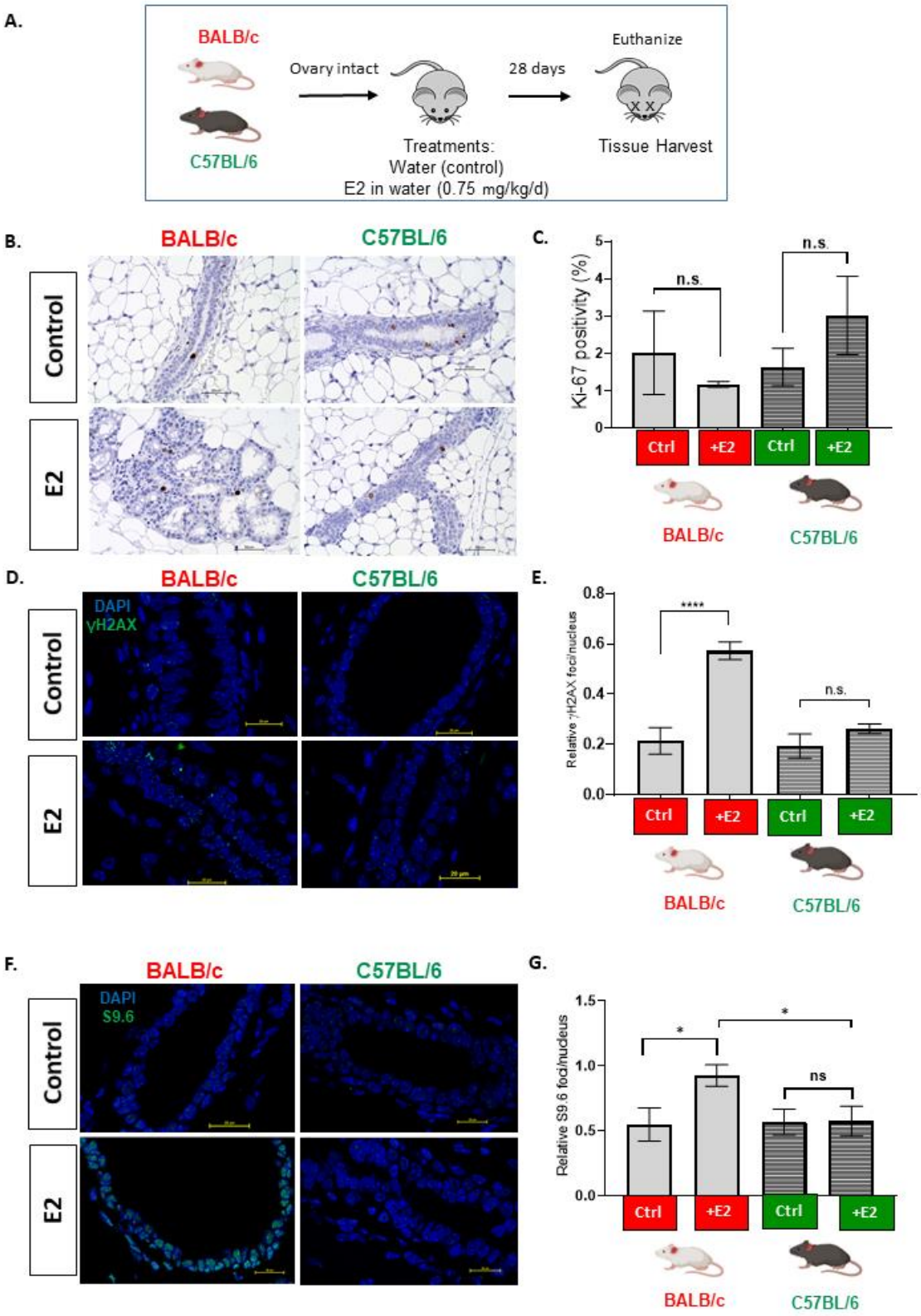
A.
BALB/c
C57BL/6
Ovary intact
28 days
Euthanize
Treatments:
Water (control)
E2 in water (0.75 mg/kg/d)
Tissue Harvest
B.
BALB/c
C57BL/6
Control
E2
C.
Ki-67 positivity (%)
n.s.
n.s.
Ctrl
+E2
Ctrl
+E2
BALB/c
C57BL/6
D.
BALB/c
C57BL/6
DAPI
γH2AX
Control
E2
E.
Relative γH2AX foci/nucleus
****
n.s.
Ctrl
+E2
Ctrl
+E2
BALB/c
C57BL/6
F.
BALB/c
C57BL/6
DAPI
S9.6
Control
E2
G.
Relative S9.6 foci/nucleus
*
*
ns
Ctrl
+E2
Ctrl
+E2
BALB/c
C57BL/6

Figure 3.4. Effect of chronic (28 days) 3xE2 treatment on mammary gland in ovary intact BALB/c and C57BL/6 mice.

(A) Workflow of experimental design and animal treatment. **(B)** Proliferation marker: Ki-67 staining of mouse mammary epithelial cells in BALB/c and C57BL/6 treated with control (n=5) or E2 (n=10). Scale bar = 50µM. **(C)** Percentage of Ki-67-stained cells were counted. **(D)** Immunostaining of mouse mammary epithelium with γH2AX antibody harvested from BALB/c and C57BL/6 mice treated with control (n=5) or E2 (n=10). Each image shows a ductal structure with a nucleus stained with DAPI (blue) and γH2AX (green). Scale bar = 20µM. **(E)** Quantification of immunostaining data of relative γH2AX foci inside the nucleus. **(F)** Immunostaining of mouse mammary epithelium with S9.6 antibody for R loops in BALB/c and C57BL/6 mice treated with control (n=5) or E2 (n=10). Scale bar = 20µM. **(G)** Quantification of immunostaining data of relative S9.6 foci inside the nucleus. ***p > 0.0001 compared to control with treatments using one-way analysis of variance (ANOVA) followed by Tukey's honestly significant difference (HSD) multiple-range test. All graphs show mean ± SEM. *Data collection in collaboration with Mary J. Hagen and Amy L. Roberts.*

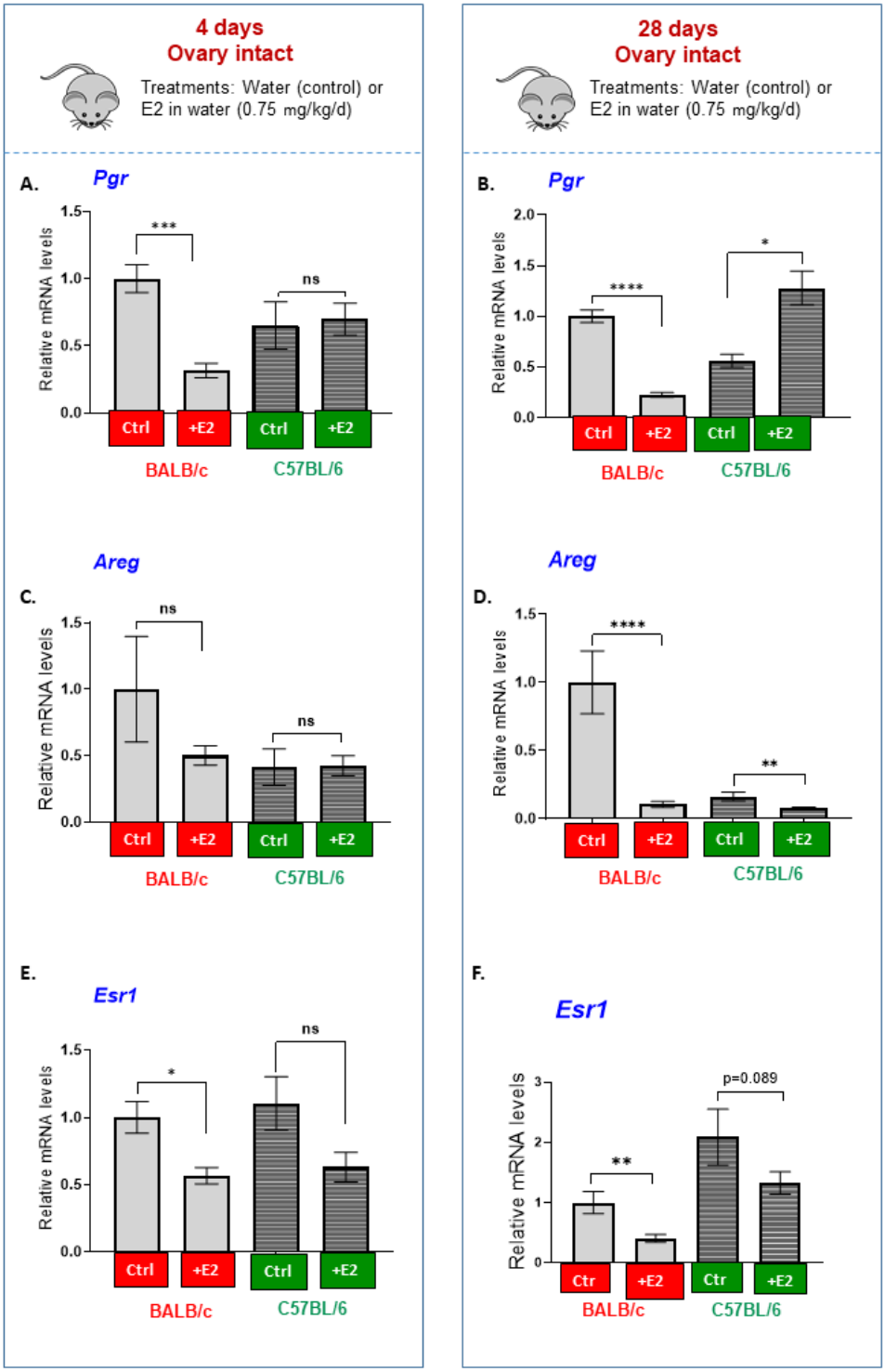
4 days
Ovary intact
Treatments: Water (control) or E2 in water (0.75 mg/kg/d)
28 days
Ovary intact
Treatments: Water (control) or E2 in water (0.75 mg/kg/d)
A.
Pgr
B.
Pgr
C.
Areg
D.
Areg
E.
Esr1
F.
Esr1
Relative mRNA levels
Ctrl
+E2
Ctr
BALB/c
C57BL/6
***
ns
****
*
**
p=0.089

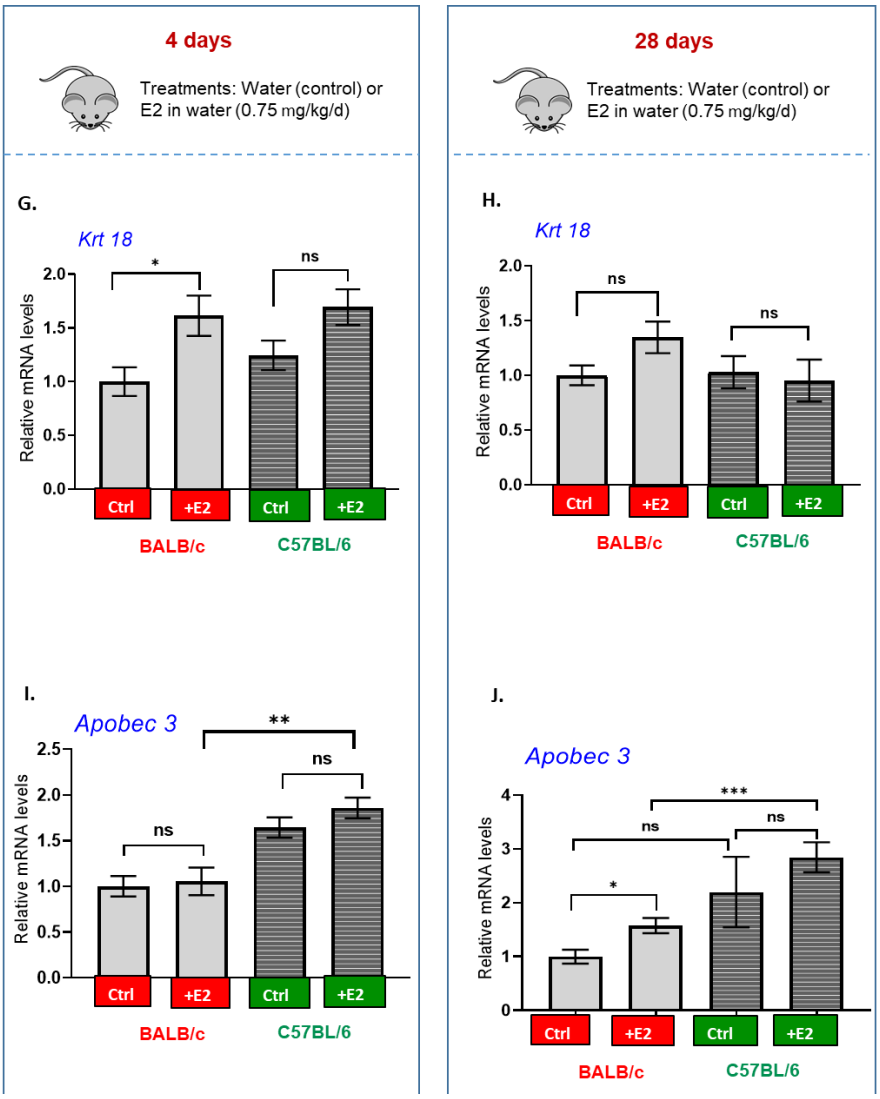

Figure 3.5. Estrogen target genes expression on acute (4 days) and chronic (28 days) treatment with 3xE2 on mammary gland in ovary intact BALB/c and C57BL/6 mice. Left panel – Gene Expression of **(A)**, *Pgr* **(C)** *Areg* **(E)** *Esr1* **(G)** *Krt18* **(I)** *Apobec3* from mammary gland tissues in ovary-intact mice treated with control or E2 (0.75mg/kg/d) for 4 days (n=5) or E2 (n=5). Right panel - Gene Expression of **(B)**, *Pgr* **(D),** and *Areg* **(F)** *Esr1* **(H)** *Krt18* **(I)** *Apobec3* from mammary gland tissue of 28 days treated ovary intact mice with control (n=5) or E2 (n=10). Gene expression was normalized with the gene *Krt18* expression – luminal epithelium marker. All graphs show mean ± SEM. *Data collection in collaboration with Mary J. Hagen.*

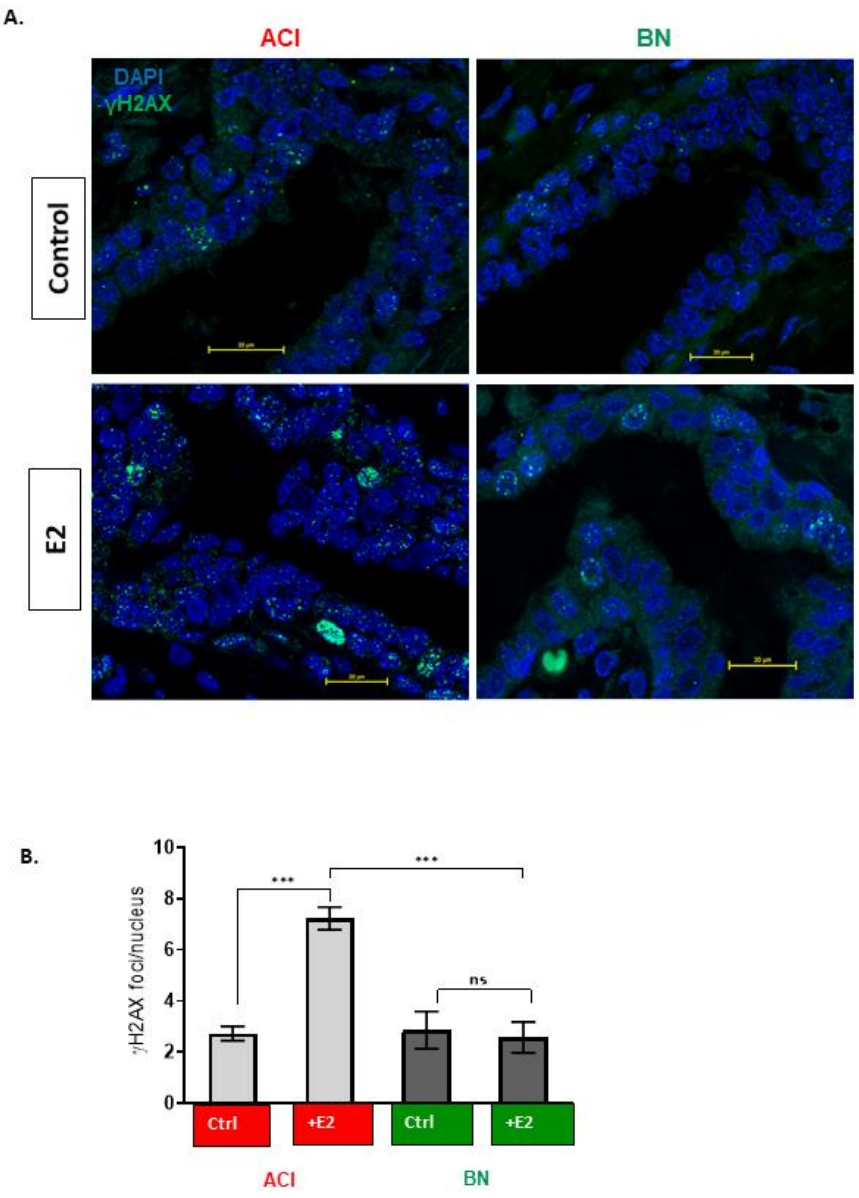

Figure 3.6: E2 induced DNA damage in mammary gland epithelium of 7 days treated ACI and BN rat strain.

(A) Immunostaining of mammary epithelium with γH2AX antibody, harvested from ACI and BN rat strain treated with control (n=5) or E2 (n=5). Each image shows a ductal structure with nucleus stained with DAPI (blue) and γH2AX (green). Scale bar = 20μM. **(B)** Quantification of immunostaining data of γH2AX foci inside the nucleus. ***p > 0.0001 compared to control with treatments using one-way analysis of variance (ANOVA) followed by Tukey's honestly significant difference (HSD) multiple-range test. All graphs show mean ± SEM. *Data collection in collaboration with Dr. James D. Shull and Amy L. Roberts.*

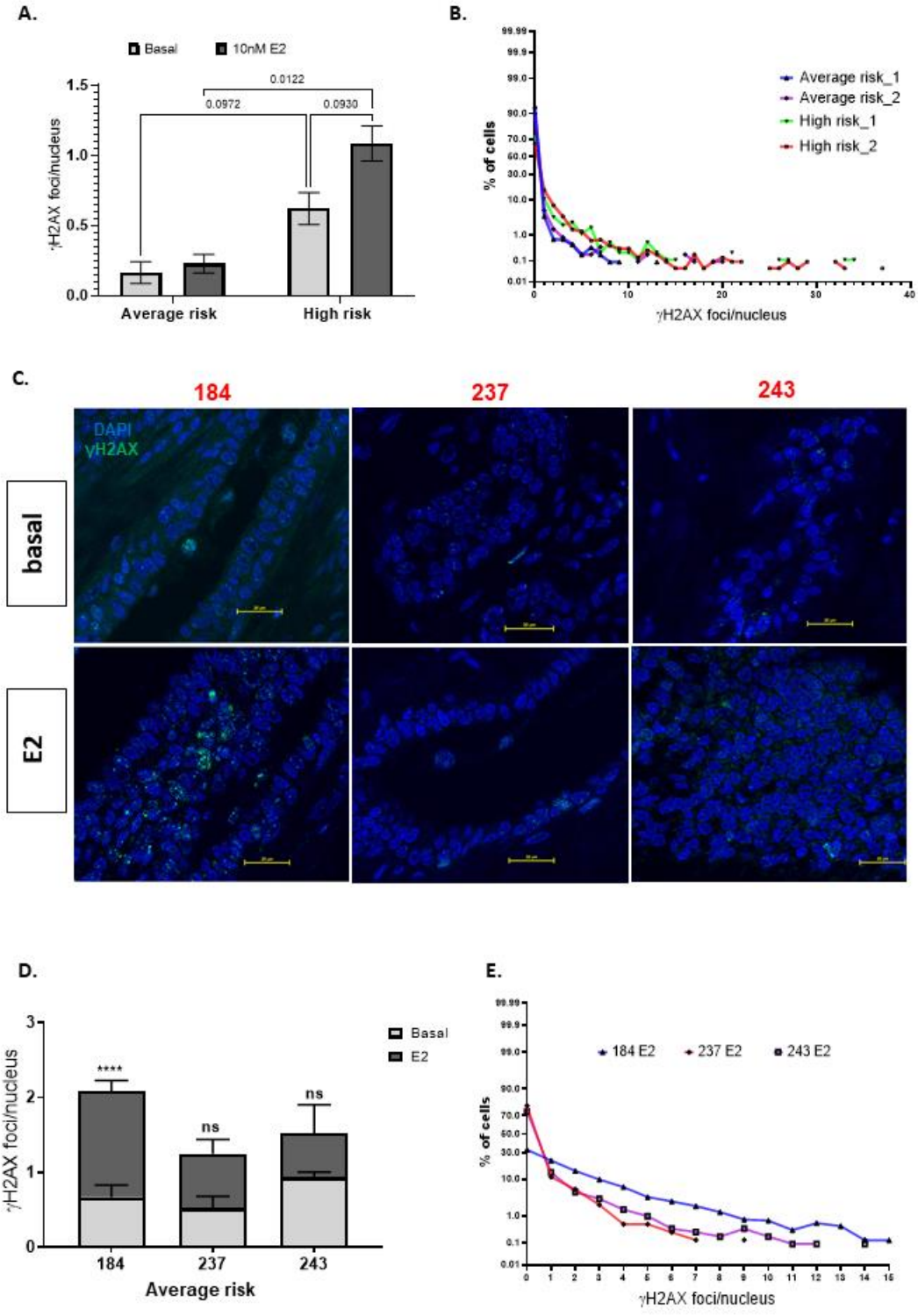
A.
Basal
10nM E2
0.0122
0.0972
0.0930
γH2AX foci/nucleus
Average risk
High risk
B.
Average risk_1
Average risk_2
High risk_1
High risk_2
% of cells
γH2AX foci/nucleus
C.
184
237
243
DAPI
γH2AX
basal
E2
D.
Basal
E2
****
ns
ns
γH2AX foci/nucleus
184
237
243
Average risk
E.
184 E2
237 E2
243 E2
% of cells
γH2AX foci/nucleus

Figure 3.7. E2 induced DNA damage in a subset of human breast tissue explants.
(A) Quantification of γH2AX foci per nucleus in the breast epithelium of average risk patients (normal) undergoing reduction mammoplasty and high-risk patients undergoing prophylactic mastectomy (n=2 in each group). **(B)** The frequency distribution graph was generated using the number of γH2AX foci/nucleus in the breast epithelial cells (%) from E2 treated average risk and high-risk patients. **(C)** Representative images of γH2AX immunostaining in human breast explants. Scale bar = 20µM. **(D)** Quantification of γH2AX foci per nucleus in the breast epithelium of 3 average risk patients treated with basal media or E2 (10nM). **(E)** The frequency distribution graph was generated using the number of γH2AX foci/nucleus in the breast epithelial cells (%) from E2 treated average risk patients. ****$p<0.0001$ compared control with treatments using one-way analysis of variance (ANOVA) followed by Tukey's honestly significant difference (HSD) multiple-range test. All graphs show mean ± SEM.

CHAPTER -4

Estrogen induces DNA damage and R-loop stabilization mediated by ROS-dependent DNA G-quadruplex (G4) structures.

Introduction

DNA can adopt multiple alternative conformations which differ from canonical B-DNA structure. Non-B DNA structures, such as co-transcriptional DNA: RNA hybrids also known as R-loops, are three-stranded nucleic acid structures. R-loops are formed when the nascent RNA hybridizes with the template DNA strand causing transient displacement of the non-template strand. R-loops are a normal consequence of transcription, however unscheduled or persistent R loops may form due to a lack of resolvases. The persistence of R loops can induce DNA damage responses that result in DNA double-strand breaks (Aguilera and García-Muse, 2012a; Skourti-Stathaki and Proudfoot, 2014; Sollier and Cimprich, 2015). Reactive oxygen species (ROS) have been shown to also play a role in R-loop formation at actively transcribed regions (Teng et al., 2018). Recently, the hormone estrogens (E2, 17β-estradiol) and endocrine-disrupting chemicals (Benzophenone-3, BP-3) were shown to induce DNA damage in breast epithelial cells by promoting R loops mediated by estrogen receptor α-mediated (ER) (Majhi et al., 2020; Stork et al., 2016). BP-3 induces DNA damage independent of proliferation (Majhi and Sharma et al., 2020). In addition, E2 also induces ER-dependent and -independent ROS causing oxidative stress

and DNA damage to promote breast cancer (Felty et al., 2005; Mobley and Brueggemeier, 2004; Okoh et al., 2011; Roy et al., 2007; Tian et al., 2016).

Similarly, another non-canonical DNA secondary structure known as G quadruplexes (G4s) is formed at single-stranded guanine-rich DNA sequences. DNA G4s arise from Hoogsteen hydrogen bonding of four guanine residues arranged within a planar G-quartet. Self-stacking of two or more G-quartets generates a G4 structure that is stabilized by monovalent cations such as K^+ and Na^+ (Kwok and Merrick, 2017). DNA G4s play a crucial role in several biological functions such as transcription, replication, and telomere maintenance but also promotes genomic instability (Rhodes and Lipps, 2015; T. Tian et al., 2018). With the advancement of Next Generation Sequencing (NGS) technologies, G4s have been mapped to critical regions such as promoters, replication origins, and telomeres (Hänsel-Hertsch et al., 2016; Langley et al., 2016; Maizels, 2006; Zahler et al., 1991).

Previous literature has shown the cooperative relationship between G4s and R loops to form a stable structure called G-loops. G-loops are the co-existence of G4 and R-loop, where R loops are formed on the template DNA and G4 on the displaced non-template DNA strand (Duquette et al., 2004; Magis et al., 2018; Tan et al., 2020; Tan and Lan, 2020). For instance, G4 ligands such as Pyridostatin (PDS) were shown to stabilize G4 structures in cancer cells and increased levels of G4s and R loops were colocalized (G-loops) as well as DNA damage (Magis et. al. 2018). Another study showed the co-existence of G4, and R-loop (G-loop) mediated by ROS at transcriptionally active sites and that, if such stable structures are unresolved, these delay the repair of DNA damage (Tan et al., 2020).

The formation of transient R-loops is a general indicator of transcription activation in response to E2. Therefore, we investigated the role of ER-mediated secondary DNA structures and their role in DNA damage in breast cells. Here, we show that treatment with E2 and BP-3 promotes DNA G4 formation in the ER+ breast cancer cells. Approximately, half of the G4 foci induced by E2 and BP-3 treatment in the cells colocalize with R-loops indicating G-loop formation, but these structures were blocked by treatment with ROS scavenger. These data suggest a mechanism in which E2, and BP-3 bind to ER to induce ROS-mediated G4 formation promoting stabilization of G-loops and leading to increased DNA damage.

Materials and Methods

Cell culture and treatments:

T47D (ATCC #HTB-1330), and MCF-7(ATCC #HTB 22) cells were passaged in growth media containing phenol-red free (PRF) DMEM-F12 (Sigma #D6434) or MEM 1x (Gibco #51200-038) with 10% heat inactivated FBS (Omega Scientific # FB-02) and 10 µg/ml insulin (Sigma #9278), 2 mM L-glutamine (Hyclone # SH30034.01), gentamycin 15 µg/ml (Gibco #15750-060) and 1X antibiotics/antimycotics (AB/AM, Gibco #15240-062) and incubated at 37^{o}C with 5% CO_2. For experiments, cells were grown in clearing media with charcoal-stripped serum (CSS) (MEM 1x with 10% charcoal-dextran treated FBS (Omega Scientific #FB-04), and 2 mM L-glutamine) for 48 h before being plated for experiments. T47D and MCF7 cells were grown in clearing media for 48 h and plated on 20 mm glass uncoated coverslips in 12 well plates with a density of 2 x 10^5 cells/well. Cells were treated with 10nM or 100nM E2, 5 µM BP3, 10uM PDS (G4 stabilizer) with or without 10 mM N-acetyl cysteine (NAC) for 16-18 hrs.

Immunostaining

Cells were fixed in 4% PFA for 20 mins at RT and quenched with 0.1 M Glycine for 15 mins. Cells were permeabilized with 0.5% Triton-X 100. Cells were washed with two times with PBS. Cells were incubated with 20ug of RNase A at 37C for 30 mins to eliminate RNA G4s and then washed 3 times with PBS. Cells were blocked in 10% goat serum with 0.1% Tween20 for 1hr at room temperature (RT), incubated overnight with anti-γH2AX antibody (Cell Signaling # 9718S), 1H6 (Millipore) or BG4 (Millipore) at 4°C

followed by 1 hour with anti-rabbit Alexa Fluor Plus-488-conjugated secondary antibody (ThermoFisher) or anti-mouse Alexa Fluor Plus-488-conjugated (ThermoFisher) at RT. Cells were mounted with Vectashield mounting medium containing DAPI (Vector Laboratories # H-1200). For BG4, Cells were incubated with 1:800 of DYKDDDDK Tag antibody (Cell Signaling ref #2368) in 5% goat serum for 1 hour at RT before the secondary incubation. Slides were imaged at 60X (immersion oil) with Nikon A1 Spectral Confocal microscope. Analysis of γH2AX, BG4 and 1H6 foci per nucleus was calculated using Nikon analysis software, where DAPI was used as a mask for the nucleus.

Co-staining of cells with BG4 and S9.6 antibodies.

Cell were fixed with ice-cold methanol at room temperature (RT) for 10 minutes. After a brief wash with PBS, cells were permeabilized with 0.5% Triton™ X-100 in PBS at RT for 15 minutes. Cells were blocked with 8% BSA/PBS and then incubated with 2 μg per slide each of BG4 and S9.6 antibodies diluted in 2% BSA/PBS for 2 hours. Cells were then incubated with 1:800 of DYKDDDDK Tag antibody (Cell Signaling ref #2368) in 2% BSA/PBS for 1 hour. Next, cells were incubated at RT with 1:1000 Alexa Fluor 594 goat Anti-Mouse IgG and Alexa Fluor 488 goat anti-rabbit IgG in 2% BSA/PBS for 1 hour. After each step, cells were washed with PBS. Cells were mounted with Vectashield mounting medium containing DAPI (Vector Laboratories # H-1200). Slides were imaged at 60X (immersion oil) with Nikon A1 Spectral Confocal microscope. Analysis of BG4 and S9.6 foci per nucleus was calculated using Nikon analysis software, where DAPI was used as a mask for the nucleus.

Statistical Analysis

Unless specified, data were analyzed by one-way or two-way analysis of variance (ANOVA) followed by Tukey's honestly significant difference (HSD) multiple-range test using GraphPad Prism 9 statistical analysis software. Results are presented as mean ± standard error of the mean (S.E.M.). Data were considered statistically significant at $p < 0.05$.

Results

E2 and BP-3 induce G4 formation.

Activation of ER by E2 stimulates both transcription of target genes within minutes and proliferation becomes evident after about 24 h when foci of γH2AX become prevalent indicating the presence of DNA double strand breaks. BP-3 was used in these studies as it also induces γH2AX foci but without significant transcription of target genes or proliferation. Therefore, the effects of transcription and proliferation can be discriminated by comparing responses to E2 and BP-3. The concentration of E2 (10 and 100nM) was selected to approximate the range found during pregnancy in women. The median urinary concentration of BP-3 in pregnant women is ~0.5μM and greater than 30μM in the 95th percentile. Therefore, 5μM BP-3 was used to reflect levels of exposure that are common in US women.

We first sought to characterize the G4 formation in response to E2 and BP-3 in ER-positive breast epithelial cancer cell lines – T47D and MCF7 cells. Cells were hormone starved for 48 hours and then treated with the compounds for 16-18 hrs. After treatment, we performed immunofluorescence with G4 specific antibody – BG4 in the breast cancer cells and measured the amount of G4 foci present inside the nucleus (**Figure 4.1A**). We observed that basal levels of G4 foci are present in the untreated (control) T47D and MCF7 cells. Cells treated with E2 causes a significant increase in the number of G4 foci when compared with control treatment in both cell lines with no differences between the 10 and 100nM concentrations. Treatment with 5uM BP-3 showed similar induction of G4 foci in

both MCF7 and T47D cells **(Figure 4.1 A, B, and C)**. Taken together, these results demonstrate that E2 and BP-3 induce G4 formation in the ER+ breast cancer cells.

E2 and BP-3 induce colocalization of G4s and R loops.

Recently, we have shown that E2 and BP3 cause R-loop formation in T47D and MCF7 cells (Majhi et al., 2020). G4 formation has been shown to co-exist with R-loop structures, forming a stable structure called G-loops (Magis et al., 2018; Tan et al., 2020). Next, we wanted to investigate whether G4, and R loop structures induced by E2, and BP-3 are formed in a similar vicinity. Therefore, we colocalized BG4 (G4 antibody) and S9.6 (R-loop antibody) immunofluorescence and measured the % of overlapping BG4 and S9.6 signals in both T47D and MCF7 cells (**Figure 4.2 A**).

Untreated T47D cells showed low levels of colocalization (median=20%) of G4 and R loop foci. In MCF7 cells, there was very little colocalization (median=0%) (**Figure 4.2 B and C**). However, cells treated with E2 (10nM and 100nM) showed a significant increase in colocalization of G4 and R-loop signals as seen by yellow foci in the merged images of green and red foci (**Figure 4.2 A, lower panel**). Treatment with 10nM E2 showed 40% colocalization and 50 – 59% colocalization was observed in 100nM E2 treatment of T47D and MCF7 cells (**Figure 4.2 B and C**). Treatment with 5uM BP-3 treatment resulted in 40% and 57% colocalization of G4 and R-loop signals in T47D and MCF7 cells (**Figure 4.2 B and C**). Almost half of the G4 foci induced by E2 and BP3 are overlapping with the R-loop signals, which suggests that E2 and BP-3 promote G-loop formation.

E2 and BP-3 induced G4s, and DNA damage is ROS dependent.

Previous studies have shown that ROS plays a role in the induction of G4 formation in cancer cells (Tan et al., 2020; Tan and Lan, 2020) and that E2 causes induction of ROS via estrogen receptor-dependent or independent mechanism (Maleki et al., 2015; Okoh et al., 2011; Roy et al., 2007; Tian et al., 2016). We hypothesized that in ER+ breast cancer cells, E2 and BP-3 could induce G4 formation mediated by the ROS mechanism. To determine the ROS-mediated G4 formation, we treated the cells with or without ROS inhibitor/scavenger - N-acetyl cysteine (NAC) along with 10nM E2, 5uM BP-3. The G4 ligand Pyridostatin (PDS) was included as a positive control to directly stabilize G4 structures. For these experiments, we performed immunostaining with another G4 specific antibody – 1H6 in an effort to confirm the results obtained with BG4 and measured the number of 1H6 foci present inside the nucleus (**Figure 4.3A**).

In control cells, treatment with the ROS scavenger (NAC) did not significantly affect basal levels of nuclear G4 foci. This indicates that a subset of G4s is present and are independent of ROS (**Figure 4.3A and B**). Cells treated with 10nM E2, 5uM BP-3, and 10uM PDS showed a significant increase in the number of G4 foci inside the nucleus. However, the presence of NAC blocked the formation of G4 foci in E2 and BP-3 treated cells resulting in levels similar to that in control cells (**Figure 4.3A and B**). Cells treated with 10uM PDS (G4 stabilizer) showed no change in the number of G4 foci with or without the presence of ROS scavenger, which is expected to observe because PDS directly stabilizes G4 structures.

We also examined the DNA damage response by immunostaining with DNA double-strand break marker - γH2AX. Previously, we have shown that E2 and BP3 cause

induction of DNA damage (Majhi and Sharma et. al., 2020). Here, we observed similar findings that E2 and BP-3 treatments showed significant increases in γH2AX foci when compared with the control-treated T47D and MCF7 cells (**Figure 4.4A, B and C**). As expected, treatment with G4 stabilizer – PDS causes significant induction of DNA damage in both cell lines. Interestingly, cells treated with E2 and BP-3 in the presence of NAC showed a significant reduction of γH2AX foci which suggests that DNA damage induced by E2 and BP3 is dependent on ROS (**Figure 4.4A, B and C**). On the other hand, PDS treatment in the presence or absence of NAC showed no significant changes in the number of γH2AX foci. Overall, our results demonstrate that E2 and BP3 induce ROS-mediated G4 formation and DNA damage.

Discussion

Since the discovery of canonical right-handed DNA double-helical structure (B-DNA) in 1953, many non-B DNA conformations have been reported to form at repetitive sequences (Ghosh and Bansal, 2003; Sharma, 2011). The non-canonical secondary structures, such as DNA: RNA hybrids (R-loops) and G-quadruplexes (G4), act as a double-edged sword that is involved in both biological and pathological functions such as transcriptional regulation, telomere maintenance, and genomic instability. Physiological R-loops and G4s are programmed processes and form transiently for their biological functions (Ohle et al., 2016; Pavri, 2017; Qiao et al., 2017). On the other side, stabilized or pathological R-loops and G4s that occur in an unscheduled manner can cause genomic instability. These non-canonical secondary structures forming during gene transcription and DNA replication can result in DNA double-strand breaks (Aguilera and García-Muse, 2012b; García-Muse and Aguilera, 2019; Rhodes and Lipps, 2015). The DNA damage and genomic instability arises from these structures due to transcriptional pausing, replication stress or transcription-replication conflicts. Multiple RNA processing factors and helicases have been shown to be involved in the resolution of R-loops and G4 structures. Failure to resolve R-loops and G4s can allow these structures to accumulate to pathological levels and cause genomic instability. Disruption of genes involved in resolution of R-loops and G4s have been linked to human diseases such as neurological disorders and cancers (Groh and Gromak, 2014; Maizels, 2015; Richard and Manley, 2017). In the context of breast cancer, the tumor suppressor proteins BRCA1 and BRCA2 have been shown to resolve pathological R loop structures as well as participating in homology-directed repair of DNA

double strand breaks (Chiang et al., 2019; D'Alessandro et al., 2018; Hatchi et al., 2015; Shivji et al., 2018).

Multiple studies have shown that R-loops are more prevalent in genomic regions that are G-rich. During transcription, the non-template DNA strand is displaced allowing G4 structures to form in the single-stranded DNA strand (Ginno et al., 2013, 2012; Reaban et al., 1994; Skourti-Stathaki and Proudfoot, 2014). Recent studies have shown the co-existence of the R-loop and G4 to form a unique stable structure called as "G-loop", where those G-rich sequences on the non-template strand fold into a G4 structure and R-loops on the template DNA strand (Lee et al., 2020). Using electron microscopy, (Duquette et al., 2004), showed the first evidence of the existence of G-loop structure *in vitro* and in *Escherichia coli*. Another study used G4 ligands, such as Pyridostatin (PDS), to stabilize G4 structures in human cancer cells and observed that G4 ligands induce DNA damage by R-loops stabilization (Magis et al., 2018). In these studies, 50 - 60% of stabilized G4s colocalized with R-loops. Importantly, R-loops allow G4 formation and those G4s reversibly stabilize the R-loop structure as a feedback loop indicating the interrelationship of G4 and R-loop (Tan et al., 2020). The kinetics of R-loop and G4 formation was found to be similar in the cells at different timepoints and failure to resolve these structures promotes DNA damage and delays the repair process.

Here we show that E2 and BP-3 induce G4 formation in the estrogen receptor-positive MCF7 and T47D breast cancer cells using two G4 specific antibodies – BG4 and 1H6 **(Figure 4.1 and Figure 4.3)**. Almost 50% of the G4 foci induced by E2 and BP3 were observed in a similar vicinity with the R-loops as performed by colocalization of S9.6 and BG4 **(Figure 4.2)**. This suggests that E2 and BP-3 induce R-loops that favor "G-loop"

formation in breast cancer cells. The extent of G4 and R loop colocalization by E2 and BP-3 treatment was found to be similar to the G4 ligands used in Magis et. al., 2018. Therefore, ER ligands have the potential to stimulate ongoing mutagenesis in ER+ breast cancer cells.

Previous literature has demonstrated the mechanistic connection between Reactive Oxygen Species (ROS) and G4 formation (Fleming et al., 2017; Fleming and Burrows, 2019; Roychoudhury et al., 2020). Recently, it was shown that ROS induces G4 formation at actively transcribed regions (Tan et al., 2020). Besides, it is already known E2 induces ROS, which causes oxidative stress and DNA damage (Felty et al., 2005; Mobley and Brueggemeier, 2004; Okoh et al., 2011; Roy et al., 2007; Tian et al., 2016). In the present study, our findings demonstrate that the levels of E2 and BP-3 induced G4 foci in the cells were significantly reduced with the presence of ROS scavenger (**Figure 4.3**). Similarly, we observed that the DNA damage marker – γH2AX foci were also significantly reduced in E2 and BP-3 treated cells when ROS was inhibited (**Figure 4.4**). This indicates that ROS plays an important role to induce G4 formation and DNA damage. We proposed a mechanistic model of E2, and BP-3 induced DNA damage **(Figure 4.5)**. According to the model, E2 and BP-3 bind with the estrogen receptor to trigger R-loop formation, and the R-loops are stabilized by G4 formation mediated by the ROS mechanism. This promotes G-loop formation and is associated with DNA damage. Therefore, we have uncovered a G4 and R-loop relationship as an intermediate of DNA damage mechanism by estrogens.

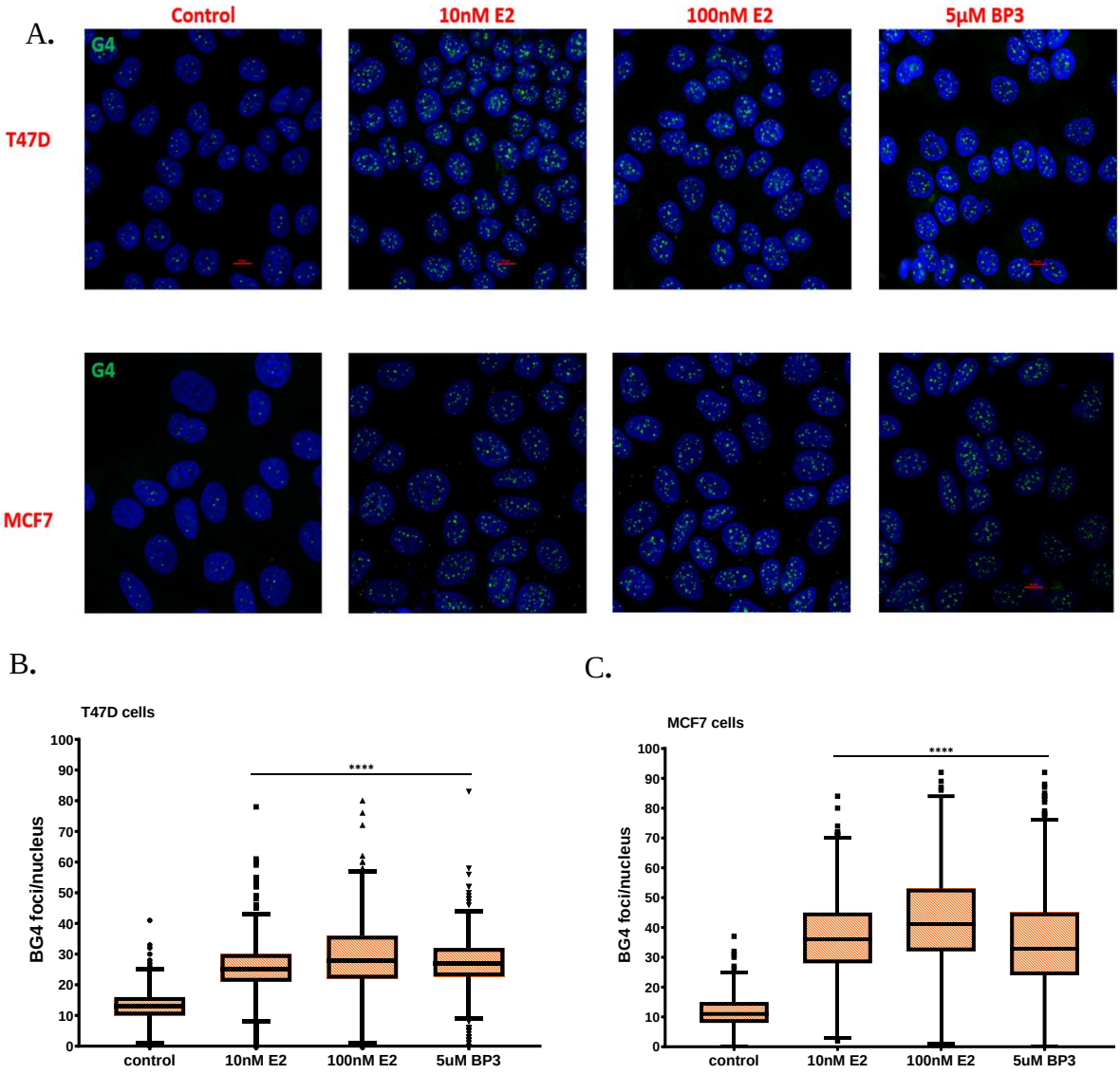

Figure 4.1. Evaluation of G4 formation in cells treated with 17β-Estradiol (E2), Benzophenone-3 (BP3).

(**A**) Immunofluorescence of BG4 foci in T47D and MCF7 cells treated with 10 or 100nM E2 and 5µM BP3. (**B and C**) Quantification of nuclear BG4 foci in T47D and MCF-7 cells treated with control, E2 and BP-3. ****p < 0.0001 compared control with treatments using one-way analysis of variance (ANOVA) followed by Tukey's honestly significant difference (HSD) multiple-range test. Scale bar = 10 µM. All graphs show box plots with interquartile range and central line as median.

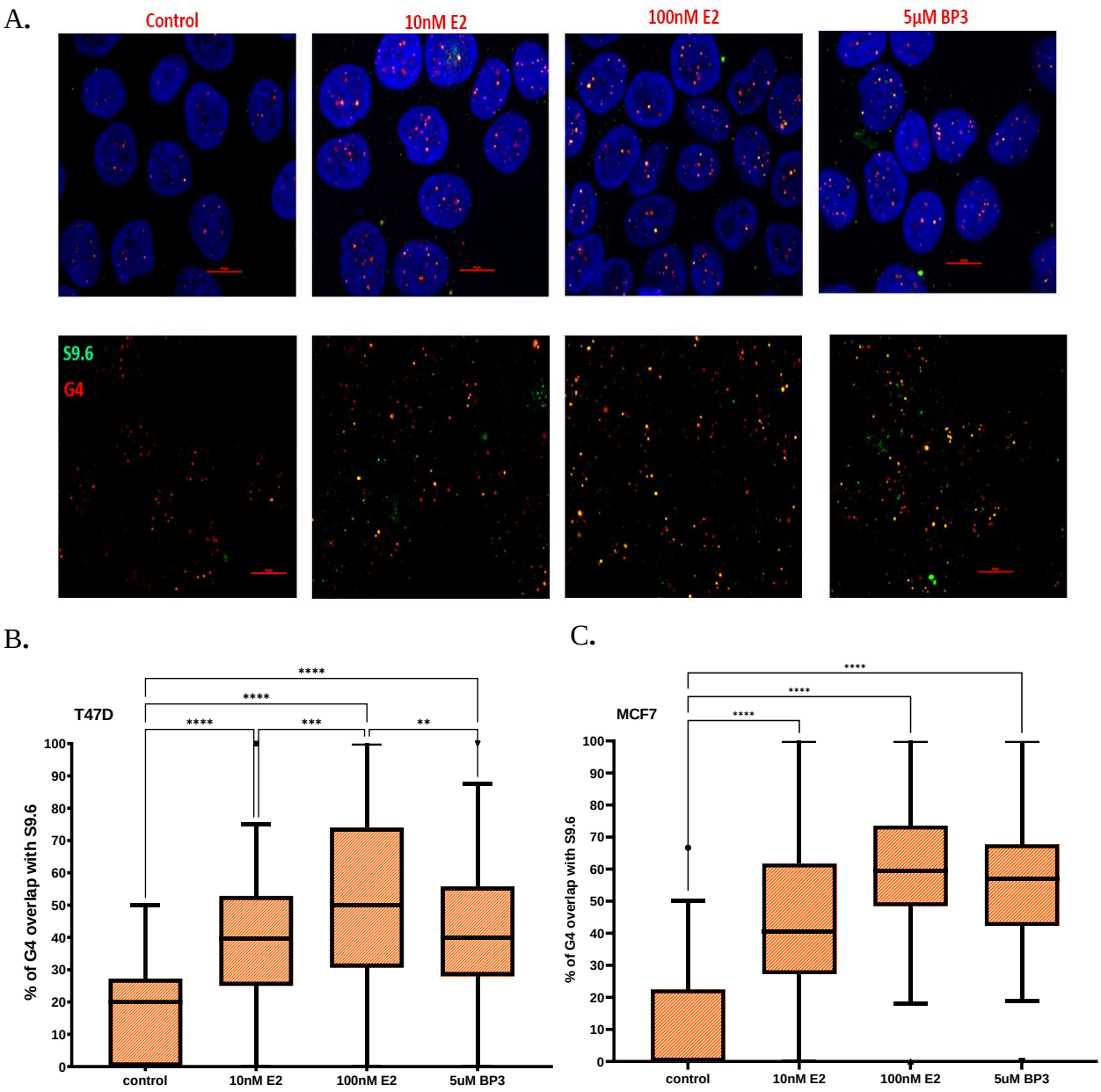

Figure 4.2 Evaluation of G4 and R loop colocalization in cells treated with E2 and BP-3. (**A**) Co-staining of BG4 and S9.6 foci in T47D and MCF7 cells treated with 10 or 100nM E2 and 5µM BP3. (Upper panel) - BG4 and S9.6 colocalization confocal images with DAPI (blue) masked as a nucleus. (Lower panel) – Only BG4 and S9.6 channel to show clear yellow foci indicating G-loops. (**B and C**) Quantification of nuclear BG4 foci in T47D and MCF-7 cells treated with control, E2 and BP-3. **p=0.003 ***p=0.0003 ****p < 0.0001 compared control with treatments using one-way analysis of variance (ANOVA) followed by Tukey's honestly significant difference (HSD) multiple-range test. Scale bar = 10 µM. All graphs show box plots with interquartile range and central line as median.

A.

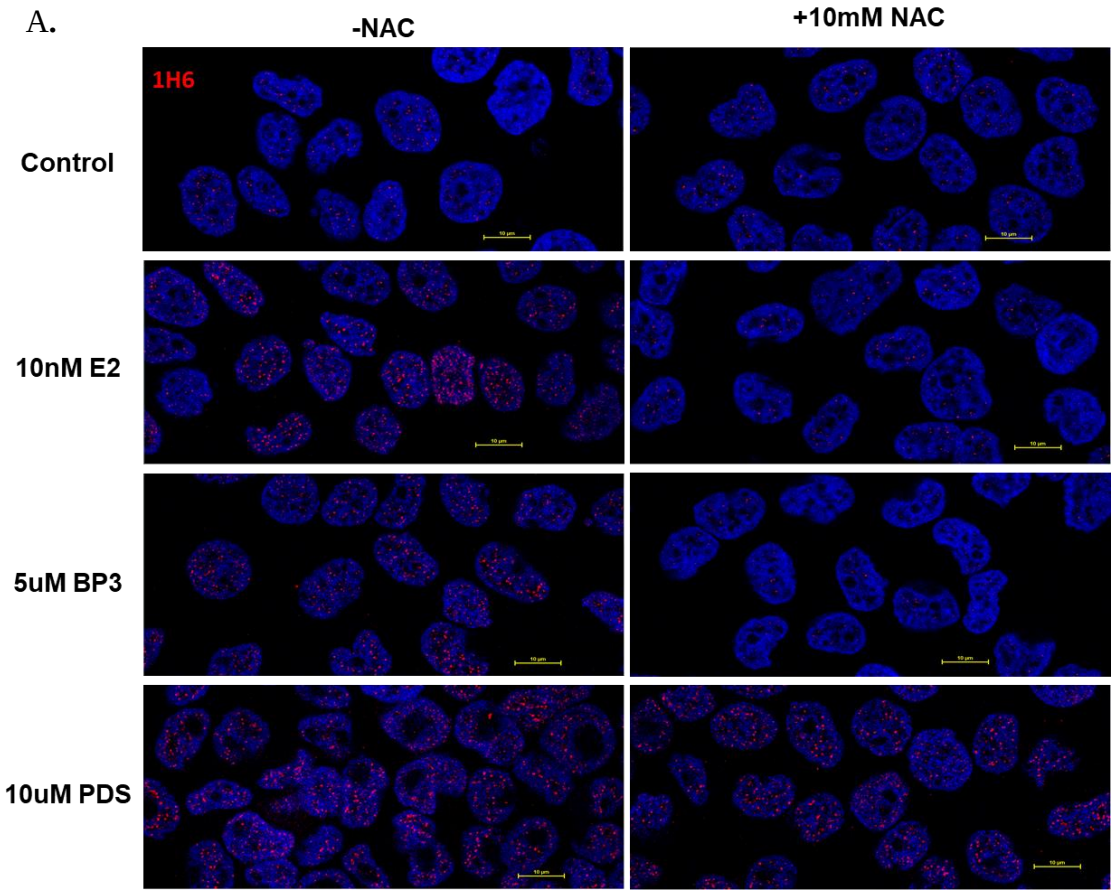
-NAC
+10mM NAC
1H6
Control
10nM E2
5uM BP3
10uM PDS

B.

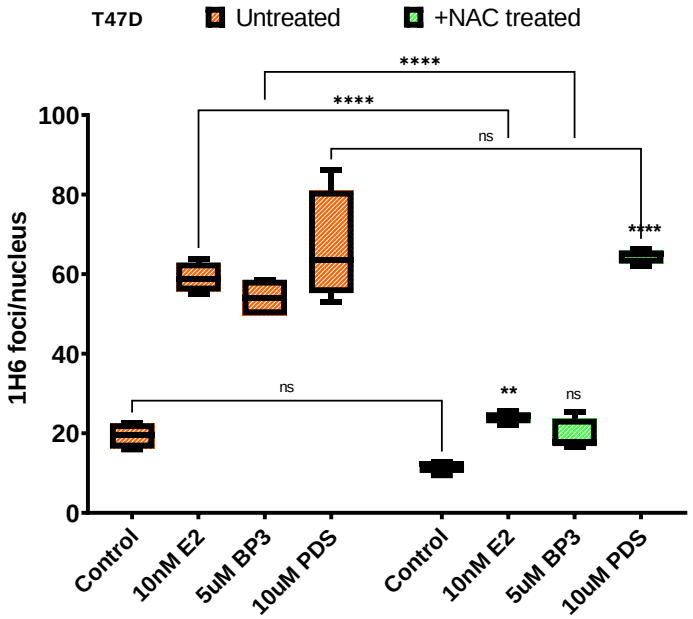
T47D
Untreated
+NAC treated
1H6 foci/nucleus
****
****
ns
****
ns
**
ns
0
20
40
60
80
100
Control
10nM E2
5uM BP3
10uM PDS
Control
10nM E2
5uM BP3
10uM PDS

Figure 4.3 Evaluation of G4 formation in cells treated with E2, BP-3 and PDS with or without the presence of ROS scavenger (NAC).

(**A**) Immunofluorescence of 1H6 foci in T47D cells treated with 10nM E2, 5μM BP3, 10uM PDS, and 10mM NAC. (**B**) Quantification of nuclear 1H6 foci in T47D treated with control, E2, BP-3, PDS and NAC. **p < 0.01 ****p < 0.0001 compared control with treatments using two-way analysis of variance (ANOVA) followed by Tukey's honestly significant difference (HSD) multiple-range test. Scale bar = 10 μM. All graphs show box plots with interquartile range and central line as median.

A.

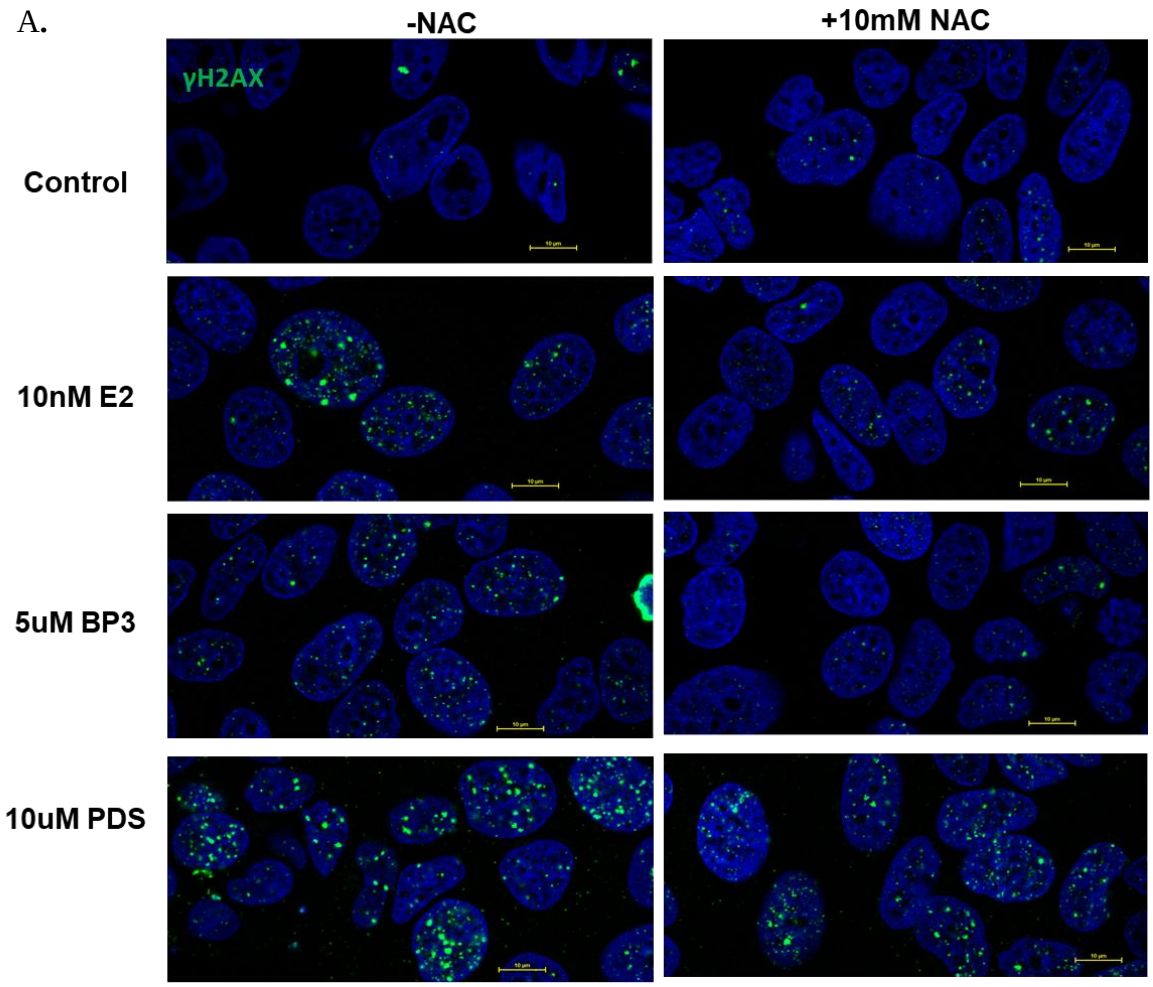
-NAC
+10mM NAC
γH2AX
Control
10nM E2
5uM BP3
10uM PDS

B.

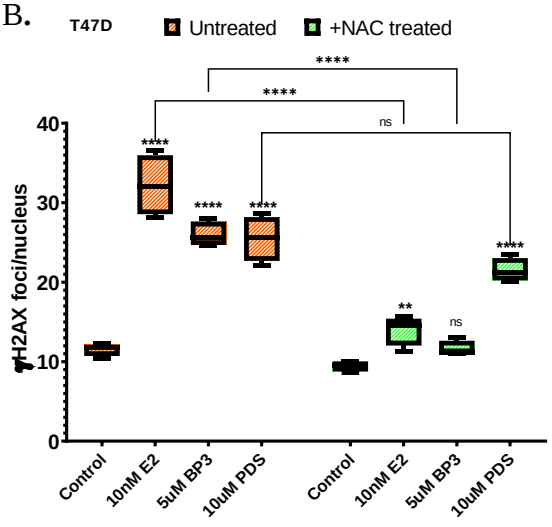
T47D
Untreated
+NAC treated
γH2AX foci/nucleus
Control
10nM E2
5uM BP3
10uM PDS

C.

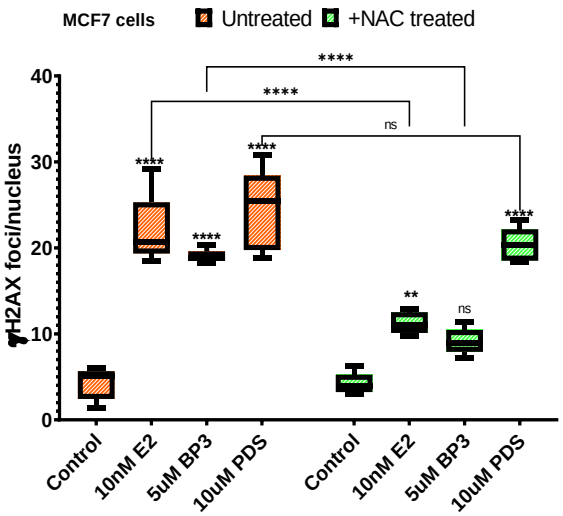
MCF7 cells
Untreated
+NAC treated
γH2AX foci/nucleus
Control
10nM E2
5uM BP3
10uM PDS

Figure 4.4. Evaluation of γH2AX formation in cells treated with E2, BP-3 and PDS with or without the presence of ROS scavenger (NAC).

(**A**) Immunofluorescence of γH2AX foci in MCF7 cells treated with 10nM E2, 5μM BP3, 10uM PDS, and 10mM NAC. (**B and C**) Quantification of nuclear γH2AX foci in T47D and MCF7 cells treated with control, E2, BP-3, PDS and NAC. **p < 0.01 ****p < 0.0001 compared control with treatments using two-way analysis of variance (ANOVA) followed by Tukey's honestly significant difference (HSD) multiple-range test. Scale bar = 10 μM. All graphs show box plots with interquartile range and central line as median.

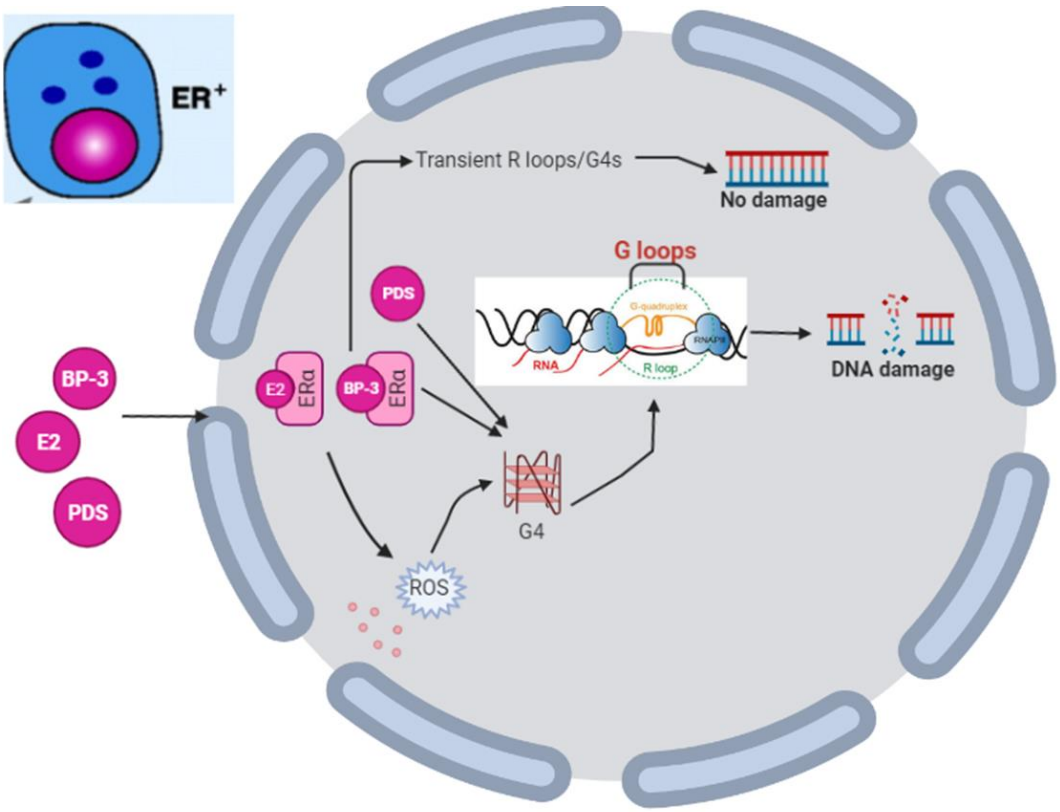

Figure 4.5. Mechanism of DNA damage induction by E2 and BP-3.
E2 and BP-3 binds with the receptor and simulates G4 and R-loops formation simultaneously to form G-loops which is associated with DNA damage. E2 and BP-3 induced G4 formation and DNA damage is mediated by ROS. PDS – a G4 ligand directly stabilizes G4 structures to cause DNA damage.

References

Adamovic, T., Roshani, L., Chen, L., Schaffer, B.S., Helou, K., Levan, G., Olsson, B., Shull, J.D., 2007. Nonrandom pattern of chromosome aberrations in 17β-estradiol-induced rat mammary tumors: Indications of distinct pathways for tumor development. Genes Chromosomes Cancer 46, 459–469. https://doi.org/10.1002/gcc.20428

Aguilera, A., García-Muse, T., 2012a. R Loops: From Transcription Byproducts to Threats to Genome Stability. Mol Cell 46, 115–124. https://doi.org/10.1016/j.molcel.2012.04.009

Aguilera, A., García-Muse, T., 2012b. R Loops: From Transcription Byproducts to Threats to Genome Stability. Mol Cell 46, 115–124. https://doi.org/10.1016/j.molcel.2012.04.009

Ahmed, S., Thomas, G., Ghoussaini, M., Healey, C.S., Humphreys, M.K., Platte, R., Morrison, J., Maranian, M., Pooley, K.A., Luben, R., Eccles, D., Evans, D.G., Fletcher, O., Johnson, N., Silva, I. dos S., Peto, J., Stratton, M.R., Rahman, N., Jacobs, K., Prentice, R., Anderson, G.L., Rajkovic, A., Curb, J.D., Ziegler, R.G., Berg, C.D., Buys, S.S., McCarty, C.A., Feigelson, H.S., Calle, E.E., Thun, M.J., Diver, W.R., Bojesen, S., Nordestgaard, B.G., Flyger, H., Dörk, T., Schürmann, P., Hillemanns, P., Karstens, J.H., Bogdanova, N.V., Antonenkova, N.N., Zalutsky, I.V., Bermisheva, M., Fedorova, S., Khusnutdinova, E., SEARCH, Kang, D., Yoo, K.-Y., Noh, D.Y., Ahn, S.-H., Devilee, P., Asperen, C.J. van, Tollenaar, R.A.E.M., Seynaeve, C., Garcia-Closas, M., Lissowska, J., Brinton, L., Peplonska, B., Nevanlinna, H., Heikkinen, T., Aittomäki, K., Blomqvist, C., Hopper, J.L., Southey, M.C., Smith, L., Spurdle, A.B., Schmidt, M.K., Broeks, A., Hien, R.R. van, Cornelissen, S., Milne, R.L., Ribas, G., González-Neira, A., Benitez, J., Schmutzler, R.K., Burwinkel, B., Bartram, C.R., Meindl, A., Brauch, H., Justenhoven, C., Hamann, U., Consortium, G., Chang-Claude, J., Hein, R., Wang-Gohrke, S., Lindblom, A., Margolin, S., Mannermaa, A., Kosma, V.-M., Kataja, V., Olson, J.E., Wang, X., Fredericksen, Z., Giles, G.G., Severi, G., Baglietto, L., English, D.R., Hankinson, S.E., Cox, D.G., Kraft, P., Vatten, L.J., Hveem, K., Kumle, M., Sigurdson, A., Doody, M., Bhatti, P., Alexander, B.H., Hooning, M.J., Ouweland, A.M.W. van den, Oldenburg, R.A., Schutte, M., Hall, P., Czene, K., Liu, J., Li, Y., Cox, A., Elliott, G., Brock, I., Reed, M.W.R., Shen, C.-Y., Yu, J.-C., Hsu, G.-C., Chen, S.-T., Anton-Culver, H., Ziogas, A., Andrulis, I.L., Knight, J.A., kConFab, Group, A.O.C.S., Beesley, J., Goode, E.L., Couch, F., Chenevix-Trench, G., Hoover, R.N., Ponder, B.A.J., Hunter, D.J., Pharoah, P.D.P., Dunning, A.M., Chanock, S.J., Easton, D.F., 2009. Newly discovered breast cancer susceptibility loci on 3p24 and 17q23.2. Nat Genet 41, 585–590. https://doi.org/10.1038/ng.354

Albrektsen, G., Heuch, I., Hansen, S., Kvåle, G., 2005. Breast cancer risk by age at birth, time since birth and time intervals between births: exploring interaction effects. Brit J Cancer 92, 167–175. https://doi.org/10.1038/sj.bjc.6602302

Anderson, E., Clarke, R.B., 2004. Steroid Receptors and Cell Cycle in Normal Mammary Epithelium. J Mammary Gland Biol 9, 3–13. https://doi.org/10.1023/b:jomg.0000023584.01750.16

Aupperlee, M.D., Drolet, A.A., Durairaj, S., Wang, W., Schwartz, R.C., Haslam, S.Z., 2008. Strain-Specific Differences in the Mechanisms of Progesterone Regulation of Murine Mammary Gland Development. Endocrinology 150, 1485–1494. https://doi.org/10.1210/en.2008-1459

Azvolinsky, A., Giresi, P.G., Lieb, J.D., Zakian, V.A., 2009. Highly Transcribed RNA Polymerase II Genes Are Impediments to Replication Fork Progression in Saccharomyces cerevisiae. Mol Cell 34, 722–734. https://doi.org/10.1016/j.molcel.2009.05.022

Bacolla, A., Tainer, J.A., Vasquez, K.M., Cooper, D.N., 2016. Translocation and deletion breakpoints in cancer genomes are associated with potential non-B DNA-forming sequences. Nucleic Acids Res 44, 5673–5688. https://doi.org/10.1093/nar/gkw261

Bacolla, A., Ye, Z., Ahmed, Z., Tainer, J.A., 2019. Cancer mutational burden is shaped by G4 DNA, replication stress and mitochondrial dysfunction. Prog Biophysics Mol Biology 147, 47–61. https://doi.org/10.1016/j.pbiomolbio.2019.03.004

Baldacci, G., Chérif-Zahar, B., Bernardi, G., 1984. The initiation of DNA replication in the mitochondrial genome of yeast. Embo J 3, 2115–2120. https://doi.org/10.1002/j.1460-2075.1984.tb02099.x

Barroso, S., Herrera-Moyano, E., Muñoz, S., García-Rubio, M., Gómez-González, B., Aguilera, A., 2019. The DNA damage response acts as a safeguard against harmful DNA–RNA hybrids of different origins. Embo Rep 20. https://doi.org/10.15252/embr.201847250

Besnard, E., Babled, A., Lapasset, L., Milhavet, O., Parrinello, H., Dantec, C., Marin, J.-M., Lemaitre, J.-M., 2012. Unraveling cell type–specific and reprogrammable human replication origin signatures associated with G-quadruplex consensus motifs. Nat Struct Mol Biol 19, 837–844. https://doi.org/10.1038/nsmb.2339

Bhatia, V., Barroso, S.I., García-Rubio, M.L., Tumini, E., Herrera-Moyano, E., Aguilera, A., 2014. BRCA2 prevents R-loop accumulation and associates with TREX-2 mRNA export factor PCID2. Nature 511, 362–365. https://doi.org/10.1038/nature13374

Blackburn, A.C., Hill, L.Z., Roberts, A.L., Wang, J., Aud, D., Jung, J., Nikolcheva, T., Allard, J., Peltz, G., Otis, C.N., Cao, Q.J., Ricketts, R.St.J., Naber, S.P., Mollenhauer, J., Poustka, A., Malamud, D., Jerry, D.J., 2007. Genetic Mapping in Mice Identifies DMBT1 as a Candidate Modifier of Mammary Tumors and Breast Cancer Risk. Am J Pathology 170, 2030–2041. https://doi.org/10.2353/ajpath.2007.060512

Blance, R.N., Sims, A.H., Anderson, E., Howell, A., Clarke, R.B., 2009. Normal Breast Tissue Implanted into Athymic Nude Mice Identifies Biomarkers of the Effects of Human Pregnancy Levels of Estrogen. Cancer Prev Res 2, 257–264. https://doi.org/10.1158/1940-6207.capr-08-0161

Bocchinfuso, W.P., Korach, K.S., 1997. Mammary Gland Development and Tumorigenesis in Estrogen Receptor Knockout Mice. J Mammary Gland Biol 2, 323–334. https://doi.org/10.1023/a:1026339111278

Böhringer, M., Obermeier, K., Griner, N., Waldraff, D., Dickinson, E., Eirich, K., Schindler, D., Hagen, M., Jerry, D.J., Wiesmüller, L., 2013. siRNA screening identifies differences in the Fanconi anemia pathway in BALB/c-Trp53+/− with susceptibility versus C57BL/6-Trp53+/− mice with resistance to mammary tumors. Oncogene 32, 5458–5470. https://doi.org/10.1038/onc.2013.38

Boubakri, H., Septenville, A.L. de, Viguera, E., Michel, B., 2010. The helicases DinG, Rep and UvrD cooperate to promote replication across transcription units in vivo. Embo J 29, 145–157. https://doi.org/10.1038/emboj.2009.308

Brinton, L.A., Hoover, R., Fraumeni, J.F., 1983. Reproductive factors in the aetiology of breast cancer. Brit J Cancer 47, 757–762. https://doi.org/10.1038/bjc.1983.128

Brinton, L.A., Schairer, C., Hoover, R.N., Fraumeni, J.F., 2009. Menstrual Factors and Risk of Breast Cancer. Cancer Invest 6, 245–254. https://doi.org/10.3109/07357908809080645

Brooks, J.D., Sung, J.S., Pike, M.C., Orlow, I., Stanczyk, F.Z., Bernstein, J.L., Morris, E.A., 2018. MRI background parenchymal enhancement, breast density and serum hormones in postmenopausal women. Int J Cancer 143, 823–830. https://doi.org/10.1002/ijc.31370

Burns, M.B., Lackey, L., Carpenter, M.A., Rathore, A., Land, A.M., Leonard, B., Refsland, E.W., Kotandeniya, D., Tretyakova, N., Nikas, J.B., Yee, D., Temiz, N.A., Donohue, D.E., McDougle, R.M., Brown, W.L., Law, E.K., Harris, R.S., 2013. APOBEC3B is an enzymatic source of mutation in breast cancer. Nature 494, 366–370. https://doi.org/10.1038/nature11881

Buteau-Lozano, H., Ancelin, M., Lardeux, B., Milanini, J., Perrot-Applanat, M., 2002. Transcriptional regulation of vascular endothelial growth factor by estradiol and

tamoxifen in breast cancer cells: a complex interplay between estrogen receptors alpha and beta. Cancer Res 62, 4977–84.

Byford, J.R., Shaw, L.E., Drew, M.G.B., Pope, G.S., Sauer, M.J., Darbre, P.D., 2002. Oestrogenic activity of parabens in MCF7 human breast cancer cells. J Steroid Biochem Mol Biology 80, 49–60. https://doi.org/10.1016/s0960-0760(01)00174-1

Calafat, A.M., Wong, L.-Y., Ye, X., Reidy, J.A., Needham, L.L., 2008. Concentrations of the Sunscreen Agent Benzophenone-3 in Residents of the United States: National Health and Nutrition Examination Survey 2003–2004. Environ Health Persp 116, 893–897. https://doi.org/10.1289/ehp.11269

Cavalieri, E.L., Rogan, E.G., 2016. Depurinating estrogen-DNA adducts, generators of cancer initiation: their minimization leads to cancer prevention. Clin Transl Medicine 5, 12. https://doi.org/10.1186/s40169-016-0088-3

Cavalieri, E.L., Stack, D.E., Devanesan, P.D., Todorovic, R., Dwivedy, I., Higginbotham, S., Johansson, S.L., Patil, K.D., Gross, M.L., Gooden, J.K., Ramanathan, R., Cerny, R.L., Rogan, E.G., 1997. Molecular origin of cancer: Catechol estrogen-3,4-quinones as endogenous tumor initiators. Proc National Acad Sci 94, 10937–10942. https://doi.org/10.1073/pnas.94.20.10937

Chambers, V.S., Marsico, G., Boutell, J.M., Antonio, M.D., Smith, G.P., Balasubramanian, S., 2015. High-throughput sequencing of DNA G-quadruplex structures in the human genome. Nat Biotechnol 33, 877–881. https://doi.org/10.1038/nbt.3295

Chiang, H.-C., Zhang, X., Li, J., Zhao, X., Chen, J., Wang, H.T.-H., Jatoi, I., Brenner, A., Hu, Y., Li, R., 2019. BRCA1-associated R-loop affects transcription and differentiation in breast luminal epithelial cells. Nucleic Acids Res 47, 5086–5099. https://doi.org/10.1093/nar/gkz262

Chiarle, R., Zhang, Y., Frock, R.L., Lewis, S.M., Molinie, B., Ho, Y.-J., Myers, D.R., Choi, V.W., Compagno, M., Malkin, D.J., Neuberg, D., Monti, S., Giallourakis, C.C., Gostissa, M., Alt, F.W., 2011. Genome-wide Translocation Sequencing Reveals Mechanisms of Chromosome Breaks and Rearrangements in B Cells. Cell 147, 107–119. https://doi.org/10.1016/j.cell.2011.07.049

Chie, W.-C., Hsieh, C., Newcomb, P.A., Longnecker, M.P., Mittendorf, R., Greenberg, E.R., Clapp, R.W., Burke, K.P., Titus-Ernstoff, L., Trentham-Dietz, A., MacMahon, B., 2000. Age at Any Full-term Pregnancy and Breast Cancer Risk. Am J Epidemiol 151, 715–722. https://doi.org/10.1093/oxfordjournals.aje.a010266

Ciarloni, L., Mallepell, S., Brisken, C., 2007. Amphiregulin is an essential mediator of estrogen receptor α function in mammary gland development. Proc National Acad Sci 104, 5455–5460. https://doi.org/10.1073/pnas.0611647104

Clarke, R.B., 2004. Complementary yet distinct roles for oestrogen receptor-α and oestrogen receptor-β in mouse mammary epithelial proliferation. Breast Cancer Res 6, 135. https://doi.org/10.1186/bcr795

Clarke, R.B., Howell, A., Potten, C.S., Anderson, E., 1997. Dissociation between steroid receptor expression and cell proliferation in the human breast. Cancer Res 57, 4987–91.

Clemons, M., Goss, P., 2001. Estrogen and the Risk of Breast Cancer. New Engl J Med 344, 276–285. https://doi.org/10.1056/nejm200101253440407

Cogoi, S., Paramasivam, M., Membrino, A., Yokoyama, K.K., Xodo, L.E., 2010. The KRAS Promoter Responds to Myc-associated Zinc Finger and Poly(ADP-ribose) Polymerase 1 Proteins, Which Recognize a Critical Quadruplex-forming GA-element. J Biol Chem 285, 22003–22016. https://doi.org/10.1074/jbc.m110.101923

Coutts, A.S., Murphy, L.C., 1998. Elevated mitogen-activated protein kinase activity in estrogen-nonresponsive human breast cancer cells. Cancer Res 58, 4071–4.

Cummings, S.R., Eckert, S., Krueger, K.A., Grady, D., Powles, T.J., Cauley, J.A., Norton, L., Nickelsen, T., Bjarnason, N.H., Morrow, M., Lippman, M.E., Black, D., Glusman, J.E., Costa, A., Jordan, V.C., 1999. The Effect of Raloxifene on Risk of Breast Cancer in Postmenopausal Women. Jama 281, 2189. https://doi.org/10.1001/jama.281.23.2189

Cuzick, J., Sestak, I., Bonanni, B., Costantino, J.P., Cummings, S., DeCensi, A., Dowsett, M., Forbes, J.F., Ford, L., LaCroix, A.Z., Mershon, J., Mitlak, B.H., Powles, T., Veronesi, U., Vogel, V., Wickerham, D.L., Group, for the S.C. of B.C.O., 2013. Selective oestrogen receptor modulators in prevention of breast cancer: an updated meta-analysis of individual participant data. Lancet 381, 1827–1834. https://doi.org/10.1016/s0140-6736(13)60140-3

D'Alessandro, G., Whelan, D.R., Howard, S.M., Vitelli, V., Renaudin, X., Adamowicz, M., Iannelli, F., Jones-Weinert, C.W., Lee, M., Matti, V., Lee, W.T.C., Morten, M.J., Venkitaraman, A.R., Cejka, P., Rothenberg, E., Fagagna, F. d'Adda di, 2018. BRCA2 controls DNA:RNA hybrid level at DSBs by mediating RNase H2 recruitment. Nat Commun 9, 5376. https://doi.org/10.1038/s41467-018-07799-2

Dall, G.V., Britt, K.L., 2017. Estrogen Effects on the Mammary Gland in Early and Late Life and Breast Cancer Risk. Frontiers Oncol 7, 110. https://doi.org/10.3389/fonc.2017.00110

Dennison, K.L., Samanas, N.B., Harenda, Q.E., Hickman, M.P., Seiler, N.L., Ding, L., Shull, J.D., 2015. Development and characterization of a novel rat model of estrogen-induced mammary cancer. Endocr-relat Cancer 22, 239–248. https://doi.org/10.1530/erc-14-0539

Ding, L., Zhao, Y., Warren, C.L., Sullivan, R., Eliceiri, K.W., Shull, J.D., 2013. Association of cellular and molecular responses in the rat mammary gland to 17β-estradiol with susceptibility to mammary cancer. Bmc Cancer 13, 573. https://doi.org/10.1186/1471-2407-13-573

Dunphy, K.A., Black, A.L., Roberts, A.L., Sharma, A., Li, Z., Suresh, S., Browne, E.P., Arcaro, K.F., Ser-Dolansky, J., Bigelow, C., Troester, M.A., Schneider, S.S., Makari-Judson, G., Crisi, G.M., Jerry, D.J., 2020. Inter-Individual Variation in Response to Estrogen in Human Breast Explants. J Mammary Gland Biol 1–18. https://doi.org/10.1007/s10911-020-09446-3

Duquette, M.L., Handa, P., Vincent, J.A., Taylor, A.F., Maizels, N., 2004. Intracellular transcription of G-rich DNAs induces formation of G-loops, novel structures containing G4 DNA. Gene Dev 18, 1618–1629. https://doi.org/10.1101/gad.1200804

Easton, D.F., Pooley, K.A., Dunning, A.M., Pharoah, P.D.P., Thompson, D., Ballinger, D.G., Struewing, J.P., Morrison, J., Field, H., Luben, R., Wareham, N., Ahmed, S., Healey, C.S., Bowman, R., Luccarini, C., Conroy, D., Shah, M., Munday, H., Jordan, C., Perkins, B., West, J., Redman, K., Driver, K., Meyer, K.B., Haiman, C.A., Kolonel, L.K., Henderson, B.E., Marchand, L.L., Brennan, P., Sangrajrang, S., Gaborieau, V., Odefrey, F., Shen, C.-Y., Wu, P.-E., Wang, H.-C., Eccles, D., Evans, D.G., Peto, J., Fletcher, O., Johnson, N., Seal, S., Stratton, M.R., Rahman, N., Chenevix-Trench, G., Bojesen, S.E., Nordestgaard, B.G., Axelsson, C.K., Garcia-Closas, M., Brinton, L., Chanock, S., Lissowska, J., Peplonska, B., Nevanlinna, H., Fagerholm, R., Eerola, H., Kang, D., Yoo, K.-Y., Noh, D.-Y., Ahn, S.-H., Hunter, D.J., Hankinson, S.E., Cox, D.G., Hall, P., Wedren, S., Liu, J., Low, Y.-L., Bogdanova, N., Schürmann, P., Dörk, T., Tollenaar, R.A.E.M., Jacobi, C.E., Devilee, P., Klijn, J.G.M., Sigurdson, A.J., Doody, M.M., Alexander, B.H., Zhang, J., Cox, A., Brock, I.W., MacPherson, G., Reed, M.W.R., Couch, F.J., Goode, E.L., Olson, J.E., Meijers-Heijboer, H., Ouweland, A. van den, Uitterlinden, A., Rivadeneira, F., Milne, R.L., Ribas, G., Gonzalez-Neira, A., Benitez, J., Hopper, J.L., McCredie, M., Southey, M., Giles, G.G., Schroen, C., Justenhoven, C., Brauch, H., Hamann, U., Ko, Y.-D., Spurdle, A.B., Beesley, J., Chen, X., Aghmesheh, M., Amor, D., Andrews, L., Antill, Y., Armes, J., Armitage, S., Arnold, L., Balleine, R., Begley, G., Beilby, J., Bennett, I., Bennett, B., Berry, G., Blackburn, A., Brennan, M., Brown, M., Buckley, M., Burke, J., Butow, P., Byron, K., Callen, D., Campbell, I., Chenevix-Trench, G., Clarke, C., Colley, A., Cotton, D., Cui, J., Culling, B., Cummings, M., Dawson, S.-J., Dixon, J., Dobrovic, A., Dudding, T., Edkins, T., Eisenbruch, M., Farshid, G., Fawcett, S., Field, M., Firgaira, F., Fleming, J., Forbes, J., Friedlander, M., Gaff, C., Gardner, M., Gattas, M., George, P., Giles, G., Gill, G., Goldblatt, J., Greening, S., Grist, S., Haan, E., Harris, M., Hart, S., Hayward, N., Hopper, J., Humphrey, E., Jenkins, M., Jones, A., Kefford, R., Kirk, J., Kollias, J., Kovalenko, S., Lakhani, S., Leary, J., Lim, J., Lindeman, G., Lipton, L., Lobb, L., Maclurcan, M., Mann, G., Marsh, D., McCredie, M., McKay, M., McLachlan, S.A., Meiser, B., Milne, R., Mitchell, G., Newman, B., O'Loughlin, I., Osborne, R., Peters, L., Phillips, K., Price, M., Reeve, J., Reeve, T., Richards, R., Rinehart, G., Robinson,

B., Rudzki, B., Salisbury, E., Sambrook, J., Saunders, C., Scott, C., Scott, E., Scott, R., Seshadri, R., Shelling, A., Southey, M., Spurdle, A., Suthers, G., Taylor, D., Tennant, C., Thorne, H., Townshend, S., Tucker, K., Tyler, J., Venter, D., Visvader, J., Walpole, I., Ward, R., Waring, P., Warner, B., Warren, G., Watson, E., Williams, R., Wilson, J., Winship, I., Young, M.A., Bowtell, D., Green, A., deFazio, A., Chenevix-Trench, G., Gertig, D., Webb, P., Mannermaa, A., Kosma, V.-M., Kataja, V., Hartikainen, J., Day, N.E., Cox, D.R., Ponder, B.A.J., 2007. Genome-wide association study identifies novel breast cancer susceptibility loci. Nature 447, 1087–1093. https://doi.org/10.1038/nature05887

Eliassen, A.H., Missmer, S.A., Tworoger, S.S., Spiegelman, D., Barbieri, R.L., Dowsett, M., Hankinson, S.E., 2006. Endogenous Steroid Hormone Concentrations and Risk of Breast Cancer Among Premenopausal Women. Jnci J National Cancer Inst 98, 1406–1415. https://doi.org/10.1093/jnci/djj376

Felty, Q., Singh, K.P., Roy, D., 2005. Estrogen-induced G1/S transition of G0-arrested estrogen-dependent breast cancer cells is regulated by mitochondrial oxidant signaling. Oncogene 24, 4883–4893. https://doi.org/10.1038/sj.onc.1208667

Fernandez, S.V., Russo, J., 2010. Estrogen and Xenoestrogens in Breast Cancer. Toxicol Pathol 38, 110–122. https://doi.org/10.1177/0192623309354108

Fleming, A.M., Burrows, C.J., 2019. Interplay of Guanine Oxidation and G-Quadruplex Folding in Gene Promoters. J Am Chem Soc 142, 1115–1136. https://doi.org/10.1021/jacs.9b11050

Fleming, A.M., Ding, Y., Burrows, C.J., 2017. Oxidative DNA damage is epigenetic by regulating gene transcription via base excision repair. Proc National Acad Sci 114, 2604–2609. https://doi.org/10.1073/pnas.1619809114

Fullwood, M.J., Liu, M.H., Pan, Y.F., Liu, J., Xu, H., Mohamed, Y.B., Orlov, Y.L., Velkov, S., Ho, A., Mei, P.H., Chew, E.G.Y., Huang, P.Y.H., Welboren, W.-J., Han, Y., Ooi, H.S., Ariyaratne, P.N., Vega, V.B., Luo, Y., Tan, P.Y., Choy, P.Y., Wansa, K.D.S.A., Zhao, B., Lim, K.S., Leow, S.C., Yow, J.S., Joseph, R., Li, H., Desai, K.V., Thomsen, J.S., Lee, Y.K., Karuturi, R.K.M., Herve, T., Bourque, G., Stunnenberg, H.G., Ruan, X., Cacheux-Rataboul, V., Sung, W.-K., Liu, E.T., Wei, C.-L., Cheung, E., Ruan, Y., 2009. An oestrogen-receptor-α-bound human chromatin interactome. Nature 462, 58–64. https://doi.org/10.1038/nature08497

Fussell, K.C., Udasin, R.G., Smith, P.J.S., Gallo, M.A., Laskin, J.D., 2011. Catechol metabolites of endogenous estrogens induce redox cycling and generate reactive oxygen species in breast epithelial cells. Carcinogenesis 32, 1285–1293. https://doi.org/10.1093/carcin/bgr109

García-Muse, T., Aguilera, A., 2019. R Loops: From Physiological to Pathological Roles. Cell 179, 604–618. https://doi.org/10.1016/j.cell.2019.08.055

Gaub, M.-P., Bellard, M., Scheuer, I., Chambon, P., Sassone-Corsi, P., 1990. Activation of the ovalbumin gene by the estrogen receptor involves the Fos-Jun complex. Cell 63, 1267–1276. https://doi.org/10.1016/0092-8674(90)90422-b

Ghosh, A., Bansal, M., 2003. A glossary of DNA structures from A to Z. Acta Crystallogr Sect D Biological Crystallogr 59, 620–626. https://doi.org/10.1107/s0907444903003251

Ginno, P.A., Lim, Y.W., Lott, P.L., Korf, I., Chédin, F., 2013. GC skew at the 5′ and 3′ ends of human genes links R-loop formation to epigenetic regulation and transcription termination. Genome Res 23, 1590–1600. https://doi.org/10.1101/gr.158436.113

Ginno, P.A., Lott, P.L., Christensen, H.C., Korf, I., Chédin, F., 2012. R-Loop Formation Is a Distinctive Characteristic of Unmethylated Human CpG Island Promoters. Mol Cell 45, 814–825. https://doi.org/10.1016/j.molcel.2012.01.017

Girard, G.M., Vanzulli, S.I., Cerliani, J.P., Bottino, M.C., Bolado, J., Vela, J., Becu-Villalobos, D., Benavides, F., Gutkind, S., Patel, V., Molinolo, A., Lanari, C., 2007. Association of estrogen receptor-α and progesterone receptor A expression with hormonal mammary carcinogenesis: role of the host microenvironment. Breast Cancer Res 9, R22. https://doi.org/10.1186/bcr1660

Gómez-González, B., Aguilera, A., 2007. Activation-induced cytidine deaminase action is strongly stimulated by mutations of the THO complex. Proc National Acad Sci 104, 8409–8414. https://doi.org/10.1073/pnas.0702836104

Gostissa, M., Alt, F.W., Chiarle, R., 2011. Mechanisms that Promote and Suppress Chromosomal Translocations in Lymphocytes. Immunology 29, 319–350. https://doi.org/10.1146/annurev-immunol-031210-101329

Gottipati, P., Cassel, T.N., Savolainen, L., Helleday, T., 2008. Transcription-Associated Recombination Is Dependent on Replication in Mammalian Cells ▿ †. Mol Cell Biol 28, 154–164. https://doi.org/10.1128/mcb.00816-07

Gould, K.A., Tochacek, M., Schaffer, B.S., Reindl, T.M., Murrin, C.R., Lachel, C.M., VanderWoude, E.A., Pennington, K.L., Flood, L.A., Bynote, K.K., Meza, J.L., Newton, M.A., Shull, J.D., 2004. Genetic Determination of Susceptibility to Estrogen-Induced Mammary Cancer in the ACI Rat Mapping of Emca1 and Emca2 to Chromosomes 5 and 18. Genetics 168, 2113–2125. https://doi.org/10.1534/genetics.104.033878

Gould, M.N., 1986. Inheritance and site of expression of genes controlling susceptibility to mammary cancer in an inbred rat model. Cancer Res 46, 1199–202.

Groh, M., Gromak, N., 2014. Out of Balance: R-loops in Human Disease. Plos Genet 10, e1004630. https://doi.org/10.1371/journal.pgen.1004630

Haag, J.D., Shepel, L.A., Kolman, B.D., Monson, D.M., Benton, M.E., Watts, K.T., Waller, J.L., Lopez-Guajardo, C.C., Samuelson, D.J., Gould, M.N., 2003. Congenic rats reveal three independent Copenhagen alleles within the Mcs1 quantitative trait locus that confer resistance to mammary cancer. Cancer Res 63, 5808–12.

Hänsel-Hertsch, R., Beraldi, D., Lensing, S.V., Marsico, G., Zyner, K., Parry, A., Antonio, M.D., Pike, J., Kimura, H., Narita, M., Tannahill, D., Balasubramanian, S., 2016. G-quadruplex structures mark human regulatory chromatin. Nat Genet 48, 1267–1272. https://doi.org/10.1038/ng.3662

Hänsel-Hertsch, R., Simeone, A., Shea, A., Hui, W.W.I., Zyner, K.G., Marsico, G., Rueda, O.M., Bruna, A., Martin, A., Zhang, X., Adhikari, S., Tannahill, D., Caldas, C., Balasubramanian, S., 2020. Landscape of G-quadruplex DNA structural regions in breast cancer. Nat Genet 52, 878–883. https://doi.org/10.1038/s41588-020-0672-8

Harvell, D.M.E., Strecker, T.E., Tochacek, M., Xie, B., Pennington, K.L., McComb, R.D., Roy, S.K., Shull, J.D., 2000. Rat strain-specific actions of 17β-estradiol in the mammary gland: Correlation between estrogen-induced lobuloalveolar hyperplasia and susceptibility to estrogen-induced mammary cancers. Proc National Acad Sci 97, 2779–2784. https://doi.org/10.1073/pnas.050569097

Hatchi, E., Skourti-Stathaki, K., Ventz, S., Pinello, L., Yen, A., Kamieniarz-Gdula, K., Dimitrov, S., Pathania, S., McKinney, K.M., Eaton, M.L., Kellis, M., Hill, S.J., Parmigiani, G., Proudfoot, N.J., Livingston, D.M., 2015. BRCA1 Recruitment to Transcriptional Pause Sites Is Required for R-Loop-Driven DNA Damage Repair. Mol Cell 57, 636–647. https://doi.org/10.1016/j.molcel.2015.01.011

Heldring, N., Pike, A., Andersson, S., Matthews, J., Cheng, G., Hartman, J., Tujague, M., Ström, A., Treuter, E., Warner, M., Gustafsson, J.-Å., 2007. Estrogen Receptors: How Do They Signal and What Are Their Targets. Physiol Rev 87, 905–931. https://doi.org/10.1152/physrev.00026.2006

Henderson, B.E., Feigelson, H.S., 2000. Hormonal carcinogenesis. Carcinogenesis 21, 427–433. https://doi.org/10.1093/carcin/21.3.427

Hoshina, S., Yura, K., Teranishi, H., Kiyasu, N., Tominaga, A., Kadoma, H., Nakatsuka, A., Kunichika, T., Obuse, C., Waga, S., 2013. Human Origin Recognition Complex Binds Preferentially to G-quadruplex-preferable RNA and Single-stranded DNA. J Biol Chem 288, 30161–30171. https://doi.org/10.1074/jbc.m113.492504

Hu, X., Jiang, L., Tang, C., Ju, Y., Jiu, L., Wei, Y., Guo, L., Zhao, Y., 2017. Association of three single nucleotide polymorphisms of ESR1 with breast cancer susceptibility: a meta-analysis. J Biomed Res 31, 213–225. https://doi.org/10.7555/jbr.31.20160087

Hunter, D.J., Kraft, P., Jacobs, K.B., Cox, D.G., Yeager, M., Hankinson, S.E., Wacholder, S., Wang, Z., Welch, R., Hutchinson, A., Wang, J., Yu, K., Chatterjee, N., Orr, N., Willett, W.C., Colditz, G.A., Ziegler, R.G., Berg, C.D., Buys, S.S., McCarty, C.A., Feigelson, H.S., Calle, E.E., Thun, M.J., Hayes, R.B., Tucker, M., Gerhard, D.S., Fraumeni, J.F., Hoover, R.N., Thomas, G., Chanock, S.J., 2007. A genome-wide association study identifies alleles in FGFR2 associated with risk of sporadic postmenopausal breast cancer. Nat Genet 39, 870–874. https://doi.org/10.1038/ng2075

Huppert, J.L., Balasubramanian, S., 2005. Prevalence of quadruplexes in the human genome. Nucleic Acids Res 33, 2908–2916. https://doi.org/10.1093/nar/gki609

Itoh, T., Tomizawa, J., 1980. Formation of an RNA primer for initiation of replication of ColE1 DNA by ribonuclease H. Proc National Acad Sci 77, 2450–2454. https://doi.org/10.1073/pnas.77.5.2450

Itou, J., Takahashi, R., Sasanuma, H., Tsuda, M., Morimoto, S., Matsumoto, Y., Ishii, T., Sato, F., Takeda, S., Toi, M., 2020. Estrogen induces mammary ductal dysplasia via the upregulation of Myc expression in a DNA-repair deficient condition. Iscience 23, 100821. https://doi.org/10.1016/j.isci.2020.100821

Jerry, D.J., Shull, J.D., Hadsell, D.L., Rijnkels, M., Dunphy, K.A., Schneider, S.S., Vandenberg, L.N., Majhi, P.D., Byrne, C., Trentham-Dietz, A., 2018. Genetic variation in sensitivity to estrogens and breast cancer risk. Mamm Genome 29, 24–37. https://doi.org/10.1007/s00335-018-9741-z

Jinek, M., Chylinski, K., Fonfara, I., Hauer, M., Doudna, J.A., Charpentier, E., 2012. A Programmable Dual-RNA–Guided DNA Endonuclease in Adaptive Bacterial Immunity. Science 337, 816–821. https://doi.org/10.1126/science.1225829

Ju, B.-G., Lunyak, V.V., Perissi, V., Garcia-Bassets, I., Rose, D.W., Glass, C.K., Rosenfeld, M.G., 2006. A Topoisomerase IIß-Mediated dsDNA Break Required for Regulated Transcription. Science 312, 1798–1802. https://doi.org/10.1126/science.1127196

Kanoh, Y., Matsumoto, S., Fukatsu, R., Kakusho, N., Kono, N., Renard-Guillet, C., Masuda, K., Iida, K., Nagasawa, K., Shirahige, K., Masai, H., 2015. Rif1 binds to G quadruplexes and suppresses replication over long distances. Nat Struct Mol Biol 22, 889–897. https://doi.org/10.1038/nsmb.3102

Kato, S., Endoh, H., Masuhiro, Y., Kitamoto, T., Uchiyama, S., Sasaki, H., Masushige, S., Gotoh, Y., Nishida, E., Kawashima, H., Metzger, D., Chambon, P., 1995. Activation of

the Estrogen Receptor Through Phosphorylation by Mitogen-Activated Protein Kinase. Science 270, 1491–1494. https://doi.org/10.1126/science.270.5241.1491

Keimling, M., Deniz, M., Varga, D., Stahl, A., Schrezenmeier, H., Kreienberg, R., Hoffmann, I., König, J., Wiesmüller, L., 2012. The power of DNA double-strand break (DSB) repair testing to predict breast cancer susceptibility. Faseb J 26, 2094–2104. https://doi.org/10.1096/fj.11-200790

Kerdivel, G., Guevel, R.L., Habauzit, D., Brion, F., Ait-Aissa, S., Pakdel, F., 2013. Estrogenic Potency of Benzophenone UV Filters in Breast Cancer Cells: Proliferative and Transcriptional Activity Substantiated by Docking Analysis. Plos One 8, e60567. https://doi.org/10.1371/journal.pone.0060567

Kordon, E.C., Molinolo, A.A., Pasqualini, C.D., Charreau, E.H., Pazos, P., Dran, G., Lanari, C., 1993. Progesterone induction of mammary carcinomas in BALB/c female mice. Breast Cancer Res Tr 28, 29–39. https://doi.org/10.1007/bf00666353

Kotsantis, P., Segura-Bayona, S., Margalef, P., Marzec, P., Ruis, P., Hewitt, G., Bellelli, R., Patel, H., Goldstone, R., Poetsch, A.R., Boulton, S.J., 2020. RTEL1 Regulates G4/R-Loops to Avert Replication-Transcription Collisions. Cell Reports 33, 108546. https://doi.org/10.1016/j.celrep.2020.108546

Krege, J.H., Hodgin, J.B., Couse, J.F., Enmark, E., Warner, M., Mahler, J.F., Sar, M., Korach, K.S., Gustafsson, J.-Å., Smithies, O., 1998. Generation and reproductive phenotypes of mice lacking estrogen receptor β. Proc National Acad Sci 95, 15677–15682. https://doi.org/10.1073/pnas.95.26.15677

Kreuzer, K.N., Brister, J.R., 2010. Initiation of bacteriophage T4 DNA replication and replication fork dynamics: a review in the Virology Journal series on bacteriophage T4 and its relatives. Virol J 7, 358. https://doi.org/10.1186/1743-422x-7-358

Kuperwasser, C., Hurlbut, G.D., Kittrell, F.S., Dickinson, E.S., Laucirica, R., Medina, D., Naber, S.P., Jerry, D.J., 2000. Development of Spontaneous Mammary Tumors in BALB/c p53 Heterozygous Mice. Am J Pathology 157, 2151–2159. https://doi.org/10.1016/s0002-9440(10)64853-5

Kwok, C.K., Merrick, C.J., 2017. G-Quadruplexes: Prediction, Characterization, and Biological Application. Trends Biotechnol 35, 997–1013. https://doi.org/10.1016/j.tibtech.2017.06.012

Lago, S., Nadai, M., Cernilogar, F.M., Kazerani, M., Moreno, H.D., Schotta, G., Richter, S.N., 2021. Promoter G-quadruplexes and transcription factors cooperate to shape the cell type-specific transcriptome. Nat Commun 12, 3885. https://doi.org/10.1038/s41467-021-24198-2

Lan, H., Kendziorski, C.M., Haag, J.D., Shepel, L.A., Gould, M.A.N. and M.N., 2001. Genetic Loci Controlling Breast Cancer Susceptibility in the Wistar-Kyoto Rat.

Lanari, C., Molinolo, A.A., Pasqualini, C.D., 1986. Induction of mammary adenocarcinomas by medroxyprogesterone acetate in BALBc female mice. Cancer Lett 33, 215–223. https://doi.org/10.1016/0304-3835(86)90027-3

Langley, A.R., Gräf, S., Smith, J.C., Krude, T., 2016. Genome-wide identification and characterisation of human DNA replication origins by initiation site sequencing (ini-seq). Nucleic Acids Res 44, 10230–10247. https://doi.org/10.1093/nar/gkw760

LaPlante, C.D., Bansal, R., Dunphy, K.A., Jerry, D.J., Vandenberg, L.N., 2018. Oxybenzone alters mammary gland morphology in mice exposed during pregnancy and lactation. J Endocr Soc 2, js.2018-00024-. https://doi.org/10.1210/js.2018-00024

Lee, C.-Y., McNerney, C., Ma, K., Zhao, W., Wang, A., Myong, S., 2020. R-loop induced G-quadruplex in non-template promotes transcription by successive R-loop formation. Nat Commun 11, 3392. https://doi.org/10.1038/s41467-020-17176-7

Lejault, P., Mitteaux, J., Sperti, F.R., Monchaud, D., 2021. How to untie G-quadruplex knots and why? Cell Chem Biol. https://doi.org/10.1016/j.chembiol.2021.01.015

Levin, E.R., 2009. Plasma membrane estrogen receptors. Trends Endocrinol Metabolism 20, 477–482. https://doi.org/10.1016/j.tem.2009.06.009

Li, S., Weroha, S., Tawfik, O., Li, J., 2002. Prevention of solely estrogen-induced mammary tumors in female aci rats by tamoxifen: evidence for estrogen receptor mediation. J Endocrinol 175, 297–305. https://doi.org/10.1677/joe.0.1750297

Lin, C.-Y., Vega, V.B., Thomsen, J.S., Zhang, T., Kong, S.L., Xie, M., Chiu, K.P., Lipovich, L., Barnett, D.H., Stossi, F., Yeo, A., George, J., Kuznetsov, V.A., Lee, Y.K., Charn, T.H., Palanisamy, N., Miller, L.D., Cheung, E., Katzenellenbogen, B.S., Ruan, Y., Bourque, G., Wei, C.-L., Liu, E.T., 2007. Whole-Genome Cartography of Estrogen Receptor α Binding Sites. Plos Genet 3, e87. https://doi.org/10.1371/journal.pgen.0030087

Lipphardt, M.F., Deryal, M., Ong, M.F., Schmidt, W., Mahlknecht, U., 2013. ESR1 single nucleotide polymorphisms predict breast cancer susceptibility in the central European Caucasian population. Int J Clin Exp Med 6, 282–8.

MacMahon, B., Cole, P., Lin, T.M., Lowe, C.R., Mirra, A.P., Ravnihar, B., Salber, E.J., Valaoras, V.G., Yuasa, S., 1970. Age at first birth and breast cancer risk. B World Health Organ 43, 209–21.

MacMillan, A.L., Kohli, R.M., Ross, S.R., 2013. APOBEC3 Inhibition of Mouse Mammary Tumor Virus Infection: the Role of Cytidine Deamination versus Inhibition of Reverse Transcription. J Virol 87, 4808–4817. https://doi.org/10.1128/jvi.00112-13

Madireddy, A., Kosiyatrakul, S.T., Boisvert, R.A., Herrera-Moyano, E., García-Rubio, M.L., Gerhardt, J., Vuono, E.A., Owen, N., Yan, Z., Olson, S., Aguilera, A., Howlett, N.G., Schildkraut, C.L., 2016. FANCD2 Facilitates Replication through Common Fragile Sites. Mol Cell 64, 388–404. https://doi.org/10.1016/j.molcel.2016.09.017

Magis, A.D., Manzo, S.G., Russo, M., Marinello, J., Morigi, R., Sordet, O., Capranico, G., 2018. DNA damage and genome instability by G-quadruplex ligands are mediated by R loops in human cancer cells. Proc National Acad Sci 116, 201810409. https://doi.org/10.1073/pnas.1810409116

Maizels, N., 2015. G4-associated human diseases. Embo Rep 16, 910–922. https://doi.org/10.15252/embr.201540607

Maizels, N., 2006. Dynamic roles for G4 DNA in the biology of eukaryotic cells. Nat Struct Mol Biol 13, 1055–1059. https://doi.org/10.1038/nsmb1171

Maizels, N., Gray, L.T., 2013. The G4 Genome. Plos Genet 9, e1003468. https://doi.org/10.1371/journal.pgen.1003468

Majewski, A.R., Chuong, L.M., Neill, H.M., Roberts, A.L., Jerry, D.J., Dunphy, K.A., 2018. Sterilization of Silastic Capsules Containing 17β-Estradiol for Effective Hormone Delivery in Mus musculus. J Am Assoc Lab Anim. https://doi.org/10.30802/aalas-jaalas-18-000030

Majhi, P.D., Sharma, A., Roberts, A.L., Daniele, E., Majewski, A.R., Chuong, L.M., Black, A.L., Vandenberg, L.N., Schneider, S.S., Dunphy, K.A., Jerry, D.J., 2020. Effects of Benzophenone-3 and Propylparaben on Estrogen Receptor–Dependent R-Loops and DNA Damage in Breast Epithelial Cells and Mice. Environ Health Persp 128, 017002. https://doi.org/10.1289/ehp5221

Maleki, J., Nourbakhsh, M., Shabani, M., Korani, M., Nourazarian, S.M., Dahaghi, M.R.O., Moghadasi, M.H., 2015. 17β-Estradiol Stimulates Generation of Reactive Species Oxygen and Nitric Oxide in Ovarian Adenocarcinoma Cells (OVCAR 3). Iranian J Cancer Prev 8, e2332. https://doi.org/10.17795/ijcp2332

Manavathi, B., Dey, O., Gajulapalli, V.N.R., Bhatia, R.S., Bugide, S., Kumar, R., 2013. Derailed Estrogen Signaling and Breast Cancer: An Authentic Couple. Endocr Rev 34, 1–32. https://doi.org/10.1210/er.2011-1057

Mao, S.-Q., Ghanbarian, A.T., Spiegel, J., Cuesta, S.M., Beraldi, D., Antonio, M.D., Marsico, G., Hänsel-Hertsch, R., Tannahill, D., Balasubramanian, S., 2018. DNA G-

quadruplex structures mold the DNA methylome. Nat Struct Mol Biol 25, 951–957. https://doi.org/10.1038/s41594-018-0131-8

Marino, M., Galluzzo, P., Ascenzi, P., 2006. Estrogen signaling multiple pathways to impact gene transcription. Curr Genomics 7, 497–508. https://doi.org/10.2174/138920206779315737

Martino, S., Cauley, J.A., Barrett-Connor, E., Powles, T.J., Mershon, J., Disch, D., Secrest, R.J., Cummings, S.R., Investigators, F. the C., 2004. Continuing Outcomes Relevant to Evista: Breast Cancer Incidence in Postmenopausal Osteoporotic Women in a Randomized Trial of Raloxifene. Jnci J National Cancer Inst 96, 1751–1761. https://doi.org/10.1093/jnci/djh319

Metcalfe, K., Lynch, H.T., Foulkes, W.D., Tung, N., Olopade, O.I., Eisen, A., Lerner-Ellis, J., Snyder, C., Kim, S.J., Sun, P., Narod, S.A., 2019. Oestrogen receptor status and survival in women with BRCA2-associated breast cancer. Brit J Cancer 120, 398–403. https://doi.org/10.1038/s41416-019-0376-y

Mobley, J.A., Brueggemeier, R.W., 2004. Estrogen receptor-mediated regulation of oxidative stress and DNA damage in breast cancer. Carcinogenesis 25, 3–9. https://doi.org/10.1093/carcin/bgg175

Molinolo, A.A., Lanari, C., Charreau, E.H., Sanjuan, N., Pasqualini, C.D., 1987. Mouse mammary tumors induced by medroxyprogesterone acetate: immunohistochemistry and hormonal receptors. J Natl Cancer I 79, 1341–50.

Möller, S., Mucci, L.A., Harris, J.R., Scheike, T., Holst, K., Halekoh, U., Adami, H.-O., Czene, K., Christensen, K., Holm, N.V., Pukkala, E., Skytthe, A., Kaprio, J., Hjelmborg, J.B., 2016. The Heritability of Breast Cancer among Women in the Nordic Twin Study of Cancer. Cancer Epidemiology Prev Biomarkers 25, 145–150. https://doi.org/10.1158/1055-9965.epi-15-0913

Mucci, L.A., Hjelmborg, J.B., Harris, J.R., Czene, K., Havelick, D.J., Scheike, T., Graff, R.E., Holst, K., Möller, S., Unger, R.H., McIntosh, C., Nuttall, E., Brandt, I., Penney, K.L., Hartman, M., Kraft, P., Parmigiani, G., Christensen, K., Koskenvuo, M., Holm, N.V., Heikkilä, K., Pukkala, E., Skytthe, A., Adami, H.-O., Kaprio, J., Collaboration, N.T.S. of C. (NorTwinCan), 2016. Familial Risk and Heritability of Cancer Among Twins in Nordic Countries. Jama 315, 68–76. https://doi.org/10.1001/jama.2015.17703

Ohle, C., Tesorero, R., Schermann, G., Dobrev, N., Sinning, I., Fischer, T., 2016. Transient RNA-DNA Hybrids Are Required for Efficient Double-Strand Break Repair. Cell 167, 1001-1013.e7. https://doi.org/10.1016/j.cell.2016.10.001

Okamoto, Y., Abe, M., Itaya, A., Tomida, J., Ishiai, M., Takaori-Kondo, A., Taoka, M., Isobe, T., Takata, M., 2019. FANCD2 protects genome stability by recruiting RNA

processing enzymes to resolve R-loops during mild replication stress. Febs J 286, 139–150. https://doi.org/10.1111/febs.14700

Okeoma, C.M., Petersen, J., Ross, S.R., 2009. Expression of Murine APOBEC3 Alleles in Different Mouse Strains and Their Effect on Mouse Mammary Tumor Virus Infection ▿ †. J Virol 83, 3029–3038. https://doi.org/10.1128/jvi.02536-08

Okoh, V., Deoraj, A., Roy, D., 2011. Estrogen-induced reactive oxygen species-mediated signalings contribute to breast cancer. Biochimica Et Biophysica Acta Bba - Rev Cancer 1815, 115–133. https://doi.org/10.1016/j.bbcan.2010.10.005

Paeschke, K., Bochman, M.L., Garcia, P.D., Cejka, P., Friedman, K.L., Kowalczykowski, S.C., Zakian, V.A., 2013. Pif1 family helicases suppress genome instability at G-quadruplex motifs. Nature 497, 458–462. https://doi.org/10.1038/nature12149

Palaniappan, M., Nguyen, L., Grimm, S.L., Xi, Y., Xia, Z., Li, W., Coarfa, C., 2019. The genomic landscape of estrogen receptor α binding sites in mouse mammary gland. Plos One 14, e0220311. https://doi.org/10.1371/journal.pone.0220311

Pavri, R., 2017. R Loops in the Regulation of Antibody Gene Diversification. Genes-basel 8, 154. https://doi.org/10.3390/genes8060154

Pedram, A., Razandi, M., Kim, J.K., O'Mahony, F., Lee, E.Y., Luderer, U., Levin, E.R., 2009. Developmental Phenotype of a Membrane Only Estrogen Receptor α (MOER) Mouse*. J Biol Chem 284, 3488–3495. https://doi.org/10.1074/jbc.m806249200

Periyasamy, M., Patel, H., Lai, C.-F., Nguyen, V.T.M., Nevedomskaya, E., Harrod, A., Russell, R., Remenyi, J., Ochocka, A.M., Thomas, R.S., Fuller-Pace, F., Győrffy, B., Caldas, C., Navaratnam, N., Carroll, J.S., Zwart, W., Coombes, R.C., Magnani, L., Buluwela, L., Ali, S., 2015. APOBEC3B-Mediated Cytidine Deamination Is Required for Estrogen Receptor Action in Breast Cancer. Cell Reports 13, 108–121. https://doi.org/10.1016/j.celrep.2015.08.066

Pohjoismäki, J.L.O., Holmes, J.B., Wood, S.R., Yang, M.-Y., Yasukawa, T., Reyes, A., Bailey, L.J., Cluett, T.J., Goffart, S., Willcox, S., Rigby, R.E., Jackson, A.P., Spelbrink, J.N., Griffith, J.D., Crouch, R.J., Jacobs, H.T., Holt, I.J., 2010. Mammalian Mitochondrial DNA Replication Intermediates Are Essentially Duplex but Contain Extensive Tracts of RNA/DNA Hybrid. J Mol Biol 397, 1144–1155. https://doi.org/10.1016/j.jmb.2010.02.029

Ponnaiya, B., Cornforth, M.N., Ullrich, R.L., 1997. Radiation-induced chromosomal instability in BALB/c and C57BL/6 mice: the difference is as clear as black and white. Radiat Res 147, 121–5.

Prado, F., Aguilera, A., 2005. Impairment of replication fork progression mediates RNA polII transcription-associated recombination. Embo J 24, 1267–1276. https://doi.org/10.1038/sj.emboj.7600602

Preston-Martin, S., Pike, M.C., Ross, R.K., Jones, P.A., Henderson, B.E., 1990. Increased cell division as a cause of human cancer. Cancer Res 50, 7415–21.

Puget, N., Miller, K., Legube, G., 2019. Non-canonical DNA/RNA structures during Transcription-Coupled Double-Strand Break Repair: Roadblocks or Bona fide repair intermediates? Dna Repair 81, 102661. https://doi.org/10.1016/j.dnarep.2019.102661

Qiao, Q., Wang, L., Meng, F.-L., Hwang, J.K., Alt, F.W., Wu, H., 2017. AID Recognizes Structured DNA for Class Switch Recombination. Mol Cell 67, 361-373.e4. https://doi.org/10.1016/j.molcel.2017.06.034

Reaban, M.E., Lebowitz, J., Griffin, J.A., 1994. Transcription induces the formation of a stable RNA.DNA hybrid in the immunoglobulin alpha switch region. J Biological Chem 269, 21850–7.

Rhodes, D., Lipps, H.J., 2015. G-quadruplexes and their regulatory roles in biology. Nucleic Acids Res 43, 8627–8637. https://doi.org/10.1093/nar/gkv862

Ribeyre, C., Lopes, J., Boulé, J.-B., Piazza, A., Guédin, A., Zakian, V.A., Mergny, J.-L., Nicolas, A., 2009. The Yeast Pif1 Helicase Prevents Genomic Instability Caused by G-Quadruplex-Forming CEB1 Sequences In Vivo. Plos Genet 5, e1000475. https://doi.org/10.1371/journal.pgen.1000475

Richard, P., Manley, J.L., 2017. R Loops and Links to Human Disease. J Mol Biol 429, 3168–3180. https://doi.org/10.1016/j.jmb.2016.08.031

Rossouw, J.E., Anderson, G.L., Prentice, R.L., LaCroix, A.Z., Kooperberg, C., Stefanick, M.L., Jackson, R.D., Beresford, S.A., Howard, B.V., Johnson, K.C., al., et, 2002. Risks and Benefits of Estrogen Plus Progestin in Healthy Postmenopausal Women: Principal Results From the Women's Health Initiative Randomized Controlled Trial. Jama 288, 321–333. https://doi.org/10.1001/jama.288.3.321

Roy, D., Cai, Q., Felty, Q., Narayan, S., 2007. Estrogen-Induced Generation of Reactive Oxygen and Nitrogen Species, Gene Damage, and Estrogen-Dependent Cancers. J Toxicol Environ Heal Part B 10, 235–257. https://doi.org/10.1080/15287390600974924

Roy, D., Liehr, J.G., 1999. Estrogen, DNA damage and mutations. Mutat Res Fundam Mol Mech Mutagen 424, 107–115. https://doi.org/10.1016/s0027-5107(99)00012-3

Roychoudhury, S., Pramanik, S., Harris, H.L., Tarpley, M., Sarkar, A., Spagnol, G., Sorgen, P.L., Chowdhury, D., Band, V., Klinkebiel, D., Bhakat, K.K., 2020. Endogenous oxidized DNA bases and APE1 regulate the formation of G-quadruplex structures in the genome. Proc National Acad Sci 201912355. https://doi.org/10.1073/pnas.1912355117

Rudolph, A., Chang-Claude, J., Schmidt, M.K., 2016. Gene–environment interaction and risk of breast cancer. Brit J Cancer 114, 125–133. https://doi.org/10.1038/bjc.2015.439

Russo, J., Ao, X., Grill, C., Russo, I.H., 1999. Pattern of distribution of cells positive for estrogen receptor α and progesterone receptor in relation to proliferating cells in the mammary gland. Breast Cancer Res Tr 53, 217–227. https://doi.org/10.1023/a:1006186719322

Russo, J., Russo, I.H., 2006. The role of estrogen in the initiation of breast cancer. J Steroid Biochem Mol Biology 102, 89–96. https://doi.org/10.1016/j.jsbmb.2006.09.004

Samavat, H., Kurzer, M.S., 2015. Estrogen metabolism and breast cancer. Cancer Lett 356, 231–243. https://doi.org/10.1016/j.canlet.2014.04.018

Santen, R., Cavalieri, E., Rogan, E., Russo, J., Guttenplan, J., Ingle, J., Yue, W., 2009. Estrogen Mediation of Breast Tumor Formation Involves Estrogen Receptor-Dependent, as Well as Independent, Genotoxic Effects. Ann Ny Acad Sci 1155, 132–140. https://doi.org/10.1111/j.1749-6632.2008.03685.x

Sasanuma, H., Tsuda, M., Morimoto, S., Saha, L.K., Rahman, M.M., Kiyooka, Y., Fujiike, H., Cherniack, A.D., Itou, J., Moreu, E.C., Toi, M., Nakada, S., Tanaka, H., Tsutsui, K., Yamada, S., Nussenzweig, A., Takeda, S., 2018. BRCA1 ensures genome integrity by eliminating estrogen-induced pathological topoisomerase II–DNA complexes. Proc National Acad Sci 115, 201803177. https://doi.org/10.1073/pnas.1803177115

Sauer, M., Paeschke, K., 2017. G-quadruplex unwinding helicases and their function in vivo. Biochem Soc T 45, 1173–1182. https://doi.org/10.1042/bst20170097

Saville, B., Wormke, M., Wang, F., Nguyen, T., Enmark, E., Kuiper, G., Gustafsson, J.A., Safe, S., 2000. Ligand-, cell-, and estrogen receptor subtype (alpha/beta)-dependent activation at GC-rich (Sp1) promoter elements. J Biological Chem 275, 5379–87. https://doi.org/10.1074/jbc.275.8.5379

Schaffer, B.S., Lachel, C.M., Pennington, K.L., Murrin, C.R., Strecker, T.E., Tochacek, M., Gould, K.A., Meza, J.L., McComb, R.D., Shull, J.D., 2006. Genetic Bases of Estrogen-Induced Tumorigenesis in the Rat: Mapping of Loci Controlling Susceptibility to Mammary Cancer in a Brown Norway × ACI Intercross. Cancer Res 66, 7793–7800. https://doi.org/10.1158/0008-5472.can-06-0143

Schlotz, N., Kim, G.-J., Jäger, S., Günther, S., Lamy, E., 2017. In vitro observations and in silico predictions of xenoestrogen mixture effects in T47D-based receptor transactivation and proliferation assays. Toxicol In Vitro 45, 146–157. https://doi.org/10.1016/j.tiv.2017.08.017

Schlumpf, M., Kypke, K., Wittassek, M., Angerer, J., Mascher, H., Mascher, D., Vökt, C., Birchler, M., Lichtensteiger, W., 2010. Exposure patterns of UV filters, fragrances, parabens, phthalates, organochlor pesticides, PBDEs, and PCBs in human milk: Correlation of UV filters with use of cosmetics. Chemosphere 81, 1171–1183. https://doi.org/10.1016/j.chemosphere.2010.09.079

Schwab, R.A., Nieminuszczy, J., Shah, F., Langton, J., Lopez Martinez, D., Liang, C.-C., Cohn, M.A., Gibbons, R.J., Deans, A.J., Niedzwiedz, W., 2015. The Fanconi Anemia Pathway Maintains Genome Stability by Coordinating Replication and Transcription. Mol Cell 60, 351–361. https://doi.org/10.1016/j.molcel.2015.09.012

Sessa, G., Gómez-González, B., Silva, S., Pérez-Calero, C., Beaurepere, R., Barroso, S., Martineau, S., Martin, C., Ehlén, Å., Martínez, J.S., Lombard, B., Loew, D., Vagner, S., Aguilera, A., Carreira, A., 2021. BRCA2 promotes R-loop resolution by DDX5 helicase at DNA breaks to facilitate their repair by homologous recombination. Embo J e106018. https://doi.org/10.15252/embj.2020106018

Sharma, S., 2011. Non-B DNA Secondary Structures and Their Resolution by RecQ Helicases. J Nucleic Acids 2011, 724215. https://doi.org/10.4061/2011/724215

Shim, W.-S., Conaway, M., Masamura, S., Yue, W., Wang, J.-P., Kumar, R., Santen, R.J., 2000. Estradiol Hypersensitivity and Mitogen-Activated Protein Kinase Expression in Long-Term Estrogen Deprived Human Breast Cancer Cells in Vivo 1. Endocrinology 141, 396–405. https://doi.org/10.1210/endo.141.1.7270

Shivji, M.K.K., Renaudin, X., Williams, Ç.H., Venkitaraman, A.R., 2018. BRCA2 Regulates Transcription Elongation by RNA Polymerase II to Prevent R-Loop Accumulation. Cell Reports 22, 1031–1039. https://doi.org/10.1016/j.celrep.2017.12.086

Shull, J.D., Dennison, K.L., Chack, A.C., Trentham-Dietz, A., 2018. Rat models of 17β-estradiol-induced mammary cancer reveal novel insights into breast cancer etiology and prevention. Physiol Genomics 50, 215–234. https://doi.org/10.1152/physiolgenomics.00105.2017

Shull, J.D., Spady, T.J., Snyder, M.C., Johansson, S.L., Pennington, K.L., 1997. Ovary-intact, but not ovariectomized female ACI rats treated with 17beta-estradiol rapidly develop mammary carcinoma. Carcinogenesis 18, 1595–1601. https://doi.org/10.1093/carcin/18.8.1595

Siegel, R.L., Miller, K.D., Fuchs, H.E., Jemal, A., 2021. Cancer Statistics, 2021. Ca Cancer J Clin 71, 7–33. https://doi.org/10.3322/caac.21654

Silva, B., Pentz, R., Figueira, A.M., Arora, R., Lee, Y.W., Hodson, C., Wischnewski, H., Deans, A.J., Azzalin, C.M., 2019. FANCM limits ALT activity by restricting telomeric replication stress induced by deregulated BLM and R-loops. Nat Commun 10, 2253. https://doi.org/10.1038/s41467-019-10179-z

Singh, B., Bhat, N.K., Bhat, H.K., 2011. Partial Inhibition of Estrogen-Induced Mammary Carcinogenesis in Rats by Tamoxifen: Balance between Oxidant Stress and Estrogen Responsiveness. Plos One 6, e25125. https://doi.org/10.1371/journal.pone.0025125

Singleton, D.W., Khan, S.A., 2003. Xenoestrogen exposure and mechanisms of endocrine disruption. Front Biosci 8, s110-118. https://doi.org/10.2741/1010

Skourti-Stathaki, K., Proudfoot, N.J., 2014. A double-edged sword: R loops as threats to genome integrity and powerful regulators of gene expression. Gene Dev 28, 1384–1396. https://doi.org/10.1101/gad.242990.114

Smith, J.S., Chen, Q., Yatsunyk, L.A., Nicoludis, J.M., Garcia, M.S., Kranaster, R., Balasubramanian, S., Monchaud, D., Teulade-Fichou, M.-P., Abramowitz, L., Schultz, D.C., Johnson, F.B., 2011. Rudimentary G-quadruplex–based telomere capping in Saccharomyces cerevisiae. Nat Struct Mol Biol 18, 478–485. https://doi.org/10.1038/nsmb.2033

Sollier, J., Cimprich, K.A., 2015. Breaking bad: R-loops and genome integrity. Trends Cell Biol 25, 514–522. https://doi.org/10.1016/j.tcb.2015.05.003

Sollier, J., Stork, C.T., García-Rubio, M.L., Paulsen, R.D., Aguilera, A., Cimprich, K.A., 2014. Transcription-Coupled Nucleotide Excision Repair Factors Promote R-Loop-Induced Genome Instability. Mol Cell 56, 777–785. https://doi.org/10.1016/j.molcel.2014.10.020

Sonnenschein, C., Soto, A.M., 1998. An updated review of environmental estrogen and androgen mimics and antagonists11Proceedings of the 13th International Symposium of the Journal of Steroid Biochemistry & Molecular Biology “Recent Advances in Steroid Biochemistry & Molecular Biology” Monaco 25–28 May 1997. J Steroid Biochem Mol Biology 65, 143–150. https://doi.org/10.1016/s0960-0760(98)00027-2

Spady, T.J., Harvell, D.M.E., Snyder, M.C., Pennington, K.L., McComb, R.D., Shull, J.D., 1998. Estrogen-induced tumorigenesis in the Copenhagen rat: disparate susceptibilities to development of prolactin-producing pituitary tumors and mammary carcinomas. Cancer Lett 124, 95–103. https://doi.org/10.1016/s0304-3835(97)00455-2

Spiegel, J., Cuesta, S.M., Adhikari, S., Hänsel-Hertsch, R., Tannahill, D., Balasubramanian, S., 2021. G-quadruplexes are transcription factor binding hubs in human chromatin. Genome Biol 22, 117. https://doi.org/10.1186/s13059-021-02324-z

Stacey, S.N., Manolescu, A., Sulem, P., Rafnar, T., Gudmundsson, J., Gudjonsson, S.A., Masson, G., Jakobsdottir, M., Thorlacius, S., Helgason, A., Aben, K.K., Strobbe, L.J., Albers-Akkers, M.T., Swinkels, D.W., Henderson, B.E., Kolonel, L.N., Marchand, L.L., Millastre, E., Andres, R., Godino, J., Garcia-Prats, M.D., Polo, E., Tres, A., Mouy, M., Saemundsdottir, J., Backman, V.M., Gudmundsson, L., Kristjansson, K., Bergthorsson, J.T., Kostic, J., Frigge, M.L., Geller, F., Gudbjartsson, D., Sigurdsson, H., Jonsdottir, T., Hrafnkelsson, J., Johannsson, J., Sveinsson, T., Myrdal, G., Grimsson, H.N., Jonsson, T., Holst, S. von, Werelius, B., Margolin, S., Lindblom, A., Mayordomo, J.I., Haiman, C.A., Kiemeney, L.A., Johannsson, O.T., Gulcher, J.R., Thorsteinsdottir, U., Kong, A., Stefansson, K., 2007. Common variants on chromosomes 2q35 and 16q12 confer susceptibility to estrogen receptor–positive breast cancer. Nat Genet 39, 865–869. https://doi.org/10.1038/ng2064

Stork, C.T., Bocek, M., Crossley, M.P., Sollier, J., Sanz, L.A., Chédin, F., Swigut, T., Cimprich, K.A., 2016. Co-transcriptional R-loops are the main cause of estrogen-induced DNA damage. Elife 5, e17548. https://doi.org/10.7554/elife.17548

Tamimi, R.M., Spiegelman, D., Smith-Warner, S.A., Wang, M., Pazaris, M., Willett, W.C., Eliassen, A.H., Hunter, D.J., 2016. Population Attributable Risk of Modifiable and Nonmodifiable Breast Cancer Risk Factors in Postmenopausal Breast Cancer. Am J Epidemiol 184, 884–893. https://doi.org/10.1093/aje/kww145

Tan, J., Lan, L., 2020. The DNA secondary structures at telomeres and genome instability. Cell Biosci 10, 47. https://doi.org/10.1186/s13578-020-00409-z

Tan, J., Wang, X., Phoon, L., Yang, H., Lan, L., 2020. Resolution of ROS-induced G-quadruplexes and R-loops at transcriptionally active sites is dependent on BLM helicase. Febs Lett 594, 1359–1367. https://doi.org/10.1002/1873-3468.13738

Técher, H., Koundrioukoff, S., Nicolas, A., Debatisse, M., 2017. The impact of replication stress on replication dynamics and DNA damage in vertebrate cells. Nat Rev Genet 18, 535–550. https://doi.org/10.1038/nrg.2017.46

Teng, Y., Yadav, T., Duan, M., Tan, J., Xiang, Y., Gao, B., Xu, J., Liang, Z., Liu, Y., Nakajima, S., Shi, Y., Levine, A.S., Zou, L., Lan, L., 2018. ROS-induced R loops trigger a transcription-coupled but BRCA1/2-independent homologous recombination pathway through CSB. Nat Commun 9, 4115. https://doi.org/10.1038/s41467-018-06586-3

Tian, H., Gao, Z., Wang, G., Li, H., Zheng, J., 2016. Estrogen potentiates reactive oxygen species (ROS) tolerance to initiate carcinogenesis and promote cancer malignant transformation. Tumor Biol 37, 141–150. https://doi.org/10.1007/s13277-015-4370-6

Tian, J.-M., Ran, B., Zhang, C.-L., Yan, D.-M., LI, X.-H., 2018. Estrogen and progesterone promote breast cancer cell proliferation by inducing cyclin G1 expression. Braz J Med Biol Res 51, 1–7. https://doi.org/10.1590/1414-431x20175612

Tian, T., Chen, Y.-Q., Wang, S.-R., Zhou, X., 2018. G-Quadruplex: A Regulator of Gene Expression and Its Chemical Targeting. Chem 4, 1314–1344. https://doi.org/10.1016/j.chempr.2018.02.014

Travis, R.C., Key, T.J., 2003. Oestrogen exposure and breast cancer risk. Breast Cancer Res 5, 239. https://doi.org/10.1186/bcr628

Trichopoulos, D., MacMahon, B., Cole, P., 1972. Menopause and breast cancer risk. J Natl Cancer I 48, 605–13.

Udquim, K.-I., Zettelmeyer, C., Banday, A.R., Lin, S.H.-Y., Prokunina-Olsson, L., 2020. APOBEC3B expression in breast cancer cell lines and tumors depends on the estrogen receptor status. Carcinogenesis. https://doi.org/10.1093/carcin/bgaa002

Ullrich, R.L., Bowles, N.D., Satterfield, L.C., Davis, C.M., 1996. Strain-Dependent Susceptibility to Radiation-Induced Mammary Cancer Is a Result of Differences in Epithelial Cell Sensitivity to Transformation. Radiat Res 146, 353. https://doi.org/10.2307/3579468

Varshney, D., Spiegel, J., Zyner, K., Tannahill, D., Balasubramanian, S., 2020. The regulation and functions of DNA and RNA G-quadruplexes. Nat Rev Mol Cell Bio 1–16. https://doi.org/10.1038/s41580-020-0236-x

Vladusic, E.A., Hornby, A.E., Guerra-Vladusic, F.K., Lakins, J., Lupu, R., 2000. Expression and regulation of estrogen receptor beta in human breast tumors and cell lines. Oncol Rep. https://doi.org/10.3892/or.7.1.157

Vocka, M., Zimovjanova, M., Bielcikova, Z., Tesarova, P., Petruzelka, L., Mateju, M., Krizova, L., Kotlas, J., Soukupova, J., Janatova, M., Zemankova, P., Kleiblova, P., Novotny, J., Konopasek, B., Chodacka, M., Brychta, M., Sochor, M., Smejkalova-Musilova, D., Cmejlova, V., Kozevnikovova, R., Miskarova, L., Argalacsova, S., Stolarova, L., Lhotova, K., Borecka, M., Kleibl, Z., 2019. Estrogen Receptor Status Oppositely Modifies Breast Cancer Prognosis in BRCA1/BRCA2 Mutation Carriers Versus Non-Carriers. Cancers 11, 738. https://doi.org/10.3390/cancers11060738

Vrtačnik, P., Ostanek, B., Mencej-Bedrač, S., Marc, J., 2014. The many faces of estrogen signaling. Biochem Medica 24, 329–342. https://doi.org/10.11613/bm.2014.035

Waks, A.G., Winer, E.P., 2019. Breast Cancer Treatment. Jama 321, 288–300. https://doi.org/10.1001/jama.2018.19323

Wang, Y., Yang, J., Wild, A.T., Wu, W.H., Shah, R., Danussi, C., Riggins, G.J., Kannan, K., Sulman, E.P., Chan, T.A., Huse, J.T., 2019. G-quadruplex DNA drives genomic instability and represents a targetable molecular abnormality in ATRX-deficient malignant glioma. Nat Commun 10, 943. https://doi.org/10.1038/s41467-019-08905-8

Wang, Z., Chandrasena, E.R., Yuan, Y., Peng, K., Breemen, R.B. van, Thatcher, G.R.J., Bolton, J.L., 2010. Redox Cycling of Catechol Estrogens Generating Apurinic/Apyrimidinic Sites and 8-oxo-Deoxyguanosine via Reactive Oxygen Species Differentiates Equine and Human Estrogens. Chem Res Toxicol 23, 1365–1373. https://doi.org/10.1021/tx1001282

Wendt, C., Margolin, S., 2019. Identifying breast cancer susceptibility genes – a review of the genetic background in familial breast cancer. Acta Oncol 58, 1–12. https://doi.org/10.1080/0284186x.2018.1529428

Wietmarschen, N. van, Merzouk, S., Halsema, N., Spierings, D.C.J., Guryev, V., Lansdorp, P.M., 2018. BLM helicase suppresses recombination at G-quadruplex motifs in transcribed genes. Nat Commun 9, 271. https://doi.org/10.1038/s41467-017-02760-1

Williamson, L.M., Lees-Miller, S.P., 2011. Estrogen receptor α-mediated transcription induces cell cycle-dependent DNA double-strand breaks. Carcinogenesis 32, 279–285. https://doi.org/10.1093/carcin/bgq255

Wu, W., Bhowmick, R., Vogel, I., Özer, Ö., Ghisays, F., Thakur, R.S., Leon, E.S. de, Richter, P.H., Ren, L., Petrini, J.H., Hickson, I.D., Liu, Y., 2020. RTEL1 suppresses G-quadruplex-associated R-loops at difficult-to-replicate loci in the human genome. Nat Struct Mol Biol 27, 424–437. https://doi.org/10.1038/s41594-020-0408-6

Wu, W., Rokutanda, N., Takeuchi, J., Lai, Y., Maruyama, R., Togashi, Y., Nishikawa, H., Arai, N., Miyoshi, Y., Suzuki, N., Saeki, Y., Tanaka, K., Ohta, T., 2018. HERC2 facilitates BLM and WRN helicase complex interaction with RPA to suppress G-quadruplex DNA. Cancer Res 78, canres.1877.2018. https://doi.org/10.1158/0008-5472.can-18-1877

Wu, Y., Shin-ya, K., Brosh, R.M., 2008. FANCJ Helicase Defective in Fanconia Anemia and Breast Cancer Unwinds G-Quadruplex DNA To Defend Genomic Stability ▿ †. Mol Cell Biol 28, 4116–4128. https://doi.org/10.1128/mcb.02210-07

Xu, B., Clayton, D.A., 1996. RNA-DNA hybrid formation at the human mitochondrial heavy-strand origin ceases at replication start sites: an implication for RNA-DNA hybrids serving as primers. Embo J 15, 3135–43.

Xu, H., Antonio, M.D., McKinney, S., Mathew, V., Ho, B., O'Neil, N.J., Santos, N.D., Silvester, J., Wei, V., Garcia, J., Kabeer, F., Lai, D., Soriano, P., Banáth, J., Chiu, D.S., Yap, D., Le, D.D., Ye, F.B., Zhang, A., Thu, K., Soong, J., Lin, S., Tsai, A.H.C., Osako, T., Algara, T., Saunders, D.N., Wong, J., Xian, J., Bally, M.B., Brenton, J.D., Brown, G.W., Shah, S.P., Cescon, D., Mak, T.W., Caldas, C., Stirling, P.C., Hieter, P., Balasubramanian, S., Aparicio, S., 2017. CX-5461 is a DNA G-quadruplex stabilizer with selective lethality in BRCA1/2 deficient tumours. Nat Commun 8, 14432. https://doi.org/10.1038/ncomms14432

Yager, J.D., Davidson, N.E., 2006. Estrogen Carcinogenesis in Breast Cancer. New Engl J Medicine 354, 270–282. https://doi.org/10.1056/nejmra050776

Yang, Y., McBride, K.M., Hensley, S., Lu, Y., Chedin, F., Bedford, M.T., 2014. Arginine Methylation Facilitates the Recruitment of TOP3B to Chromatin to Prevent R Loop Accumulation. Mol Cell 53, 484–497. https://doi.org/10.1016/j.molcel.2014.01.011

Yaşar, P., Ayaz, G., User, S.D., Güpür, G., Muyan, M., 2017. Molecular mechanism of estrogen–estrogen receptor signaling. Reproductive Medicine Biology 16, 4–20. https://doi.org/10.1002/rmb2.12006

Ye, X., Bishop, A.M., Reidy, J.A., Needham, L.L., Calafat, A.M., 2006. Parabens as Urinary Biomarkers of Exposure in Humans. Environ Health Persp 114, 1843–1846. https://doi.org/10.1289/ehp.9413

Yersal, O., Barutca, S., 2014. Biological subtypes of breast cancer: Prognostic and therapeutic implications. World J Clin Oncol 5, 412. https://doi.org/10.5306/wjco.v5.i3.412

Yi, P., Wang, Z., Feng, Q., Chou, C.-K., Pintilie, G.D., Shen, H., Foulds, C.E., Fan, G., Serysheva, I., Ludtke, S.J., Schmid, M.F., Hung, M.-C., Chiu, W., O'Malley, B.W., 2017. Structural and Functional Impacts of ER Coactivator Sequential Recruitment. Mol Cell 67, 733-743.e4. https://doi.org/10.1016/j.molcel.2017.07.026

Yu, J.-C., Hsiung, C.-N., Hsu, H.-M., Bao, B.-Y., Chen, S.-T., Hsu, G.-C., Chou, W.-C., Hu, L.-Y., Ding, S.-L., Cheng, C.-W., Wu, P.-E., Shen, C.-Y., 2011. Genetic variation in the genome-wide predicted estrogen response element-related sequences is associated with breast cancer development. Breast Cancer Res 13, R13. https://doi.org/10.1186/bcr2821

Yu, K., Chedin, F., Hsieh, C.-L., Wilson, T.E., Lieber, M.R., 2003. R-loops at immunoglobulin class switch regions in the chromosomes of stimulated B cells. Nat Immunol 4, 442–451. https://doi.org/10.1038/ni919

Yu, Y., Okayasu, R., Weil, M.M., Silver, A., McCarthy, M., Zabriskie, R., Long, S., Cox, R., Ullrich, R.L., 2001. Elevated breast cancer risk in irradiated BALB/c mice associates

with unique functional polymorphism of the Prkdc (DNA-dependent protein kinase catalytic subunit) gene. Cancer Res 61, 1820–4.

Zahid, M., Kohli, E., Saeed, M., Rogan, E., Cavalieri, E., 2006. The Greater Reactivity of Estradiol-3,4-quinone vs Estradiol-2,3-quinone with DNA in the Formation of Depurinating Adducts: Implications for Tumor-Initiating Activity. Chem Res Toxicol 19, 164–172. https://doi.org/10.1021/tx050229y

Zahler, A.M., Williamson, J.R., Cech, T.R., Prescott, D.M., 1991. Inhibition of telomerase by G-quartet DMA structures. Nature 350, 718–720. https://doi.org/10.1038/350718a0

Zhu, M., Wu, W., Togashi, Y., Liang, W., Miyoshi, Y., Ohta, T., 2021. HERC2 inactivation abrogates nucleolar localization of RecQ helicases BLM and WRN. Sci Rep-uk 11, 360. https://doi.org/10.1038/s41598-020-79715-y